THERMAL CHARACTERISTICS OF SCREENHOUSE CONFIGURATIONS IN A WEST-AFRICAN TROPICAL CLIMATE

A thesis submitted to the Faculty of Graduate Studies

and Research of McGill University

by

Gaétan Desmarais

In partial fulfilment

of the requirements of the degree of

Doctor of Philosophy

Department of Agricultural and Biosystems Engineering

Macdonald Campus of McGill University

Ste-Anne de Bellevue, Québec,

Canada, H9X 3V9

ABSTRACT

Gaétan Desmarais Ph.D. (Agric. and Biosystems Eng.)

Thermal Characteristics of Screenhouse Configurations in a West-African Tropical Climate.

The Biological Control Program (BCP) for Africa operates from Cotonou, Benin, which is part of the International Institute of Tropical Agriculture (IITA). Its present mandate includes the provision of Biological Control Labs to African National Biological Control Programs. Thirty tropical countries are targeted. The challenge presently faced by the BCP is to develop biological control structures adapted to the climatic and economic conditions of those countries. Specifically, structures such as greenhouses, screenhouses and growth chambers must provide, at reasonable expense, protection of experimental material against insects and airborne pathogens, as well as close to ambient temperature and sunlight. A recent innovation, the "screenhouse", is a promising technology with respect to its inherent capacity of providing near-ambient conditions by passive cooling (natural ventilation, radiation absorption and evaporative cooling) alone. However, overheating is still a problem in many conditions. In order to characterize the thermal performance of such structures, and to optimize their cooling performances, various screenhouse architectural configurations, screen types and water cooling options were evaluated during three seasons at the IITA, BCP research station.

Results show that in the climatic conditions tested, the architectural configuration is the most influential factor affecting the inside temperatures of the screenhouse followed by the type of screen used. Water cooling had more effect in the rainy season. Heat transfer models were formulated for every screenhouse configuration and set of options tested. Computer simulations generated the predicted inside temperatures of the screenhouses using the heat transfer characteristics calculated from the experimental data. The research aimed and succeeded at establishing fundamental understanding of the heat transfer of the screenhouse system in order to develop criteria for better designs.

RÉSUMÉ

Gaétan Desmarais Ph.D. (Génie agricole et Biosystèmes)

Caractéristiques thermiques des configurations de serres grillagées sous un climat tropical d'Afrique de l'Ouest

Le Programme de lutte biologique (PLB) pour l'Afrique de l'Institut international d'agriculture tropicale (IITA), basé à Cotonou (Bénin), a notamment pour mandat de fournir des laboratoires de recherche sur la lutte biologique aux programmes nationaux de lutte biologique des pays africains. Trente pays tropicaux sont visés. A l'heure actuelle, le PLB est confronté au défi du développement de structures de lutte biologique adaptées aux conditions climatiques et économiques de ces pays. Plus précisément, les structures telles que les serres, les serres grillagées et les chambres de croissance doivent protéger, à des coûts raisonnables, le matériel expérimental contre les insectes et les pathogènes véhiculés par l'air, tout en présentant des températures proches de la température ambiante et tout en laissant passer les rayons du soleil. La nouvelle technologie des "serres grillagées" semble prometteuse en ce qu'elle fournit des conditions proches des conditions ambiantes grâce au refroidissement passif (ventilation naturelle, absorption des radiations et évapotranspiration). Cependant, la surchauffe reste un problème dans de nombreuses conditions. Afin de caractériser les performances thermiques de ces structures et d'optimiser leurs performances de refroidissement, plusieurs configurations architecturales, types de moustiquaire et options de refroidissement par l'eau, ont été évalués dans des serres grillagées au cours de trois saisons à la station de recherche du programme de lutte biologique de l'IITA.

Les résultats montrent que, dans les conditions climatiques testées, le facteur le plus influent sur les températures intérieures est la configuration architecturale, suivie du type de moustiquaire utilisé. Le refroidissement par l'eau offre une efficacité maximum pendant la saison des pluies. Des modèles de transfert de chaleur ont été formulés pour chaque configuration de serre grillagée et pour chaque série d'options testées. Grâce aux caractéristiques de transfert de chaleur calculées d'après les données expérimentales, les simulations informatiques permettent de prédire les températures intérieures dans les serres grillagées. Cette recherche avait pour but de formuler les bases d'une compréhension fondamentale de transferts de chaleur du système de serre grillagée afin de déterminer des critères permettant l'amélioration de la conception de ces structures.

Cet ouvrage est dédié à ma mère

Denise

qui a tracé mon chemin

et qui depuis son départ est restée

et restera pour toujours,

plus présente que jamais.

ACKNOWLEDGMENTS

I would like to express my sincere appreciation to my thesis supervisor, Dr. G.S.V. Raghavan, Department of Agricultural and Biosystems Engineering. Beyond his supervisory role, Dr. Raghavan has been a mentor whose encouragement, persistence, focus and faith throughout the course of this study were a constant and stimulating source of progress for the completion of this thesis.

I would like to sincerely thank Dr. Hans R. Herren, Director General of the International Center of Insect Physiology and Ecology, who believed in the project from the beginning and allowed me to pursue the study at the Benin station of the International Institute of Tropical Agriculture (IITA). I would also like to thank Dr. Peter Neuenschwander, Director of Plant Health Management Division (IITA) who also permitted the continuation of the project at IITA-Benin.

I am grateful to the members of my advisory committee, Dr. S. F. Barrington and Dr. E. Norris, of the Department of Agricultural and Biosystems Engineering for their advice and encouragement throughout the various phases of this project.

My heartfelt appreciation goes to Mr. Bob Akinwumi, IITA Benin station Chief Engineer, who through the course of this project has become a very close friend, not to say a brother, and whose assistance and collegiality, both professional and personal while I was in Africa were invaluable. I express my gratitude and sincere thanks to him and his family for their help and friendship.

I also would like to sincerely thank Dr. Benoit Megevand (IITA) and his wife Dr. Conceçao Boavida (IITA) who have been extremely supportive during my stay in Benin.

I am indebted to Dr. C. Ratti, Post Doctoral Fellow, for giving me directions and recommendations on the formulation of the mathematical models and the simulation program. My sincere thanks to Cristina for her time and assistance.

I would like to sincerely thank Peter Alvo for his precious involvement in the statistical analysis aspects and throughout the writing stages of the thesis. His editorial comments through numerous drafts, perceptive and challenging discussions have been invaluable. I am indebted for his help and value his friendship.

Many grateful thanks are due to Valérie Orsat and to Yvan Gariepy, Department of Agricultural and Biosystems Engineering, for their constant support in the communications from Benin to Canada and especially during the equipment shipping phase.

My appreciation is extended to Mr. Cyprien Atcha (Ingénieur Agronome, IITA) who did everything in his power for this project to be successful. I am very grateful for his help and friendship. I would also like to thank Mr. M. Nobime and Mr. O. Piau for their faithful assistance.

The assistance of the Canadian International Development Research Center (IDRC) through the Young Canadian Researcher Award (YCRA) that was granted from the start of the project in May 1993 till December 1994, has provided the opportunity for this project to take place. The financial assistance of the International Institute of Tropical Agriculture (IITA) for purchasing the equipment necessary for the project is also sincerely acknowledged.

The journey has been tumultuous but worth it. Many people have given their uncalculated help along the way. Unfortunately it is impossible to name them all here, but I would like to give special thanks to all these people and I am convinced that these persons will recognise themselves in these words.

J'aimerais remercier sincèrement M. Alain Ratié (IITA) pour son inestimable soutien moral et logistique, ainsi que pour la sérénité et la sagesse de ses conseils.

Les sacrifices et le support que m'a fournis ma famille tout au long de mon parcours sont inestimables. Je désire remercier tout spécialement mon père, Roger, et son épouse Ghyslaine. Je veux profiter de l'occasion pour remercier mes deux frères Michel et Patrice ainsi que ma soeur Brigitte qui se sont toujours dévoués corps et âmes lorsque j'ai eu besoin d'eux. Leurs épouses et époux, Lyne, Brigitte et Pierre ainsi que mes nièces et neveux, Julie, Patrick, Elysa, Francois et Olivier sont également près de mon coeur.

Je veux lancer un merci tout spécial à Johanne et Yves qui m'ont apporté beaucoup de soutien et d'amitié durant plusieurs étapes de mon cheminement.

Je veux finalement exprimer toute ma gratitude à ma "blonde", Valérie, pour son support enthousiaste et sa patience du début à la fin de ce projet. Sa compréhension et sa générosité sont les éléments indispensables sans lesquels nous n'aurions pu passer au travers de ce défi.

TABLE OF CONTENTS

LIST OF FIGURES

LIST OF TABLES

NOTATIONS

a	Heating efficiency of solar radiation
A_c	Area of green/screenhouse cover [m^2]
A_{c1}	Area of first layer oc cover [m^2]
A_f	Floor Area [m^2]
A_T	Area of opening [m^2]
c_t	Cover thickness [m]
C	Heat capacity of greenhouse [J /m^3 °C]
C_p	Heat capacity or specific heat of air [J/m^3 °C]
C_{pc}	Heat capacity or specific heat of cover [J/m^3 °C]
C_{pg}	Heat capacity or specific heat of ground [J/m^3 °C]
C_q	Air flow discharge coefficient
C_v	Air velocity coefficient
$D_{g,ss}$	Conductive heat flux from ground to subsoil [W]
g	Acceleration of gravity [m/s^2]
h	Height difference between inlet and outlet [m]
h_g	Convective heat transfer coefficient from ground to air [W/m^2 °C].
h_i	Convective heat transfer coefficient from cover to air within the screenhouse [W/m^2 °C].
h_o	Heat transfer coefficient from cover to the air outside [W/m^2 °C].
H	Heat input from the heating system [W]
H_i	Enthalpy inside the green/screenhouse [J/kg]

H_o	Enthalpy outside the green/screenhouse [joule/kg]
I	Global radiation [W/m^2]
I_i	Global radiation inside the screenhouse [W/m^2]
I_o	Global radiation outside the screenhouse [W/m^2]
k_c	Thermal conductivity of the cover [W/m °C].
k_g	Thermal conductivity of the ground [W/m °C].
L	Thickness of concrete slab [m]
m_a	mass of air [kg]
m_c	mass of cover [kg]
m_g	mass of ground [kg]
N	Air exchange rate [Air exchange/min]
N_υ	Natural ventilation rate [Air change/min]
q_{cd}	Conduction heat loss or gain [W]
q_C	Air conditioning heat [W]
q_e	Equipment heat [W]
q_f	Furnace heat [W]
q_g	Convection heat transfer from the ground [W]
q_i	Heat of infiltration [W]
q_I	Solar heat gain [W]
q_{Ieff}	Effective heat gain of the screenhouse inside air by short wavelength radiation energy (sun temperature) [W]
q_{Ieffd}	Effective heat gain of the double roof screenhouse inside air by short wavelength radiation energy (sun temperature) [W]

q_{leffdw} Effective heat gain of the inside air of a double roof screenhouse with water irrigation by short wavelength radiation energy (sun temperature) [W]

q_{leffw} Effective heat gain of the inside air of a screenhouse with water irrigation by short wavelength radiation energy (sun temperature) [W]

q_{lw} Heat transfer of long wave radiation [W]

q_{lwsky} Heat transfer of long wave radiation to the sky [W]

$q_{N\upsilon}$ Heat of Natural ventilation [W]

q_p Heat transfer of photosynthesis [W]

q_r Heat of respiration from plant tissues [W]

q_t Heat of thermal radiation [W]

q_{teff} Effective heat gain of the single layered screenhouse inside air by long wavelength radiation energy (screenhouse air temperature) [W]

q_{teffw} Effective heat gain of the double roof screenhouse inside air by long wavelength radiation energy (screenhouse air temperature) [W]

q_{υ} Heat of ventilation [W]

q_{RD} Heat of conduction-convection including radiation [W]

Q Air flow rate [m^3/s]

r Correction factor for radiative heat transfer

R Long wave radiation through the cover [W]

So Solar radiation [W]

t Time

T	Surface temperature [°K]
T_a	Air temperature [°K]
T_{dp}	Dew point temperature [°C]
T_g	Ground temperature [°C]
T_i	Inside temperature [°C]
T_m	Temperature of the mass [°C]
T_o	Outside temperature [°C]
T_s	Sky temperature [°K]
T_{soil}	Soil temperature [°C]
U	Global heat transfer coefficient [W/m^2 °C]
U_w	Global heat transfer coefficient for screenhouse irrigated with water [W/m^2 °C]
υ	Air velocity [m/s]
υ_a	Air approach velocity [m/s]
υ_r	Air remaining velocity [m/s]
V	Green/screenhouse volume [m^3]
V_g	Ground volume [m^3]
W_i	Interior humidity ratio [kg H_2O/ kg dry air]
W_o	Exterior humidity ratio [kg H_2O/ kg dry air]
W_p	Moisture added to the greenhouse environment by evapotranspiration [kg/s]
W_{ve}	Moisture exchange in the ventilated air [kg/s]
x	Distance [m]

Greek

α	Absorptivity [%]
ε	Emissivity of surface [%]
ε_a	Apparent emissivity of atmosphere [%]
ε_g	Emissivity of ground [%]
ε_s	Emissivity of internal surface [%]
η	Reflectivity [%]
θ	Reduction (friction) factor for air flow
ρ	Air density [kg/m^3]
ρ_g	Ground density [kg/m^3]
σ	Stefan- Boltzman's constant [5.670 X 10^{-8} $W/m^2\,{}^{\circ}C^4$]
τ	Transmissivity of materials to solar radiation [%]
τ_{c1}	Transmissivity of cover 1 to solar radiation [%]
τ_{c2}	Transmissivity of cover 2 to solar radiation [%]
τ_g	Transmissivity of materials to radiation coming from ground [%]
τ_t	Transmissivity of materials to radiation coming from surfaces near the ground (also called Thermal transmissivity) [%]
τ_w	Transmissivity of water to solar radiation [%]

I. INTRODUCTION

Africa has serious problems in feeding its people. If the situation does not improve soon, catastrophe threatens the continent. The development of the agriculture production capacity is a priority in Africa and is at the top of the agenda for the overall development of the continent. An urgent strategic emphasis is put on food production systems that are stressed by climatic changes, water storage, desertification, environmental deterioration, soil degradation, modifications of bioclimatic factors, pest infestations, and natural disasters. The future well-being of African countries is clearly perceived to depend on the rate at which they can generate and implement environmentally sound and sustainable technologies in all sectors of exploitation, and particularly in agriculture (I.D.R.C., 1993).

The international community has reached the consensus that the development and implementation of adapted technologies in agriculture must take place through aid aimed at strengthening the research structures and capacities of the countries. The underlying philosophy is that through an adequate research infrastructure, African countries will be in a position to make their own decisions about the technologies they choose to favour for their own development. I.D.R.C. (1991) states: "Research provides the means for the acquisition of appropriate knowledge and, thence, for development. The capacity to conduct research, therefore, is a necessary condition for empowerment".

In the case of Agricultural research, there is a definite trend by the worldwide donor community to support the establishment of stable research structures for African national research programs (I.D.R.C and A.U.C.C, 1992). As a member of the Consultative Group of International Agricultural Research (CGIAR), the International Institute of Tropical Agriculture (IITA) located in Ibadan, Nigeria, has a mandate to provide strong support and assistance to the national African research programs aimed at improving research and development capacity in agriculture. IITA is putting a lot of emphasis on technology transfer and training for research within the countries. The technology transfer mandate includes supplying the national research programs with agricultural research infrastructures (IITA, 1990, 1991, 1992, 1993).

In Africa, agricultural research necessarily addresses the prolific and diverse biological communities inherent to African ecologies. Aside from climate, biological enemies represent the greatest constraint to production capacity. Natural biological means of improving agricultural production through pest control and improved varietal resistance are favoured for economic considerations and to protect the delicate ecological balance of the continent.

A very good example is the Biological Control Program (IITA BCP) that has been initiated by IITA to overcome the Cassava Mealeybug (*Phenacoccus manihoti*) by one of its natural predators *Epidinocarsis lopezi* (Herren and

Yaninek, 1989). This program is now based at the Biological Control Centre for Africa which is located in Cotonou, Republic of Benin (Figure 1.1), and is part of the Plant Health Management Division of IITA.

Apart from cases using the "systems" approach where the whole system is observed with no control, when a specific problem must be investigated in biological research for agricultural production there is always a need to isolate wanted from unwanted biological elements or to isolate dependent from independent biological variables or parameters. For the sake of not being biased, most of the research protocols seek to reproduce real conditions with the exception of one or two varied parameters. This type of research is done in biological containment facilities because the biological factors present in the humid tropics, the semi-arid tropics and the arid regions are too numerous to study all at once. Facilities permitting isolation of all but those of interest are therefore essential to agriculture research centres.

Biological containment can either be performed in completely artificial climates such as growth rooms or growth chambers, or in facilities open to some but not all natural elements. Containment facilities are usually categorized as: 1) glasshouses, greenhouses, screenhouses or walk-in tunnels, 2) low tunnels or flat films and 3) others (windbreaks and hot beds). At worst, a plant protection enclosure should permit natural lighting. In Africa it is usually the biological factors (insects, viruses, bacteria, birds and animal pests)

Africa

Figure 1.1: Location of Experiment

that must be excluded or included. Thus, categories 1) and 2) are the most important to research on biological control.

Following the mandate given to IITA, IITA BCP is in the process of supplying Biological Control Labs to the African National Biological Control Programs (ANBCP). Up to thirty (30) countries are targeted and will be supplied with Biological Control Labs in the very near future. Almost all of the National Agricultural Research Programs in Africa will need biological containment facilities as part of the infrastructure of their agricultural research centres. The standard technologies that will be used will necessarily follow the trends activated by the International Research Centres like IITA and IITA BCP. The national centres do not have many choices as to what technologies they will use. Greenhouses and screenhouses are already considered as being the standard technologies to use. In this context, the International Research Centres like IITA face many challenges. One of them is that specifically adapted greenhouse technologies for humid tropical and subtropical climates do not yet exist (Rault, 1988). The main problems faced are non-representative interior temperatures, difficulties in maintaining proper isolation from pests, rapid deterioration of materials, inadequate or unavailable power for cooling, and high capital and maintenance costs.

The possibilities for combining technologies to develop containment facilities adapted to the specific needs at a particular location are numerous. Ideally, the containment facility should be: modular, easy to build, inexpensive to operate and maintain, require low energy input, expendable, durable and easy to cool. However, such near-optimal design is not the norm.

The screenhouse concept put forward by Rossel et al. (1979) offers a number of advantages over the greenhouse or glasshouse in humid tropical climatic conditions. The major advantage being its intrinsic zero energy input needs during operation. The screenhouse system is inherently naturally ventilated by the air going through the screens that cover the structure. However, overheating is still a problem under many conditions.

The screens used as a covering material for the screenhouse restrict the outside air from getting inside the screenhouse resulting in low ventilation rates especially in low wind conditions. A judicious choice of screen coverings has to be made. Screening is selected in relation to its ability to exclude or include small insect pests but the effects of the size of mesh used, on the inside climate conditions of the screenhouse, are not known.

The architectural design of the screenhouse also has an effect on the inside climatic conditions. For example, the temperatures inside the screenhouse are different for a double roof than for a single roof screenhouse. The tunnel shape screenhouse will not give the same inside temperatures as the Quonset shape. Yet these effects have neither been quantified nor analyzed in a systematic manner. Other methods requiring very low energy inputs can also be utilized to cool the screenhouse. A water curtain spread on the outside surface of the screenhouse can be used to both filter the incoming radiation heat load and to evaporate heat by evaporation. Conditions of high humidity certainly limit the potential of evaporation as a cooling method for the humid tropics but no one has tried to estimate these limits when applied to the screenhouse case. Standard ventilation could be used for ventilating the screenhouse but it is expensive and uniformity of ventilation is physically difficult to achieve when only screens are used as covering. Other active technologies like air conditioning could also be used to cool screenhouses but these technologies defeat the purpose of the energy and resource saving objectives that humanity has fixed for the future of this planet.

There is an urgent need to achieve a fundamental understanding of the heat transfer characteristics of screenhouses and to identify the design components that may most easily be manipulated for cooling optimization. This research is an attempt to characterize the thermal performance of the screenhouse structures, and to optimize their cooling performances. Various screenhouse structural configurations, screen types and water cooling options were evaluated in three seasons at the IITA, BCP research station. The data were analyzed following the engineering design approach. Heat transfer models were formulated for every screenhouse configuration and set of options tested. Computer simulations generated the predicted inside air temperatures of the screenhouses based on the heat transfer characteristics calculated using the experimental data. This research is a first step aiming to establish a fundamental understanding of the heat transfer of the screenhouse system, from which it will be possible to develop criteria for future designs of screenhouses in humid and sub-humid tropical regions and for other climatic regions of the world where screenhouses are presently needed.

II. REVIEW OF LITERATURE

2.1 Greenhouse Technologies for the Tropics

Brochier (1979) points out that growing vegetables in humid tropical climates at low altitude is very difficult. The limiting factors are numerous. Heavy rains cause physical damage to the crops and destroy the surface of the soil. The diurnal temperature cycle does not permit for optimal photosynthesis/respiration ratios. Insolation levels are low because of short days and heavy cloud cover for most of the growing season. Continuous high humidity favours parasitism. Brochier (1979) also stated that because of these factors protective structures and specially developed cultivation practices relying on the use of plastics have appeared around the towns of the tropical lowland regions to counter the very low productions obtained during the very short dry season. Brochier (1979) asserts that, in effect, the only way of producing vegetables during the long rainy season is to erect structures to protect them from the rain.

The plastic greenhouse structures that have been used in Gabon, in Manaus (Brazilian Amazon) and in French Guyana are of three types: 1) small wooden framed structures, 2) large wooden framed structures and 3) galvanized metal framed tunnels 7 meters wide. Brochier (1979) mentions that the 7m X 54 m galvanized tunnel framework is more resistant to tornadoes (120 km/hour wind speeds) and more durable than the wooden structures. Brochier states that they also have performed well with respect to temperature, luminosity and air-tightness but the author gives little scientific evidence of such performances.

After reviewing most of the techniques for cooling and ventilating greenhouses in the humid tropics, Rault (1988) clearly introduces a contradiction to Brochier's (1979) work: "no polyvalent greenhouse has really been designed specifically for tropical humid areas". The main constraints he noted were: i) inadequate materials for the cover and the structure, ii) the lack of effective ventilation and cooling techniques, and iii) maintenance and energy consumption and costs.

Rault (1988) mentions that according to the climate, the specificity of protected cultivation has clearly been settled. The "greenhouse effect" is desired in a mild climate and the "oasis effect" will be wished in an arid tropical climate. The "umbrella effect" will be expected in humid tropical regions but will induce excessive increases of daytime temperatures. Rault (1988) says that particularly during the rainy season, none of the commonly used methods of shading, ventilation and cooling, including cooling by evaporation, are completely satisfactory. Even by using plastic cladding materials instead of glass which, according to the same author, is the most promising direction, the improvement of internal climatic surroundings in greenhouse design for the tropics is a challenge.

In the same period, Von Zabeltitz (1988, 1990) summarized the general design criteria for greenhouses in mild climates. Three different climatic divisions are distinguished: 1) the Mediterranean climates, 2) the tropical desert conditions and 3) the humid tropical climates. Von Zabeltitz (1988) states that in addition to the general demands on plastic-film greenhouses, the climatic conditions prevailing in each region have an influence on the construction design. Von Zabeltitz (1988, 1990) enumerates the advantages and disadvantages of many different models of greenhouses that have been developed for the three climates and used worldwide but says very little about their inside climatic performances. Although very useful information for deciding among the numerous possibilities of greenhouse designs for the Mediterranean climate can be found in FAO (1990), the paper is also a clear report on the complexity of choosing the appropriate greenhouse technology for a specific climatic region. Rault (1990) describes the performance of a tunnel greenhouse with side and top ventilation under the tropical lowland climate in French Guyana. The author mentions that there are still some improvements to be made to the design.

Greenhouse design for tropical regions still faces many challenges. Von Zabeltitz (1990) summarized general design criteria for plastic film greenhouses in warm climates: physical and photochemical resistance; simple method to change the film; insulation of parts of the structure which are heated by solar radiation; effective ventilation; tightness of structure; prevention of dropping of condensation water from the roof; vertical sidewalls. In the specific case of humid tropical regions the same author enumerates the main demands on plastic-film greenhouse designs: i) protection from rain; ii) very good ventilation efficiency; iii) durability of the film and iv) rain water collection. Many of these parameters for design can be improved with new technologies or new arrangements of existing technologies. The temperature regulation of greenhouse interior air is of fundamental importance in the design. Rault (1988) mentions that the technologies that have been used to date have not been fully satisfactory.

2.2 Cooling Technologies for Greenhouses in the Tropics

Garzoli (1989) affirms that unlike heating, for which technology is well established, greenhouse cooling frequently presents considerable problems. This argument is reaffirmed by FAO (1990) which states: "one of the major problems encountered by greenhouse producers in the Mediterranean region as a whole is the control of excess heat". Chandra et al. (1990) mention that the most important environmental control requirement under the tropical conditions in India is cooling.

Garzoli (1989) and FAO (1990) have listed ventilation (forced and natural), shading, evaporative cooling (fan and pad systems) and refrigerated cooling as the four known and presently implementable techniques for cooling greenhouses. FAO (1990) emphasizes that to date, it is unaware of any inexpensive greenhouse cooling system that can keep the temperature inside the shelter below ambient. Many authors (FAO (1990); Garzoli (1989); Rault (1988)) agree that the cost of greenhouse cooling by refrigeration can mean high and even prohibitive capital and running costs, especially in tropical humid climates (Rault, 1988).

Some researchers have experimented with the concept of closed systems for cooling greenhouses, especially for desert climates. For most closed system greenhouses, a water film on the surface ("fluid roof") of the greenhouse provides the cooling effect. The precursors of these techniques are described by Fontes (1975), Daunitch (1975), Chiapale (1981) and Gale (1981). Many others have investigated the concept. Some, such as Strauch et al. (1989) and Zeroni et al. (1990) are still testing the performances of such systems. Mannan et al. (1979) tested two small scale, non ventilated greenhouses in a hot climate in India and obtained measurements of inside temperatures in the summer ranging as high as 55 to 60 °C. They found that a thin layer of water on the roof is very effective in keeping a greenhouse cool in summer by as much as 10 to 12 °C but the authors made no report of the relative humidity conditions. Lawson (1986) and Ménard (1991) studied the performance of a water film to conserve energy in a greenhouse. Kurosaki et al. (1978) describe the heat transfer involved in a solar radiation absorbing fluid layer flowing over a substrate and conclude that too large concentrations of additives (or opacities) to capture incoming solar radiation in the fluid layer are undesirable since they result in the deterioration of the system performance.

In the case of humid tropical climates, the objective of temperature regulation is to maintain the inside temperature as close as possible to ambient ("umbrella effect"). Rault (1988) considers thermic regulation as one of the determining factors for success in cultivation under a plastic shelter. He points out thermic regulation as an easy parameter to control in arid climatic conditions but much more difficult to control in humid tropical surroundings. Rault (1988) considers the most commonly used cooling techniques as unsatisfactory for application in the humid tropics. He gave the following comments: 1) Shading: unwanted due to limited external luminosity; 2) Evaporative systems: effectiveness reduced because of high relative humidity of the air; 3) Cooling, by refrigeration or dehumidification of the atmosphere: requires high investment and operating costs; 4) Dynamic ventilation: difficult due to the high and rapid "greenhouse effect" in a completely closed area.

From FAO (1990) and Rault (1988), it is obvious that the techniques that are used to date for the cooling of the greenhouses in tropical regions are not satisfactory and represent a burden for the application of greenhouse technologies as a whole in these regions. There is therefore still a lot of incentive to find new, natural, cheap to build/to run/to maintain ways of cooling greenhouses for use in tropical climates. Development of applicable cooling technologies is an important research endeavour.

2.3 Screenhouses

A technology for protecting crops that shows a lot of promise for tropical climates but has never been studied in terms of its thermal properties, is the "screenhouse". Rossel et al. (1979) report a model of a screenhouse that was developed for virus research at the International Institute of Tropical Agriculture, Ibadan, Nigeria. The screenhouse is described as a screened cage equipped with a high capacity ventilation fan. The author admits that without forced ventilation, the fine mesh screen tends to reduce the airflow and temperature rises of 3.5 °C were noted in the tested screenhouse models. The structure is provided with a second and separate roof over and on top of the screen cage to provide for adequate rain protection. The authors claim that the shading effect of the screen proved to be beneficial for symptom expression in most test plants but admitted that the same plant species have a tendency to etiolate slightly. Picture 2.1 shows the Tunnel type screenhouse and Picture 2.2 shows the Rossel type screenhouse. Both types of screenhouse were developed at IITA.

Many researchers have used the screenhouse in their experiments. Desmarais (1992) points out the main problems encountered by the screenhouse users in various research centres in Africa: 1) lack of adequate instructions to build the screenhouses; 2) missing parts in the shipments; 3) design anomalies (e.g.. proper double door design to conserve insect tightness, proper attachment system (grip strip) design used to tie the screens on the screenhouse structure, proper rain protection roof design); 4) deterioration of materials; 5) level of precision needed at construction time; 6) insect tightness; 7) inside climate; 8) cost and 9) the lack of competitive suppliers. For the insect tightness and the inside climate of the screenhouse, Desmarais (1992) stated

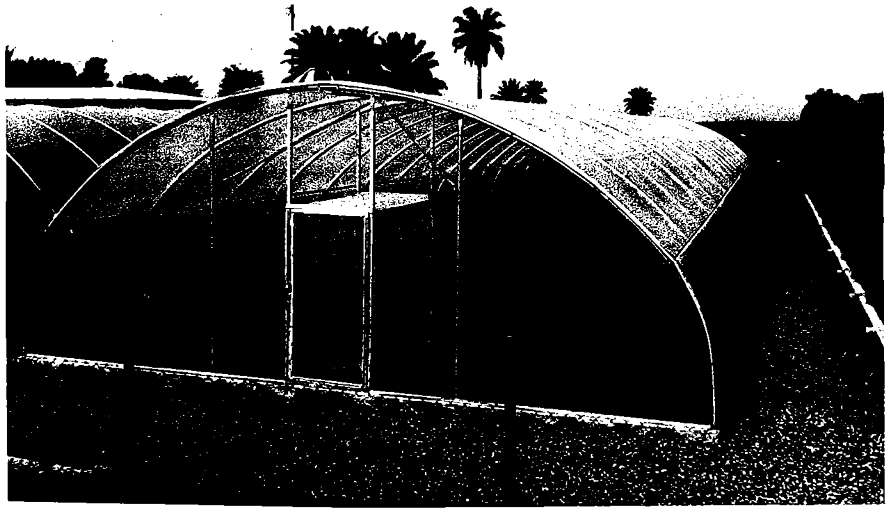

Picture 2.1: The Tunnel Type Screenhouse (8m x 20m)

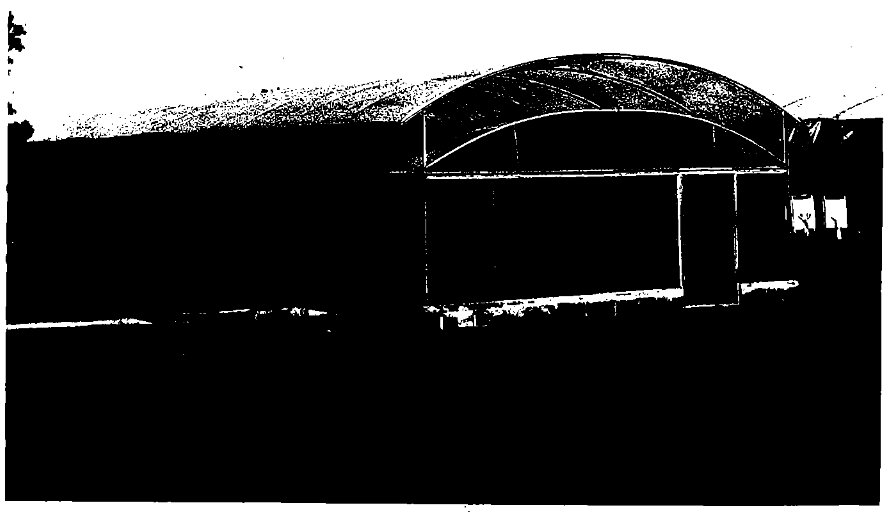

Picture 2.2: The Rossel Type Screenhouse (6m x 20m)

that more basic analysis and research is needed to better understand the evolution of the inside conditions of the screenhouse. To the author's knowledge, no extensive studies characterizing screenhouse climate have been performed. A shade-house design (Williamson et al. 1984) has been developed in Hawaii for dendrobium orchids but there are no indications of the thermal performance. Ross (1995) reported that an naturally ventilated screenhouse in Honduras, covered on four side walls with insect screening and on the roof with plastic were overheating and presented a special design problem.

2.4 Screening for Greenhouses

In Canada and United States, screens have been used for years to limit access of insects to dwellings and commercial buildings. The predominance of total air conditioning has limited the use of screens in commercial buildings but their use in homes is still important. In recent years, screening has been used in greenhouse applications. Greenhouse screening is generally achieved with much finer mesh than windows for house screening because all the insects have to be excluded, some of which are minuscule in size (Roberts et al. 1995). Bethke (1990) presents a table of screen hole sizes to use for various greenhouse pests to be excluded from the greenhouse. Some examples are presented in Table 2.1.

Impatiens Necrotic Spot Virus (INSV) and Tomato Spotted Wilt Virus (TSWV) are two major diseases that can devastate a wide range of greenhouse plants. Both diseases are vector transmitted by Western flower thrips

(*Frankliniella occidentalis*). Thrips often migrate into greenhouses from spring to fall and are among the most difficult pests to control. Thrips and whiteflies are also very common in Africa and represent a big problem. Flower thrips

Table 2.1 - Recommended size of holes for insect screening

Insect	Size of holes microns
Serpentine leaf miner (*Liriomyza trifolii*)	640
Sweet potato whitefly (*Bemisia tabaci*)	462
Melon aphids (*Aphis gossypii*)	340
Greenhouse whitefly (*Trialenrodes vaporiarorum*)	288
Silver leaf whitefly (*Bemisia argentifolii*)	239
Western flower thrips (*Frankliniella occidentalis*)	192

have developed resistance to several synthetic insecticides. Excluding thrips from greenhouses should be one of the highest priorities of greenhouse growers. To prevent inward migration of nymphs of the Western flower thrips, a very fine mesh screening must be installed.

Microscreening also works to keep insect predators and parasites from migrating out of the greenhouse if biological release of beneficial insects and mites is done. Pesticide-use reductions in the range of 50 and 90 percent have occurred in North America, Europe and Israel for fine mesh users (Roberts et al., 1995).

For greenhouses, screening is used on all air inlet louvres and other vents. Exhaust fan openings need to be covered by tightly closing louvres. Any opening along the perimeter of the greenhouse base and cracks around doors and vents must be sealed.

Roberts et al. (1995) stated that the mesh fineness which is required in greenhouse applications can limit the movement of air in the greenhouse and promote undesirable growing conditions. Ross et al. (1994) mention that small screen openings restrict air movement and thus a large screened surface must be provided to allow the necessary ventilation air into the greenhouse. Three design approaches are presented to size a screening system: A- The United States National Greenhouse Manufacturers Association (NGMA) which makes use of a manometer to measure existing greenhouse static pressure and uses information about the static pressure versus the air velocity relationship of the screening material to size the screened area; B- The second method uses the air flow velocity or air "approach velocity" established by equation or from air flow tests at 0.76 mm of water static pressure loss through the screening material; and C- The third method uses free open area calculations for the screening materials that do not have known air velocity versus static air pressure relationships.

Ross et al. (1994) specify that method A is best and most direct from an engineering viewpoint and that method B and C could result in erroneous designs if the greenhouse was poorly designed initially.

2.5 Screens

Screens are found and used today in many different forms, shapes and types and have many applications. The key element to the heat transfer characteristics of the screenhouse is the screen that is used as a cover. The screen properties and the interactions of the screens with the environment in terms of flow of air, water and/or radiation affect the inside conditions in the screenhouse.

2.5.1 Properties of Screens.

Screens can be characterized by various parameters. Some authors have already made some classifications. For example, Jaubourg (1988) and Tillie (1988) mentioned the porosity, the structure and the texture of screens as determining the resistance to wind flow-through. Kozai et al.(1991) have made an attempt to define the permeability of screen wicks by experimental and analytic techniques. Depending on the application for which the screen is intended, the authors studied particular parameters. There are many parameters that could be used for classification. The materials used in the fabrication is one of them. The colour of the screen is also important. A classification of screens can also be looked at in terms of their heat transfer properties. Another classification could also be done with the properties of screens defined by the interactions (flow-through, capillarity, etc.) of screens with water. A classification made in terms of both thermal performance and its interaction with water could be made. In the particular context of this study, a classification of screens can be made in terms of the ability to stop insects crossing the screen (Bethke, 1990). A precise description of the screen can be made only by using its physical characteristics. A differentiation has to be made between a description of the screen and the performance of the screen in various application.

2.5.1.1 Materials.

The most common materials used in the fabrication of screens are metals and plastics. The most common metals and alloys used are aluminium, steel, copper and bronze. With the advent of polymers, many different varieties of plastic screens are available. The most commonly used are Nylon and Fibreglass but many other types of plastics (PVC, Polyethylene, Polypropylene, Polyester, Teflon) are also used to make screens. The choice of material for fabrication of the screen influences its performance (resistance, longevity, etc.) in specific applications. Hindeleh et al. (1990) have demonstrated that crystallinity enhances light transmissivity through low-density polyethylene sheets.

2.5.1.2 Geometric parameters.

Screens vary in their geometric design. The parameters that play a role aside from the material used are: the size (thickness, area, volume) of the threads, the number of threads that are made to cross horizontally and vertically (warp and weft) which has been named a mesh (or pics) and the shape of the thread used. These geometric parameters also vary and are determined by the structure and/or textures of the screens.

2.5.1.3 Structure and texture.

Jaubourg (1988) and Tillie (1988) have listed 4 different types of structures and/or textures for screens: extruded, thermowelded (thermosoudé), knitted, woven and woven coated.

2.5.1.4 Porosity.

The geometric porosity of screens is defined by Jaubourg (1988) as being the ratio of open area to the total area of the screen. Kozai (1991) has defined mathematical equations for calculation of the porosity of screens determined by a model of the screen geometry based on microscopic observations.

2.1.1.5 Permeability.

Kozai (1991) has also given equations to predict the permeability of metal screens for a water flow and mentions that permeability of screens varies greatly with the packing number defined as how the screen meshes are "packed" together.

2.5.2 Interactions of screens and airflow.

Jaubourg (1988) mentions that the porosity, the nature of the thread used in the fabrication and the form of the edges of each openings of the screen are important in determining the interaction of wind with screens. The author has evaluated the efficiency of screens and defines it as being the residual speed of air downstream of a screen as a function of the airspeed upstream.

The author used a helicoidal fan of large diameter in a wind tunnel to generate a constant and homogeneous airflow to test the screens. The screens were drawn tight on a metallic frame (120 cm x 120 cm) so that they could be placed perpendicular to airflow. Three different wind speeds were used: 4.3, 6.4 and 10 m/s. Measurements of airspeed were taken at 0.5 m and 1.5 m downstream of the screen on a width of 0.8 m. Jaubourg (1988) concludes that in general, porosity is inversely proportional to the efficiency of the screen and that for screens with asymmetric sides there were no noteworthy differences in efficiency with respect to the side facing the wind. The author was able to formulate equations of efficiency as a function of porosity specific to three categories of screen structures in the range of wind speed measured. Jaubourg (1988) also tested and formulated an equation for the efficiency of double layers of identical screens placed at 12 cm of each other.

Tillie (1988) performed the same measurements with screens of the same dimensions and types but the screens were placed in natural wind conditions. All the screens were not tested at the same wind speed. The author was trying to differentiate between the various behaviours of the different types of screens. An evaluation of efficiencies of screens was also performed with screens attached to the side openings of a barn. The values of porosity were not measured but taken from the manufacturer. The author has noted gaps in efficiencies of screens of the same porosity. He admits that this might be because the values of porosity given by the manufacturers were not exact.

Tillie (1988) noticed a great variability in the efficiency of screens of various textures. He concludes that the efficiency of a screen, as defined by Jaubourg (1988), is affected by the porosity, the texture and the shape of holes of the screens. Su et al. (1991) used air and helium as testing fluid to evaluate the pressure drops of the flow through single wire screen gauges of various open area ratios.

2.5.3 Interactions of screens with water.

Some authors have studied the interactions of screens with water. Hayashi et al. (1990) studied the liquid film formation on mist cooled heat exchanger and heat transfer tubes with a variety of surface configurations such as grooved, wire-wound, and screen mesh wound tubes. The authors used the wetness parameter G* defined in a previous report by Matsuda et al. (1986). In their study on permeability of screens Kozai et al. (1991) used distilled water as the test liquid to evaluate 48, 70, 100 and 200 mesh stainless steel plain square weave screen samples. Pruzan et al. (1990) investigated the use of water-ethanol mixtures in an experiment on evaluating two phase flow and dry-out of screen wicks. Ng (1990) studied the dewatering performance of screens used to dewater wet coal. Results showed that three parameters can quantify the vibrating screen performance: i) the separation of free water, ii) the removal of surface moisture of the wet coal and iii) the vibratory excitation.

2.5.4 Heat transfer properties of screens.

Many researchers have looked at the heat transfer properties of screens. Zhang et al. (1991) determined the thermal insulation effect that is due to a mid plane screen in a two-dimensional air cavity. One function of the tilting-blade screen in the window is to modulate the radiative heat transfer through the window. Another function is to interfere with the buoyancy-induced air circulation and to increase the insulation capability of trapped air. The authors concluded that the use of a vertical screen can reduce significantly the overall heat transfer rate by natural convection through a tall enclosure. In a study on turbulent heat transfer processes Ueda et al. (1992) used a heated screen in their experimental set up to heat the turbulent air flow pattern generated by a turbulence generating grid. The temperature profiles could then be plotted to elucidate the turbulent airflow. The study was conducted as basic research on the interaction of flow and motion. Beard et al. (1989) evaluated the thermal performance of a heated plate with open-channel infrared radiation shields. Four different radiation shields of opaque fabric were tested under simulated typical outdoor conditions to determine the relative performance of the four screens as well as of the bare plate configuration. The testing for each plate-screen configuration included conditions with and without wind simulation for three different plate heating conditions. Solar radiation was simulated using a square array of sixteen 300 W reflector flood-lamps. The authors also developed lumped parameter computer models to characterize the heat transfer phenomena associated with the bare plate, with and without the continuous screens. Velocity and temperature profiles in the channel were measured for each test. The velocity in the channel was found to be most greatly influenced by the type of screen used. Temperature profiles are characterized in two groups corresponding to testing without and with wind simulation. The introduction of solar radiation to the various plate/screen configurations resulted in the bare plate experiencing the greatest temperature rise. The addition of wind-driven forced convection caused the plate temperature to decrease for all tests with the incised screens as well as for the test with bare plate. Wind-driven forced convection did not significantly change the average plate temperature in any of the continuous screen tests. The use of radiation screening lowered the infrared signal in all cases, with the double layer-screen yielding the lowest infrared signal for all tests. The authors conclude that among all the screens tested, the double-layer incised screen was the most effective in suppressing the infrared signature of the heated plate under outdoor conditions, because it allowed air to flow through its incisions while still providing a totally opaque radiation shield.

2.5.5 Heat transfer properties of screens interacting with water or air or mixtures of fluids.

Many of the studies performed on screen interactions with air or water or with mixtures of these with other fluids were done with the purpose of evaluating heat transfer properties of screens with these fluids. Hayashi et al. (1990) differentiated between the heat transfer characteristics of various configurations, geometry and dimension of heat transfer tubes. Some of the configurations used wire wound screens with water, the result being an increase of the heat transfer coefficient in comparison to the smooth tubes. Lewandowski et al. (1991) reported results of experimental investigations of convective heat transfer from a circular screened horizontal plate to ambient liquid. The authors affirm that the results presented in this study have been used in investigations on heat transfer in devices for solar radiation absorption such as collectors and solar ponds. The interest in the study of Pruzan et al. (1990) was to examine the effect of fluid composition on the maximum dry out heat flux (DHF). This heat flux is the highest steady state heat flux that a heat pipe can dissipate. At higher fluxes the mass evaporation rate exceeds the rate at which liquid can be resupplied by capillary action in the screen wick. The authors conclude that any reductions in surface tension for the fluid mixture should be avoided as this reduces the capillary pumping capability of the screen wick and limits heat pipe performance at large capillary rise heights. Su et al. (1991) studied the ratio of specific heats of fluids on the pressure drop of the flow through wire screen. The gauzes tested were of ten different values of open area ratio (porosity). Air and helium were used as test fluids. The authors found that the effect of the ratio of specific heats of the fluid on the pressure loss coefficient was negligible.

2.6 Natural Ventilation

The air exchange rate inside a screenhouse is greatly influenced by the outside wind conditions. The screenhouse is said to be naturally ventilated. Rault (1990) demonstrates the importance of natural ventilation parameters to get good performance out of a greenhouse in the humid tropics. He pointed out three important parameters: i) the ratio of ventilation opening per unit area of soil surface; ii) the ratio of plastic cover per unit area of soil surface; iii) the ratio of ventilation opening to plastic cover surface area.

Aynsley et al. (1977) present various methods of wind and air movement measurements for the aerodynamic study of naturally ventilated buildings. ASHRAE (1981) presents a model of natural ventilation for buildings. Hellickson et al. (1983) focus on greenhouse natural ventilation. Choinière (1991) studied natural ventilation for low-rise building for livestock housing. All these authors used the following simple model to characterize wind induced natural ventilation.

$$Q = C_q \, v \, A_T \tag{1}$$

where, Q is the flow rate of the air passing through an opening of area A_T at velocity v and C_q is the restriction coefficient for the air flow. Hellickson et al. (1983) describe natural ventilation as being a combination of wind pressure differences and temperature differences effects. The temperature difference forces also called "stack effect" are described by the following equation.

$$\left(\frac{Q}{A_T}\right)^2 = \frac{\Theta^2\ 2gH(Ti-To)}{Ti} \qquad (2)$$

ASHRAE (1981) demonstrate that the relative flow due to temperature differences decreases with increasing wind pressure differences.

Hellickson et al. (1983) emphasize the importance of mapping local meteorological data to comprehend natural ventilation effects on buildings. Arbel et al. (1990) have studied natural ventilation on greenhouse in desert climates and concluded that the technique needed improvements but could be considered as an efficient and low cost method of ventilation in these climates. These studies on natural ventilation show the possibilities of quantifying the effects of natural winds for ventilation of buildings. No report of natural ventilation studies of buildings completely covered with fine mesh screen like the one used for screenhouse was found in the literature. The present study makes an attempt to describe the natural ventilation phenomena in screenhouses.

2.7 Greenhouse Climate Modelling

Researchers have used modelling as a tool to better understand greenhouse climatic characteristics. Lacroix (1988) explains that the productivity of research is enhanced by modelling since the number of experiments needed is reduced. Lacroix et al. (1988, 1990) make an extensive review of the existing heat and mass transfer greenhouses models. Two main groups of models have been identified, 1) the one-component (or lumped parameters) models which establish the heat and mass balance of the inside of the greenhouse and 2) the multi-component models which also consider the cover, the soil and the plants. In these two groups the models can be static or dynamic. Modelling for greenhouse climates concentrates on energy and mass balance models.

Walker et al. (1983) solved a steady state energy balance equation for a standard greenhouse with a single cover layer. The authors consider ventilation as part of their model. Figure 2.1 shows the terms that were used for their derivation. The energy balance equation is shown below:

$$q_I + q_e + q_f + q_r = +/-(q_{cd} + q_g) + q_v + q_i + q_t + q_p + q_C \qquad (3)$$

where, q_I is the solar heat gain; q_e is the equipment heat; q_f is the furnace heat; q_r is the heat of respiration from plant tissues; q_{cd} is the heat of convection-conduction; q_g is the convection heat transfer from the ground; q_v is the heat of ventilation ; q_i is the heat of infiltration; q_t is the heat of thermal radiation; q_p is the heat transfer of photosynthesis and q_C is the cooling heat.

Although not specifically stated by Walker et al. (1983), many assumptions were made to deduce the above heat transfer equations. For example, the authors considered that thermal energy is transferred directly from the air (T_i) to the outside (T_o), which means that the temperature of the surfaces, including the ground, are considered the same as the air temperature. All the incoming heat is considered to be transferred directly to the inside air of the greenhouse.

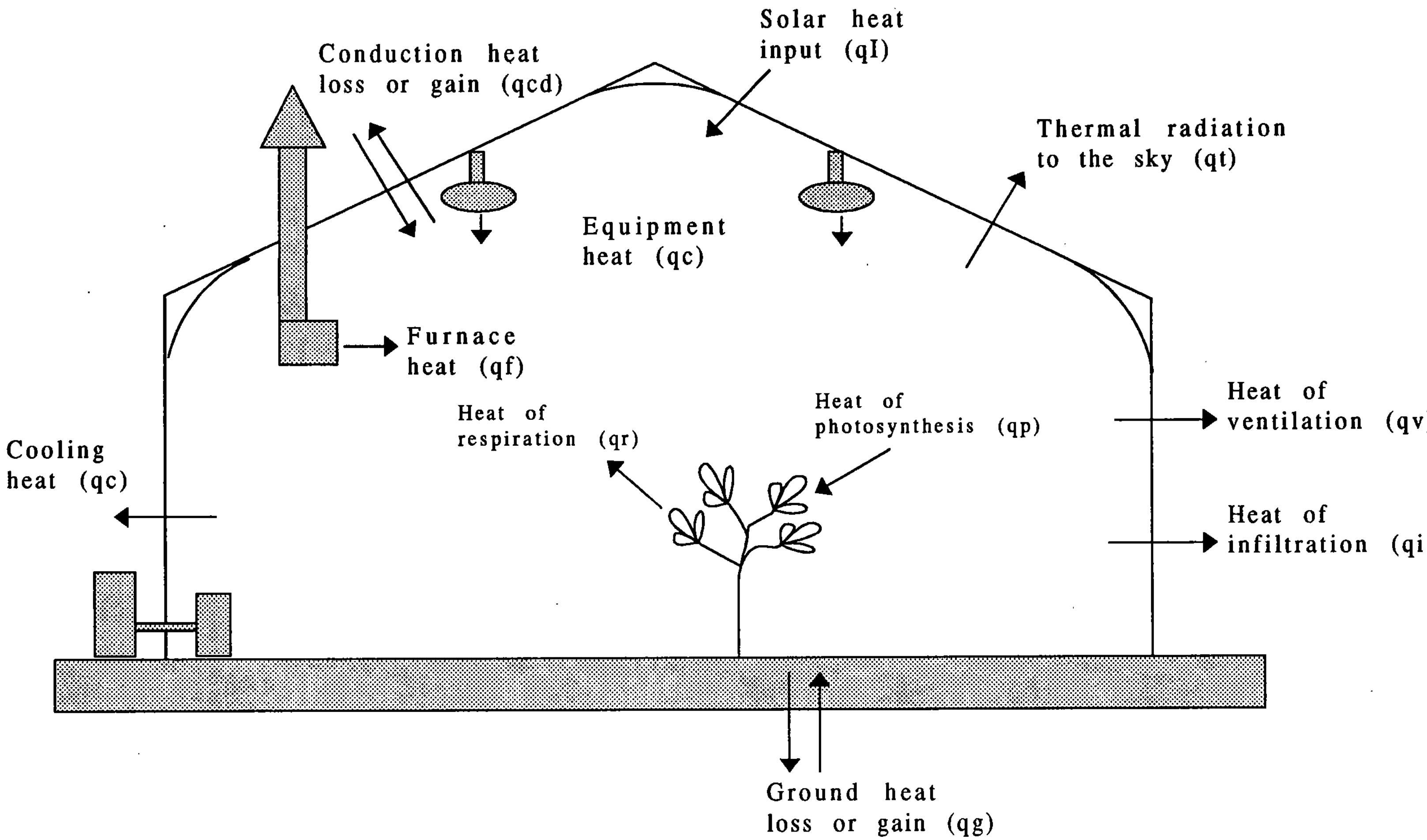

Figure 2.1: Energy losses and gains in a ventilated greenhouse

Walker et al. (1983) also defined equations for mass balance of a ventilated greenhouse. Two categories of equations describe summer humidity levels and winter humidity levels. The mass balance for summer conditions under steady state conditions is described by:

$$W_p = W_{ve} \tag{4}$$

where, W_p is the moisture added to the greenhouse environment by evapotranspiration and W_{ve} is the moisture exchange in the ventilation air. W_{ve} can be described by:

$$W_{ve} = N\ V\ \rho\ (W_i - W_o) \tag{5}$$

where, N is the air exchange rate, V is the volume of the greenhouse, ρ (rho) is the air density, W_i is the water content of the air inside the greenhouse and W_o is the outside air water content. Walker (1983) mentions that equations 4 and 5 can be used to predict the relative humidity levels inside the greenhouse.

Albright et al. (1985) developed a one-component heat transfer dynamic model of a greenhouse to perform an on site thermal calibration of an unventilated greenhouse. The model used was of the following form:

$$H + aSo - C(\frac{dTm}{dt}) - U(T_i - T_o) - R = 0 \tag{6}$$

where, the five terms represent:

i) H: the heat input from the heating system,

ii) aSo: the heat input by solar radiation (So),

iii) C(dTm/dt): the rate of heat storage in the system,

iv) U(Ti-To): the loss by conduction, convection and infiltration due the temperature difference, and

v) R: the long wave radiation through the cover.

The parameters that are evaluated are U, the overall heat transfer coefficient; a, the heating efficiency of the solar radiation; C, the heat capacity of the greenhouse. Latent heat transfer is not considered explicitly, but does affect the value of U.

Seginer et al. (1986) performed night time experiments to eliminate the solar radiation effects to determine transfer coefficients for heat and water vapour in small greenhouse.

The Gembloux Greenhouse Dynamic Model (GGDM) (Nijskens et al., 1991) examines the dynamic exchange of heat and water vapour between the various layers of a greenhouse which are assumed to be homogeneous and infinite in the horizontal plane. The GGDM model has the advantage of isolating many layers of the greenhouse which can be considered separately for the heat and mass balances. But the disadvantage of such a model is its inherent complexity especially at times of solving many simultaneous differential equations for the different heat balance layers of the system. The model also includes two layers of cover as part of its components. The authors mention that the GGDM2 model analyses a single-glazing screen fitted greenhouse but give no description of such a system. Nijskens et al. (1991)

show the usefulness of a sensitivity study of a dynamic model in determining the most influential parameters and/or boundary conditions of the system.

No report of extensive study of screenhouse heat and mass transfer characteristics was found in the literature. Excessive temperature levels of inside screenhouse climates is problematic for research and production in the tropical countries (Desmarais, 1992). In order to properly assess the potential of implementing screenhouse technologies in the tropical climates, it is necessary to know the intrinsic characteristics of screenhouse design, principally in terms of their thermal performance. This research wants to look at the global effect of different structural shapes of screenhouses, the effect of different screens and the effect of a water curtain on the inside climate of the screenhouse to establish engineering foundations for present and future designs.

III. BACKGROUND AND HYPOTHESES

In the context of an engineering consulting contract with the International Institute of Tropical Agriculture in Ibadan, Nigeria, Desmarais (1992) performed some observations and trials related to the thermal performance of screenhouses and greenhouses in the warm and humid climate of that tropical region.

3.1 Observations and Trials

A primary and fundamental observation was the fact that in comparable outside weather conditions, the inside climate of a screenhouse is different from the inside climate of a greenhouse.

A second observation was that the modifications of the physical configurations of the screenhouse had definite effects on the inside climate. The main effects were observed with the change of three specific parameters of the physical configurations of the screenhouse (Figures 3.1, 3.2, 3.3 and 3.4). The first one was the structural or architectural shape of the screenhouse. For example the inside climate is different in a Quonset shape screenhouse (Figure 3.1) than in a Tunnel shape screenhouse (Figure 3.4). The double roof (Figure 3.3) or rain cover plays a role in warming up the inside climate of the screenhouse. The second main parameter was the hole size of the screen used as cover for the screenhouse. A screenhouse covered with a screen with very small holes seems to have more overheating problems than a screenhouse covered with a screen with larger hole size. The third main characteristic

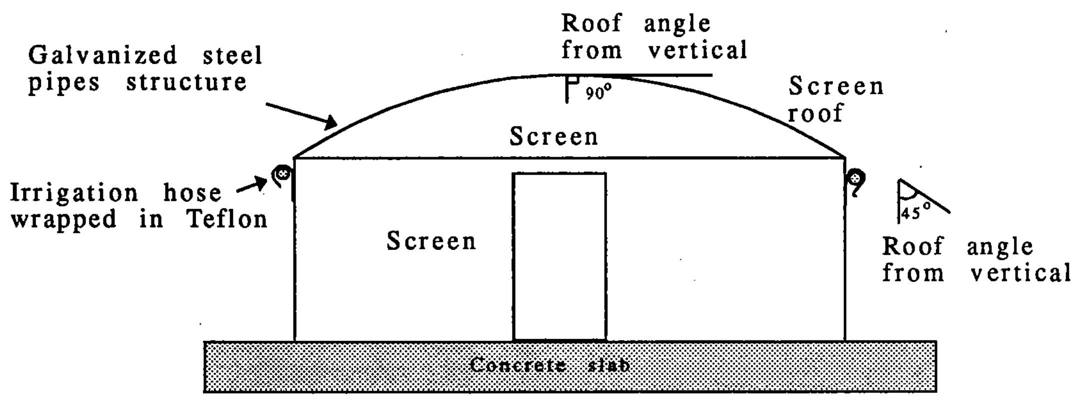

Figure 3.1: Screenhouse #1: Rossel Modified (front view)

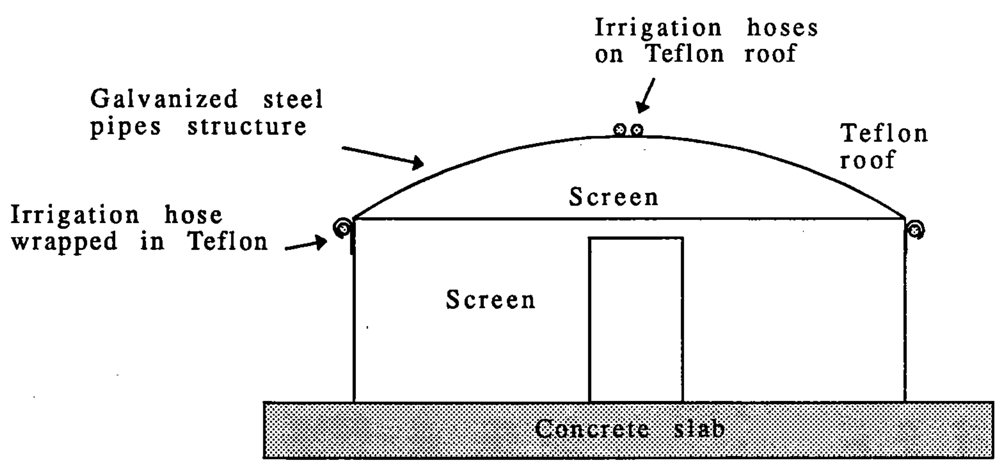

Figure 3.2: Screenhouse #2: Rossel Modified (front view)

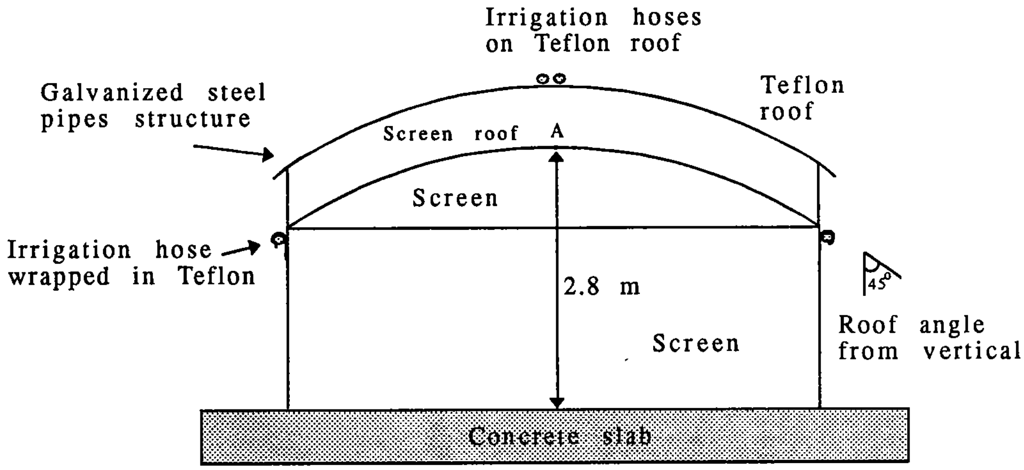

Figure 3.3: Screenhouse #3: Rossel type (front view)

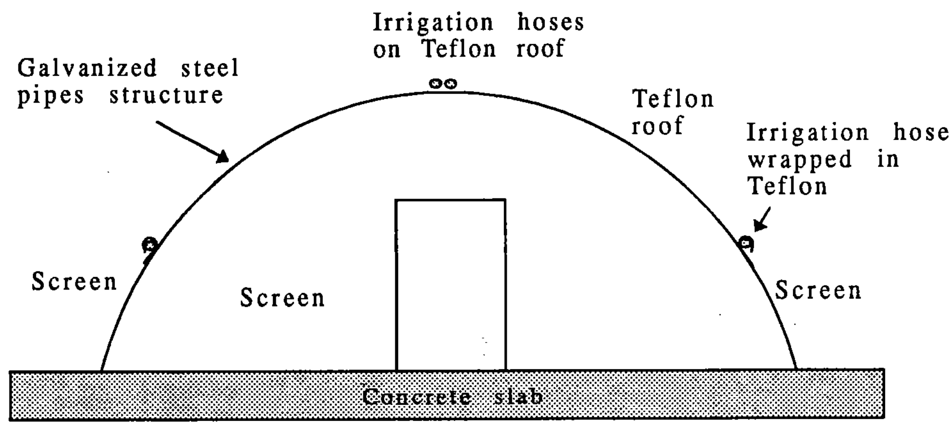

Figure 3.4: Screenhouse #4:Tunnel type (front view)

was the colour of the screen cover. The light levels are much higher in a screenhouse with a white screen than in a screenhouse covered with an amber screen. These three parameters were retained as the three principal characteristics that are used as testing variables for the study.

Researchers at the International Institute of Tropical Agriculture, Ibadan and Cotonou centres observed and reported that, in many cases, the inside climates in screenhouses were not always as would be desired for many of their experiments (Desmarais, 1992). Temperatures over 40 °C inside the screenhouse were reported when outside ambient temperatures were at 32 °C and global radiation was at 600 W/m^2. The new models of screenhouses used in Ibadan and elsewhere in Africa do not use the high capacity fans (forced ventilation system) since they have been proven to be inefficient considering that the openings in the screens do not allow the establishment of the static pressure essential for air movement to take place.

Trials were conducted on a small tunnel greenhouse to investigate the effect on the inside greenhouse climate of a water film flowing on the cover of the greenhouse. A reduction of the inside greenhouse temperature of as much as 7 °C was observed when the outside relative humidity was at 70 %. This result shows a potential for the application of the "fluid roof" or "water spraying on the roof" techniques for greenhouses in humid tropics.

3.2 Questions and Basis for Formulation of Hypotheses

The questions arising from these observations and trials were the following :

i) What causes the differences observed between climates inside screenhouses and greenhouses? Is it temperature, relative humidity, radiation or wind?

The fundamental difference is that a screen with holes is used as a cover for the screenhouse instead of the usual unperforated plastic film or glass for greenhouse. This aspect is fundamental to the extent that the screenhouse climate has an entirely different reaction to the outside climate stimuli. To date, no study has been performed to determine how the screenhouse inside climate reacts to external conditions.

ii) What exact reactions of the screenhouse inside climate are caused by the modification of the screenhouse physical configurations: a) shape, b) screen cover hole size which is related to the mesh size, c) the colour of the screen, d) the material used to make the screen, e) the shape of the screen holes and f) others?

iii) The screen used for screenhouse construction are chosen for their capacity of preventing insect pests to enter or exit the screenhouse. The smaller the hole size, the better the protection. But, small hole size will decrease natural ventilation efficiency. Therefore what is the optimal choices or limits of choices for the screen hole sizes to obtain desirable inside screenhouse climatic conditions?

iv) The seven degree celsius temperature reduction obtained with water spraying on the small tunnel greenhouse, as described in 3.1 above, leads to the hypothesis that water spraying on the screen caused evaporative cooling and/or absorption of radiative energy and that neither effect is negligible even in a humid tropical climate. Will water have the same effects on screenhouses?

3.3 Hypotheses

The line of questions developed in 3.2 were the basis for the hypotheses formulated for this research. These hypotheses are:

1) It is possible to minimize the difference in temperature between the screenhouse interior and ambient temperature by optimizing the screenhouse's thermal characteristics.

2) The screenhouse thermal characteristics are affected by the physical configurations of the screenhouse namely i) the structural or architectural shape, ii) the size of the hole of the screen used as a cover and iii) the colour of the screen cover.

3) Screenhouse with water cooling allows for the combination of three natural cooling methods: i) natural ventilation, ii) evaporative cooling and iii) radiation absorption.

4) Water cooling is an energy efficient method to cool screenhouses in humid tropical climates.

IV. OBJECTIVES

The specific objectives of the proposed investigation were:

A) To measure the effects of i) the structural or architectural shape of the screenhouse, ii) the screen hole size used as cover for the screenhouse, iii) the colours of screens and iv) water irrigation on the inside air temperatures of the screenhouses for three different seasons of the Forest-Savanna transitional zone climate of the Cotonou region.

B) To derive the mathematical models that describe the heat transfer of the various configurations of the screenhouses tested. The data obtained in A) are used to validate the heat transfer models and/or obtain information to improve the models.

C) To determine the effects of the parameters measured in the objective A) on three screenhouse heat transfer characteristics: i) τ, the overall transmissivity of the screenhouse, ii) Nv, the natural ventilation coefficient and iii) U, the global heat transfer coefficient.

D) To use computer simulations, based on the derived heat transfer models, as a tool, to calibrate the heat transfer models, to optimize the screenhouse heat transfer characteristics and to predict screenhouse inside temperatures in various tropical climates.

of GNP while imports were at 21,9 %. The external debt of the country in 1991 was at 1.4 billion US dollars (Larousse, 1993).

5.1.2 Climatic characteristics of the Cotonou region

The Cotonou region lies in the southern part of the Republic of Benin, by the coast. It has a sub-equatorial climate characterized by four more or less clearly marked seasons in the year. These are:

- a long dry season from mid-November to mid-March;
- a long rainy season from mid-March to mid-July;
- a short dry season from mid-July to mid-September;
- a short rainy season from mid-September to mid-November.

There are two peaks in the rains, in June and October, separated by a fall-off in August (when there is an average of 50 mm rainfall). The June peak is the highest (Cotonou town: an average of 366.5 mm in June compared to 137.4 mm in October). Total annual rainfall is around 1300 mm over a period of 90 to 110 days.

Because of the effect of the sea, air temperatures do not vary greatly. Daily differences are between 3 and 8 °C in the rainy season, and around 10 °C in the dry season. Annual variations are between 2 and 6 °C. The highest temperatures (between 32 and 37 °C) occur in March/April, and the lowest in December/January (between 17 and 24 °C). The average temperature for the whole year is around 27 °C. The proximity of the sea also raises the atmospheric humidity, which remains fairly constant throughout the year (minimum atmospheric humidity of 65%, maximum of 95%).

The dominant wind at ground level is from the South-West, with an average speed of 5 m/s (18 km/h), but there are seasonal fluctuations. The long dry season brings the Harmattan (Besancenot, 1992), which is a dry wind from the North-East (2 to 3 m/s). During the rainy seasons, there is often rainstorm disturbance of the squall line type, with winds from the east and speeds of sometimes more than 20 m/s (72 km/h). Daily sunshine ranges from 7 to 8 hours during November and April to 5 hours during June and September, with a minimum (approximately 4 hours) in July. The potential evapotranspiration (PET) varies between 3 and 5 mm per day. Table 5.1 summarises the normal types of weather of the Cotonou region.

Table 5.1 - Normal types of weather during the four seasons of the Cotonou region

1. The long dry season
    - fairly clear sky with low and higher clouds;
    - occasional rains generally in the form of rainstorms;
    - morning fog especially in December, January and February;
    - sometimes the Harmattan blows as far as the coast, accompanied or not by a dry mist or a dust;
    - the climate is generally hot and dry;

2. Normal weather during the long rainy season: sky generally very cloudy.
    - March-May: daytime storms often accompanied by rain;
    - increasing frequency of rainstorms as the period progresses, together with disturbances (squall line type);
    - June-July: monsoon (continuous) rains, sometimes stormy, often occurring at night between 22.00 hrs and 6.00 hrs, followed by some migratory squall lines;
    - Maximum rainfall in June
    - The climate is hot and humid;

Table 5.1 - Normal types of weather during the four seasons of the Cotonou region (cont'd)

---

3. Normal weather during the short dry season
   - generally cloudy sky with mainly low stratiform clouds;
   - slight rainfall, often in the form of fine rain or mist;
   - the climate is relatively humid and cold;

4. Normal weather during the short rainy season
   - similar characteristics to those of the long rainy season, except less abundant rain over a shorter period;
   - from the end of September to mid-November, daytime storms with moderate rains and sometimes squall line disturbances;
   - peak rainfall in October (generally less than in June);
   - climate relatively hot and humid.

5.2 Screenhouse Structures

Four small scale experimental screenhouses were constructed on site at IITA-Benin station. Each of the four screenhouses had a different structural configuration (Figures 3.1, 3.2, 3.3, 3.4).

Two of the four structural configurations chosen were originally designed by researchers at IITA and are used for various agricultural research projects in many tropical countries of Africa, Indonesia and South America. They are the Rossel type screenhouse (screenhouse #3 in the experiments) and the Tunnel type screenhouse (screenhouse #4 in the experiments). Pictures 5.1 and 5.2 show the model screenhouses tested in this research.

The Rossel type screenhouse (Figure 3.3: screenhouse #3 in the experiment) was equipped with the structural components necessary for the installation of a double roof mainly used as a rain cover. The rain cover was

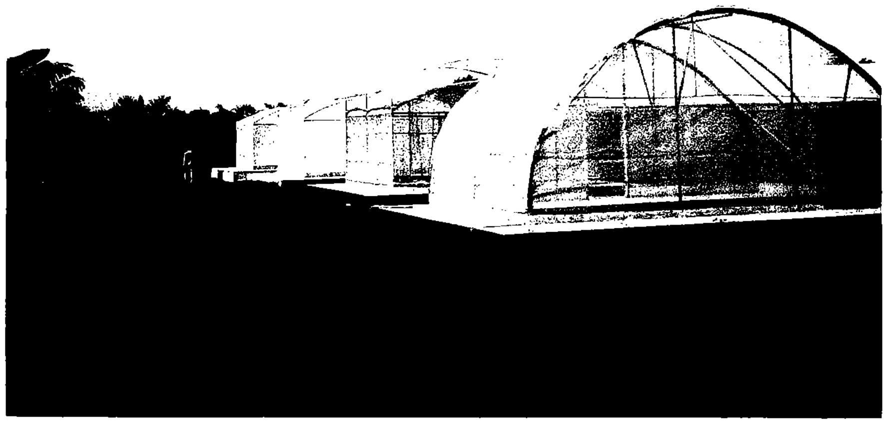

Picture 5.1: The 4 experimental screenhouses: From South to North: #4 (Tunnel), #3 (Rossel), #2, #1.

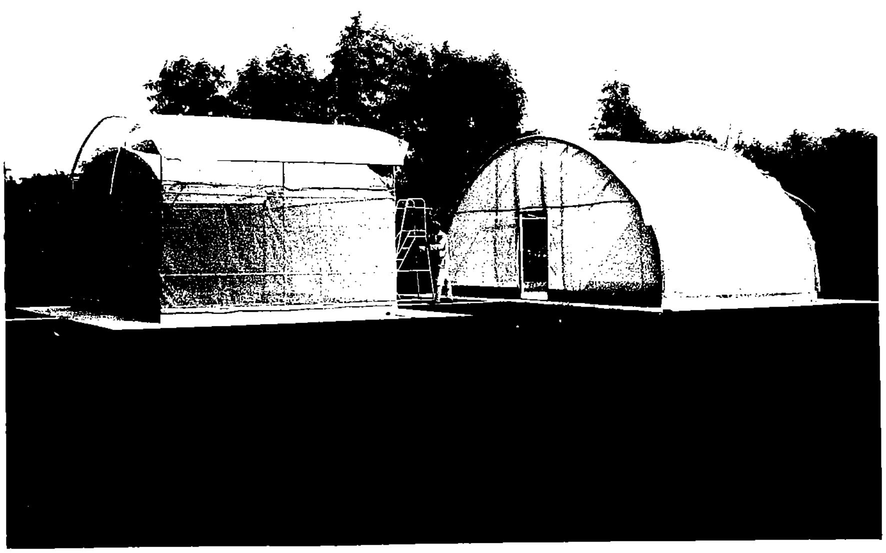

Picture 5.2: Experimental Screenhouses; from left to right: #3 (Rossel) and #4 (Tunnel)

made of a plastic film (Polyethylene or Teflon). For the experiments, a Teflon roofing sheet was installed on the double roof layer of the Rossel type screenhouse. This Teflon roofing sheet remained on the double roof layer of the Rossel type screenhouse during all the experiments because it determined the specificity of the Rossel type screenhouse structural configuration. The lower level (first layer roof, the 2 walls, the door and end extremities) of the Rossel type screenhouse were completely screened. The double roof layer was shaped as a half cylinder and was 0.6 m above the first layer roof. The walls of the screenhouse were 2 m high and the highest point of the first layer roof was at 2.8 m (Point A on Figure 3.3). The screenhouse was 6 m wide. Rossel type screenhouses come in sections of 2 m length and are usually used in length of 20 or 32 m. For the experiment a Rossel type screenhouse of 4 m length was built. The screenhouse was equipped with a 1 m wide by 2 m high door. The door was also made of screen and could be opened and closed with a zip lock system. The left side of the door was 3 m from the East side of the screenhouse and the right side of the door is 2 m from the West side of the screenhouse.

The Tunnel type screenhouse (Figure 3.4: screenhouse #4 in the experiment) was shaped as a tunnel. The highest point of its semi-cylindrical shape was 3.0 m high. The screenhouse was 8 m wide and also came in sections of 2 m length. The usual length of the Tunnel type screenhouse was either 20 or 32 m. For the experiments a length of 4 m was chosen. The Tunnel type screenhouse can be either completely screened or covered by a plastic film

(Polyethylene or Teflon) rain cover. For the experiment, the rain cover version was chosen because of its similarity with the Rossel type screenhouse for rain protection. The rain covered version of the Tunnel type screenhouse was also expected to show more critical high temperatures because of the greenhouse effect of the rain cover. The rain cover extended on the middle of the semi-cylindrical surface of the screenhouse roof leaving an opening of 1.85 m high on both sides of the screenhouse and all along its length. These openings are covered with screen. The Tunnel type screenhouse was also equipped with a 1 m wide by 2 m high screened zip lock door. The door and the end extremities of the Tunnel type screenhouse were completely screened. The door was centred on the northern face of the screenhouse leaving 3.5 m on each side.

The two other screenhouses used in the experiment are modifications of the Rossel type screenhouse. For the two remaining screenhouses the double roof rain cover had been taken off.

The first of the two remaining screenhouses (Figure 3.1: screenhouse #1 in the experiment) was completely screened. The roof, the walls, the door and end extremities were covered with screen. This screenhouse configuration was chosen to look at the effect of the double roof on inside screenhouse climate for days without rain. The dimensions of screenhouse #1 were the same as those of the experimental Rossel type screenhouse. Only the double roof was absent on this screenhouse. Screenhouse #1 was also equipped with a 1 m wide by 2 m high screened zip lock door.

The last screenhouse (Figure 3.2: screenhouse #2 in the experiments) was also a modification of the Rossel type screenhouse in that the double roof was also taken off. The particularity of screenhouse #2 was that its remaining roof was covered with a layer of Teflon sheet. The rest of the screenhouse (walls and end extremities) was covered with screen. The dimensions of the door, the walls, the end extremities and the roof of screenhouse #2 were the same as the one of screenhouse #1.

The length of the experimental screenhouses was chosen to be 4 m for practicality of experimentation and also to reduce the cost of the experiments. The temperature differences measured between the inside and the outside of the experimental (4 m long) screenhouses were found to be in the same ranges as in the full scale screenhouses.

The structural components of the four experimental screenhouses were prefabricated galvanized steel pipes and clamps that were made of necessary length and shape for the various types of screenhouses. For the Rossel type screenhouse, the pipe outside diameter was 3.2 cm and the inside diameter was 2.5 cm. For the Tunnel type, the pipe outside diameter was 6 cm with an inside diameter of 5.6 cm. Some structural reinforcing pipes for the Tunnel type screenhouse were 4.6 cm OD and 4.2 ID. The screens and plastic sheets were attached to the screenhouse with the help of extruded aluminum profiles and plastic infills.

All four screenhouses were built on a concrete slab (Figure 5.1). Concrete was chosen as the floor construction material for the experiments because it is the material used in standard constructions of screenhouses. Also, the concrete slab were built for the purpose of uniformity in the characterization of the floor properties. Screenhouses #1, #2 and #3 were centred on a 8 m wide by 6 m long slabs. Screenhouse #4 was also centred on a 10 m wide by 6 m long concrete slab. The thickness of the slabs were built so as to level the top floor of the 4 screenhouses. For purpose of levelling, the concrete slabs were constructed with varying thickness. Small sections of concrete slabs of 0.5 m wide and 3 m long were also built as sidewalk to connect the four screenhouse slabs for ease of movements between the screenhouses.

The four screenhouses structures were built in line centred on their slabs so that the actual structures are separated from one another by 5 meters. The line pattern was chosen for purpose of uniformity in the parameters affecting their thermal performances.

The four screenhouses were built next to an existing laboratory. The lab is 7.5 m away from the North-East corner of screenhouse #1 (Figure 5.1).

5.3 Orientation of the Screenhouses

The orientation of the longitudinal line of the four screenhouses was chosen to be North-South. All the screenhouse doors were in line facing North and all the screenhouse ends were in line facing South. Screenhouse # 1 door

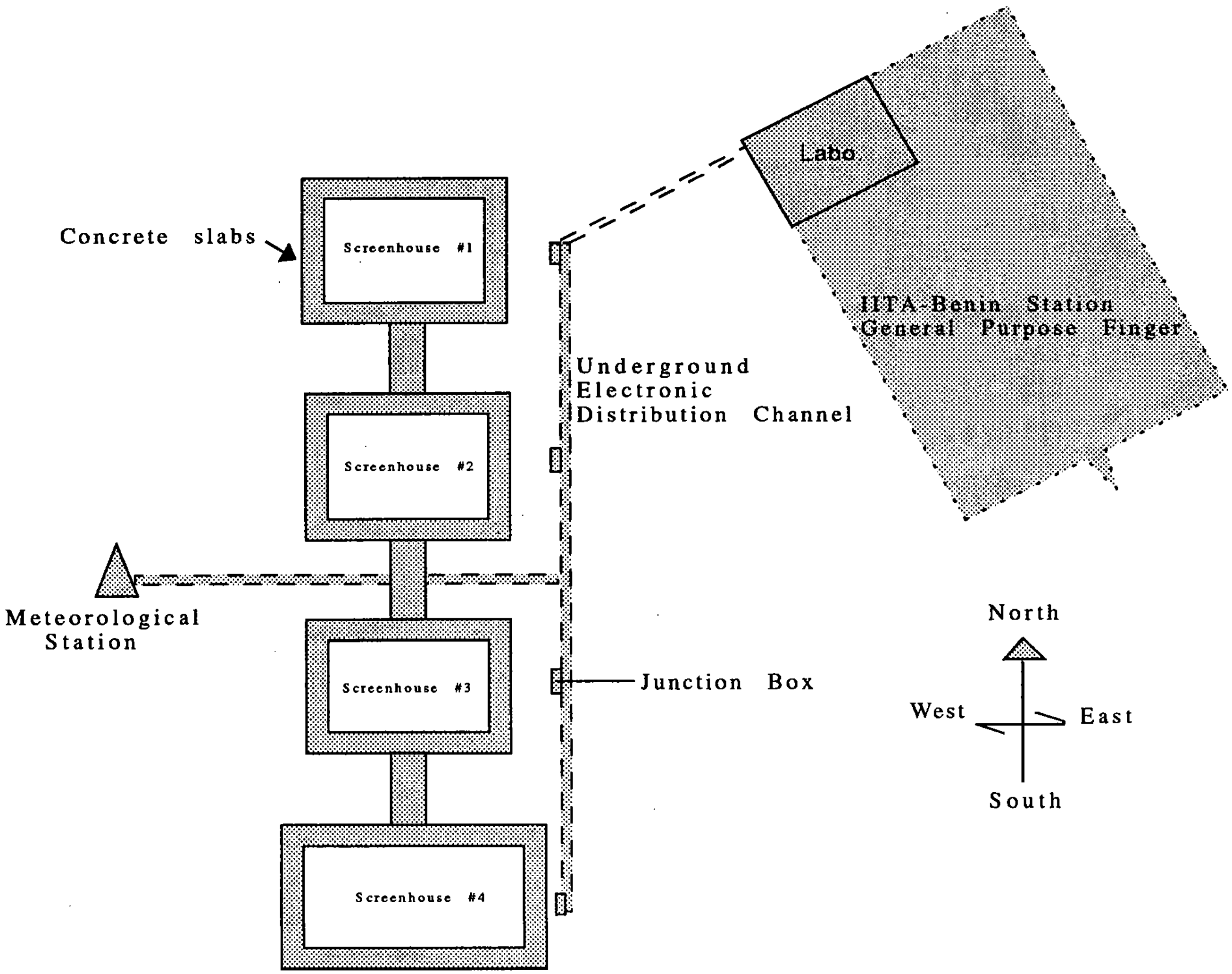

Figure 5.1: Experimental screenhouse layout

extremity was closest to North and screenhouse #4 end extremity was closest to South.

The North-South outlay was chosen in relation to the orientation of the sun for the four screenhouses. The objective was to avoid as much inter-shading as possible of the four screenhouses on each other. Larousse (1992) mentions that the year division in seasons result from the angle of 23° 26' of the rotation axis of the earth in relation to its translation plane around the sun. At the spring and fall equinoxes, the sun is exactly in the plane of the equator. For the northern hemisphere, at the summer solstice, the sun is exactly in the plane of the tropic of Cancer which corresponds to a sun angle of 23° 26' north of the equator. Since the experimental set up was located in Cotonou (Latitude: 6° 25' North) the sun angles seen on the experimental site was 6° 25'south at the spring and fall equinoxes, and 17° 1' north at the summer solstice and 20° 51' south at the winter solstice. The exact North-South orientation of the longitudinal line of the screenhouses was chosen because of the very small differences of the sun angle compared to if it was located exactly on the equator.

The orientation of the longitudinal line of the screenhouse was also chosen in relation to the main wind direction. Ideally the longitudinal line of the screenhouses would be oriented perpendicular to the main wind direction. As described in section 5.1.2, main wind direction for the Cotonou region is South-West. As far as wind direction is concerned, the orientation of the longitudinal line of the screenhouse would have to be on the North-West - South East axis. A compromise had to be made between the main wind direction, sun orientation and physical characteristics of the close environment of the screenhouses to give the final orientation of the screenhouses. Priority was given to the North-South orientation.

5.4 Watering Systems

Before the installation of the watering systems on the experimental screenhouses it was necessary to proceed to a series of hydrodynamic tests to describe the best possible hose-water-screen configuration (angle and flow). The purpose of the tests was to obtain the most uniform flow of the water curtain on the whole surface of the screens.

5.4.1 Hydrodynamic tests

A set of water-screen hydrodynamic bench tests were performed in the laboratory at Macdonald Campus of McGill University prior to the start of the construction of the experimental screenhouses on the study site at IITA-Benin station.

The bench test was composed of a black nylon screen being attached to a PVC pipe structure as shown on Figure 5.2. The angle of the screen from vertical could be set by varying the angle of the PVC structure. A water irrigation hose was attached to the top arm of the PVC structure to irrigate the screen. The tests consisted in varying the angle of the screens and the water flow so as to observe the behaviour of the water curtain on the screen.

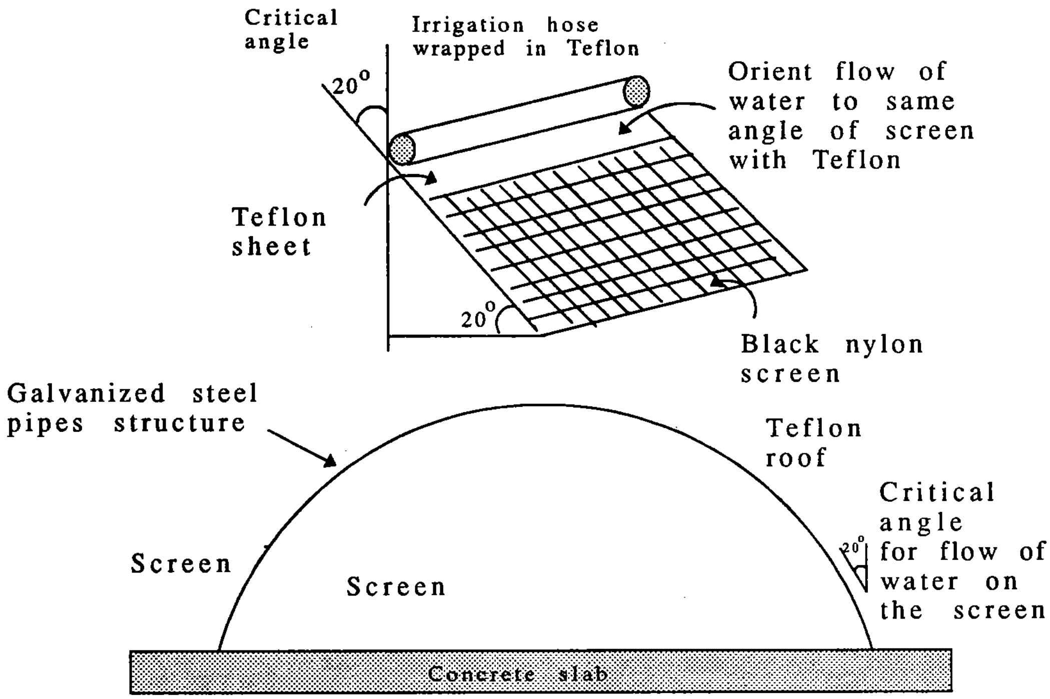

Figure 5.2: Hydrodynamic tests: Critical angle for water flow on screen

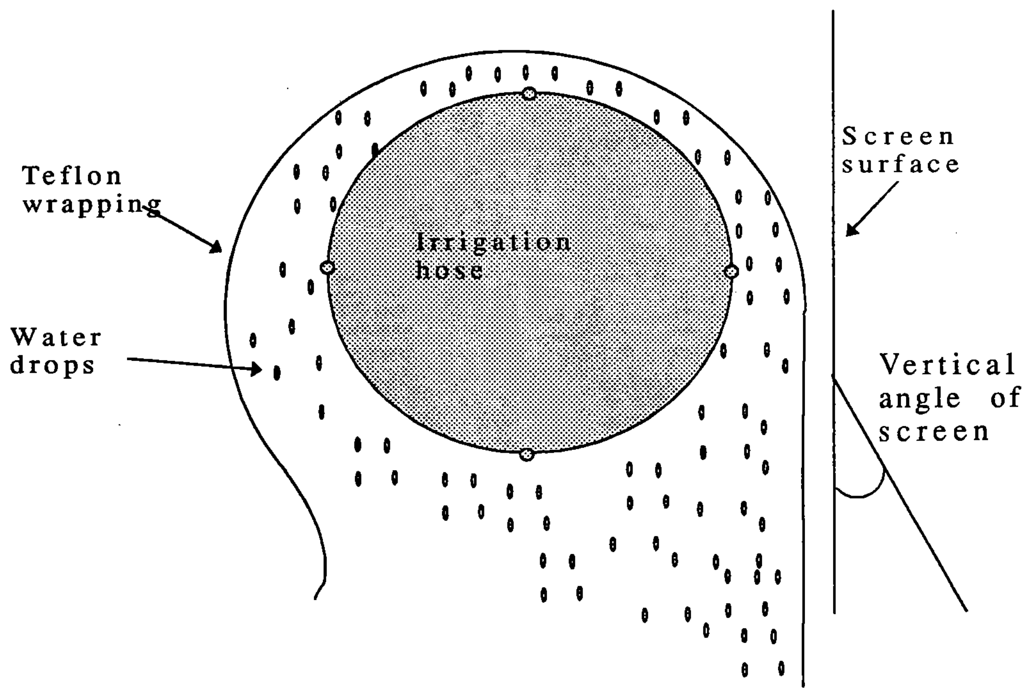

Figure 5.3: Irrigation hose wrapped in Teflon close to screen

From these tests, it was found that the angle of the screen has an impact on the flow of water on the screen. Screen angles as low as 5° from the vertical would allow the water to fall across the screen. More importantly, it was found that the orientation of the flow of water before and when it reaches the screen has the most critical impact on the distribution of water on the screen. To create the best possible uniform water curtain on the screen, it was found that there was a need to orient the flow of water as close as possible to the vertical angle of the screen before the water touches the screen. For that purpose, the hoses were wrapped in polyethylene sheets so as to let the water flow in the same vertical angle of the screen (Figure 5.3). With that configuration it was possible to have vertical screen angles of 20° (Figure 5.2) without having much water flowing across the screen. It was also found that all the screens used in the experiments would retain some water in the inside interstice of the screen mesh. This phenomenon helped creating a more uniform water curtain on the screen. The water inside the interstice attracted some other water by surface tension and helps create a whole surface of filled water interstices.

The configuration results of the hydrodynamic bench tests were implemented on the experimental screenhouses. The hose-plastic wrapping configuration that was sketched in the bench tests proved to be very satisfactory for the purpose of the experiments. A fairly uniform water curtain could be observed on the screenhouses. Water pressure had to be maintained to a minimum of 2 bar in the water circuit to obtain a satisfactory water distribution on the screens.

A set of hydrodynamic tests performed on the experimental screenhouses demonstrated that it was possible to obtain a uniform flow of water over the teflon roof, the vertical screen walls and over a screen cover when a maximum screen angle of 20° from vertical was respected (Figure 5.2). These results were helpful in designing the irrigation system on the small scale screenhouse models that were used in the experiments. The goal was to obtain a uniform thin water layer (not more then 5 mm) over as many of the screenhouse roofs or walls. The first layer roof of screenhouse #1 and #3 were the only two surfaces that were not covered with water mainly because they were completely screened and because the screen angle from the vertical was always much more than 20°. The roof screen angles for these screenhouses were in the order of 45 to 90° from the vertical (Figures 3.1 and 3.3). On all other walls and roof surfaces of the 4 small scale screenhouse models, it was possible to obtain a quite uniform thin water flow layer. The hydrophillic properties of the screen interstices helped obtaining the uniform flow of water over the screens. Water was retained by capillarity or surface tension in the interstices of all the screens tested. This created a thin film of water in the screen holes and helped the formation of a uniform flow of water over the whole screen surface. The screen water surface tension forces were enough to retain the weight of the water curtain up to a certain depth of water and up to a certain screen angle from vertical.

5.4.2 Watering systems installation

Watering systems were installed on the four screenhouses. The watering system consisted of irrigation hoses attached to the structural elements of the screenhouses so as to create a water curtain on the roof, the walls and the end extremities of the screenhouses. Since data had to be taken manually inside the screenhouses during all the experiments, the door extremities of the four screenhouses were left without a water curtain because of practicality of experimentation. Even in a real case situation, a water curtain on the door extremity of the screenhouse would prove to be impractical.

The Supersoaker hose and Teflon sheet wrapping configuration were attached to the two walls and end extremities at the top edge for screenhouses #1, #2 and #3 (Figures 3.1, 3.2, 3.3). As mentioned above, the door extremities did not have a water curtain. Irrigation was installed on the first layer Teflon roof for screenhouse #2 and on the second layer Teflon roof for screenhouse #3. Irrigation was also installed on the sides and on the roof of screenhouse #4.

Screenhouse #1 did not have a water curtain on the roof (Figure 3.1). It was not possible to obtain a hose-water-screen configuration that would not let the water flow across the roof screen. As shown on Figure 3.1, the screen roof angle from vertical was always larger than 45°. It was decided that this screenhouse would be studied without a water curtain on the roof.

The water curtain on the roof of screenhouse #2 was made by simply laying two lines of the soaker hose at the top edge of the Teflon roof in the longitudinal line of the screenhouse (Figure 3.2). No Teflon sheet wrapping was utilized. The jet sprayed by the Supersoaker hoses created a quite uniform water curtain on all the surface of the Teflon roof. The water flowed downward by gravity and most of this water was recuperated by the screen walls on both side of the screenhouse.

Screenhouse #3 was equipped with a water curtain on the double roof of the screenhouse (Figure 3.3). No water curtain was made on the first layer roof of the screenhouse for the same reasons as for screenhouse #1: the roof was screened. The hose-water configuration on the double roof of screenhouse #3 was installed the same way as for screenhouse #2. A satisfactory uniform water curtain was obtained on the double roof.

The hose-water-screen configuration on screenhouse #4 was installed keeping in mind the same above mentioned principles (Figure 3.4). Two lines of soaker hoses were installed at the top edge of the screenhouse in the longitudinal axis without the Teflon sheet wrapping. This created a quite uniform water curtain on the Teflon roof. The water flowed down by gravity and followed the angle of the Teflon all along its vertical length. When it reached the screen section the water already followed naturally the angle of the screen and Teflon intersection. This way, the water followed the screen in its vertical angle with very little of the water going across the screen. The vertical angle at the Teflon-screen intersection was found to be 60° from horizontal. A line of soaker hose and Teflon sheet wrapping was also installed at the Teflon-screen intersection on both walls of the screenhouse because of the insufficient amount of water furnished by the roof lines to have a satisfactory uniform water curtain on the screen walls. The same line was used in continuity for the end extremity of the Tunnel screenhouse (Figure 3.4).

5.5 Screens

Four different types of screens were chosen. Originally, the intent was to test two different colours of screens (white and amber) and two different mesh sizes (32 and 50). These two colours and two mesh sizes of screens were chosen because they are the ones most used on existing screenhouse structures in research centres in Africa. The four types of screens were: Screen #0 (S0): Tildenet 50 (white), Screen #1 (S1): Lumite 50 (amber), Screen #2 (S2): Lumite 32 (amber), Screen #3 (S3): Tildenet 32 (white). All the screens are made of high density polyethylene fibres. Table 5.2 summarises the principle physical characteristics of the four types of screens used in the experiment. Samples of these four screen types are presented in Appendix A.

During the experiment, all of the four screens were rotated from one screenhouse structure to the other. Four screens on four structures were tested at one time.

Table 5.2 - Screen physical characteristics

	Screen Types (by Brand name)			
	Tildenet	Lumite 25	Lumite 25	Tildenet
Screen # in experiment	S0	S1	S2	S3
Company Number	IN 50	50062	50060	IN 32
Material	HDPE	HDPE	HDPE	HDPE
Mesh construction	50x50	52x52	32x32	32x32
Mesh count per cm	18.9	20.8	12.54	from 10 to 10.8
Mesh count per inch	48.0	52.9	31.7	25.4 to 27.4
Thread diameter (µm)	200	225	250	225
Mesh opening (µm)	350	300 to 325	575	700 to 775
Free open area (%)	40.5	32.7 to 34.9	48.5	57.2 to 60.1
Thickness (mm)	0.16	0.25	0.25	0.16

5.6 Instrumentation

The instrumentation was planned for as many measurements as possible of climatic data inside and outside of the four screenhouses.

5.6.1 Inside the screenhouse

Temperatures were measured in three different locations in each screenhouse (Figure 5.4) and at similar location from one screenhouse to the other. The locations of the temperature measurements in the screenhouse were chosen to obtain an average of the air temperature conditions in the screenhouse. The measurement of temperatures were made with Cole-Palmer Type T (copper-constantin) thermocouples. The thermocouples were centred and hung 2.5 cm down underneath a 45 cm long by 30 cm wide by 1.5 cm thick wooden plate to hide the thermocouple measuring tip from direct sunlight radiation.

Two relative humidity measurements were taken in each screenhouse during all the experiments. The location is shown on Figure 5.4 and was chosen as such for the same reasons as for the temperature measurement location. The relative humidity sensor were Vaisala RH transmitter (G-37303, +/-5% accuracy in the 10 to 90%). The relative humidity sensors were placed underneath the same wooden plate as the thermocouple.

Two measurements of the Quantum PAR (Photosynthetic Active Radiation: 400-700 nm) solar radiation and two measurements of the Global (sun + sky (400-1100 nm)) solar radiation were made at one time during the

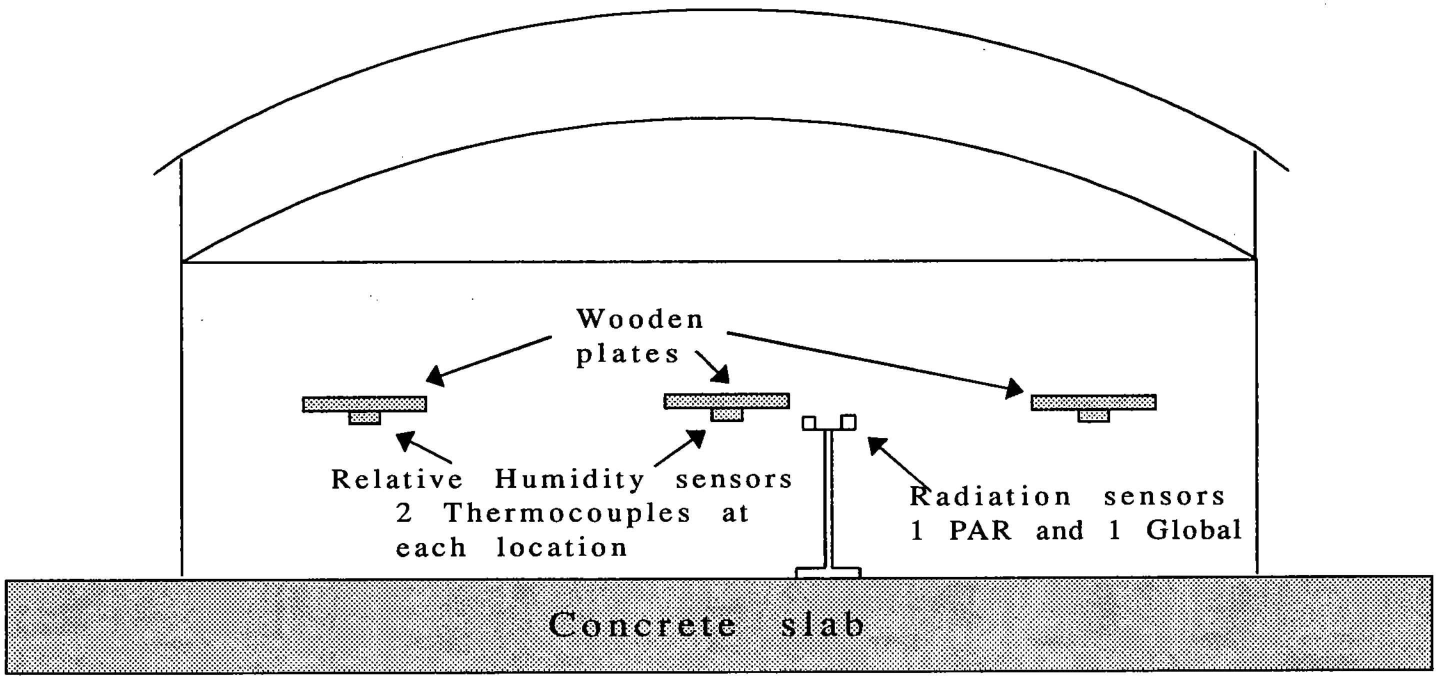

Figure 5.4: Location of sensors

experiment. The PAR and the Global solar radiation were defined by Thimidjan et al. (1983). The measurements were done in pairs (PAR-Quantum). Only two screenhouses could be monitored at one time. The pairs of sensors had to be changed each day from one house to the other according to a procedure allowing for the maximum possibilities of alternative measurements. The sensors were located very close to the centre of the screenhouse (Figure 5.4). The Quantum PAR sensors were Li-Cor sensor (LI-190) and the Global radiation sensors were Li-Cor Pyranometer sensor (LI-200).

Wind speed inside the screenhouse was measured with a Pacer DTA4000 Anemometer-Thermometer/Data logger. The Data logger was connected to a 7 cm diameter vane anemometer that is sensitive down to 0.2 m/s. The portable data logger had various averaging, storing and communication features.

5.6.2 Outside the screenhouse

A local meteorological station was installed close to the experimental screenhouse site (Figure 5.1) to measure as many of the external weather conditions as possible. A MET-ONE (model 010B) wind speed sensor (sensitivity: 0.27 m/s, range: 0 to 50 m/s +/- 1% accuracy) and a MET-ONE wind direction sensor were installed on a mast 3.2 high to have local wind measurements. On that same mast at 2.6 m height, a Li-Cor 190 PAR and a Li-Cor 200 Global radiation sensors were installed to measure outside solar close to the ground and the concrete slabs to connect the outside distribution boxes to the inside screenhouse. The 4 cm PVC tube crossed the wall of the screenhouse through the lower concrete brick wall of the screenhouse and was raised to a height of 1 m to outlet inside the screenhouse.

The cables then ran inside the screenhouse, attached to the structure of the screenhouses and were connected to the instruments at their location as described above.

5.8 Data Acquisition System

5.8.1 Hardware

A Doric data acquisition system was connected to the sensors via cables. The Doric Model 245 data logger is a microprocessor based modular data acquisition system that can measure and record as many as 500 analog inputs. These inputs may be from various sources such as thermocouples, voltage outputs, current outputs and RTD's. There are three basic components in the Model 245 data logger system, the mainframe unit, the front end modules (FEM) and the satellite unit.

The system is equipped with a day calendar/24-hour clock and two serial communication ports (RS-232C).

The configuration chosen for the experiments was the mainframe unit with two front end modules (FEMs) giving access to a total of 40 analog inputs. No satellite unit was used in the experiment. Table 5.3 lists the various sensor connection to the channels of the Doric system.

Table 5.3 - Doric system connection to sensors

01.	Radiation sensor P.A.R	Meteo station
02.	Radiation sensor GLOBAL	Meteo station
03.	Wind speed sensor	Meteo station
04.	Wind direction sensor	Meteo station
05.	Temperature # 1	Meteo station
06.	Temperature # 2	Meteo station
07.	Relative humidity	Meteo station
08.	Temperature Suppl. #1	Floor
09.	Temperature Suppl. #2	Water hose
10.	Radiation sensor P.A.R # 1	All Screenhouses
11.	Radiation sensor GLOBAL # 1	All Screenhouses
12.	Radiation sensor P.A.R #2	All Screenhouses
13.	Radiation sensor GLOBAL # 2	All Screenhouses
14.	Temperature Portable	All Screenhouses
15.	Wind speed sensor - Portable	All Screenhouses
16.	Temperature # 1	Screenhouse # 1
17.	Temperature # 2	Screenhouse # 1
18.	Temperature # 3	Screenhouse # 1
19.	Relative Humidity # 1	Screenhouse # 1
20.	Relative humidity # 2	Screenhouse # 1
21.		
22.	Temperature # 1	Screenhouse # 2
23.	Temperature # 2	Screenhouse # 2
24.	Temperature # 3	Screenhouse # 2
25.	Relative Humidity # 1	Screenhouse # 2
26.	Relative Humidity # 2	Screenhouse # 2
27.	Temperature Suppl. #4	Dry screen
28.	Temperature # 1	Screenhouse # 3
29.	Temperature # 2	Screenhouse # 3
30.	Temperature # 3	Screenhouse # 3
31.	Relative Humidity # 1	Screenhouse # 3
32.	Relative Humidity # 2	Screenhouse # 3
33.	Temperature Suppl. #5	Dry screen
34.	Temperature # 1	Screenhouse # 4
35.	Temperature # 2	Screenhouse # 4
36.	Temperature # 3	Screenhouse # 4
37.	Relative Humidity # 1	Screenhouse # 4
38.	Relative Humidity # 2	Screenhouse # 4
39.	Temperature Suppl. #5	Wet screen
40.	Temperature Suppl. #6	Wet screen

5.8.2 Software

The Doric system was programmed with basic commands accessible through a front end display panel. There are five major command types: 1- Program commands, 2- Display commands, 3-List commands, 4- Log commands and 5- Reset commands. The first key pressed after [CLEAR] determines the command type. There are also commands for specialized functions including alarm commands, math commands, commands for use with a Digital input card and calibration commands. The 40 Doric channel chosen for the experiment were programmed with the function needed for the specific sensor utilized (thermocouple, humidity sensor (current input) and others).

A general Log command was programmed into the Doric to send average data through the serial communication port every 10 minutes. The data logger scanned a sample of all the 40 channel data every 7 seconds, made an average at the end of a 10 minute period and sent the average values through the serial communication port repeatedly, 24 hours a day.

5.9 Permanent Data Storage

A TEC MASTER Advance System XT+ (IBM compatible) was connected to the Doric system via RS-232C serial connection. The TEC MASTER XT was located in the laboratory close the Doric system. The TEC MASTER XT was permanently running and connected to the Doric for purpose of data storage.

5.9.1 Hardware

The TEC MASTER computer was equipped with a 20 Mbytes Hard disk, with a 640 Kbytes RAM memory and was connected to a Data Train V242A monochrome display monitor.

5.9.2 Software

The TEC MASTER computer ran on DOS. A program named CAPTURE.EXE was used to log data from the DORIC. Once the data was logged onto the TEC MASTER computer, the DATA could be transferred to any other computer or permanent DATA storage medium.

The data were transferred from the TEC MASTER computer to an EPSON EQUITY LT-286 through a serial communication connection using LAPLINK as a transfer program. The data could then be treated as needed.

A program named CONVERT.EXE (QUICK BASIC) was used to convert the data from the DORIC format to a format usable by any spreadsheet. The EXCELL spreadsheet program was used.

5.10 Experimental Procedure

The first objective of this research was to measure the effects of i) the structural or architectural shape of the screenhouse, ii) the size of holes of the screen used as cover for the screenhouse, iii) the colours of screens and iv) water irrigation on the inside climate of the screenhouses for three different seasons of the warm humid climate of the Cotonou region. An experimental procedure was developed and repeated exactly the same way for the three experimental seasons chosen. The experimental procedure was planned and based on the statistical design.

5.10.1 Statistical Design

Mead (1984) states that confounded designs have considerable advantages in comparison to split plot designs. The major advantages underlined are the simplicity of conception and the economies of resources because confounded designs provide more information with fewer factors in the same block sizes than the most popular split-plot designs. Cochran et al. (1957) and Kempthorne (1975) also have described the principles and applicability of the confounded design for agriculture experiments.

The confounded design was implemented and a tabular description of the resulting experimental procedure is summarised in Table 5.4.

The four screens and the two water irrigation statuses were rotated on the four screenhouse structures. For example, during Period #2 and sub-Period #3, Screen #3 (S_3) was installed on screenhouse #1, Screen #1 (S_1) was installed on screenhouse #2, Screen #0 (S_0) was installed on screenhouse #3 and Screen #2 (S_2) was put on screenhouse #4. During sub-Period #3, water irrigation was put on screenhouse #1 and #2 (S_{3-1} and S_{1-1}). Screenhouse #3 and #4 were left dry (S_{0-0} and S_{2-0}). In Table 5.4, the water irrigation state is indicated by the 0 or 1 indices: 0 means no water while 1 means that the screenhouse was being irrigated.

Table 5.4 - Experimental procedure

Period	Sub-Period	Screenhouses number #1	#2	#3	#4
		Screen - Water configurations			
1	1	S_{0-0}	S_{2-0}	S_{3-1}	S_{2-1} : 5 days
1	2	S_{0-1}	S_{2-1}	S_{3-0}	S_{2-0} : 5 days
2	3	S_{3-1}	S_{1-1}	S_{0-0}	S_{2-0} : 5 days
2	4	S_{3-0}	S_{1-0}	S_{0-1}	S_{2-1} : 5 days
3	5	S_{2-0}	S_{0-0}	S_{1-1}	S_{0-1} : 5 days
3	6	S_{2-1}	S_{0-1}	S_{1-0}	S_{0-0} : 5 days
4	7	S_{1-0}	S_{3-0}	S_{2-1}	S_{0-1} : 5 days
4	8	S_{1-1}	S_{3-1}	S_{2-0}	S_{0-0} : 5 days

Screens:

S_0 - Tildenet 50, White, 40% open area
S_1 - Lumite 50, Amber, 35% open area
S_2 - Lumite 32, Amber, 49% open area
S_3 - Tildenet 32, White, 60% open area

Water states:

0 - No water irrigation
1 - With water irrigation

There are four blocks which were the four screenhouses. The treatments were the four mesh sizes, the two colours of the screens and the two water states. The confounded parameters were Period and Sub-Period. Each Sub-Period was repeated for five days. There are two sub-Periods within one Period. One Period duration lasts ten days. Within one Period, the only difference between the two Sub-Periods were the water irrigation status which were alternated. Within one Period, the same screen stayed on the same screenhouse. The screens were rotated from one screenhouse to the other at each change of Period.

The thirty two possibilities of screenhouse architectural types, screen and water state combinations were tested in three different seasons. The procedure described in Table 5.4 was repeated exactly the same way for each of the three seasons. Experiment #1 was performed during the long rainy season from June to mid-August 1994. Experiment #2 took place during the intermediate short dry-short rainy season (mid-August to November 1994). Experiment #3 was performed during the dry season (January to March 1995). One complete set of tests in one season took 40 days. Two or three days in between each Period were necessary to interchange the screens on the screenhouses. A total of 120 days of sampling was done. For each day of sampling, a complete vector of data, including the readings from all the 40 channels of the Doric data acquisition system, was read every 7 seconds and averaged over 10 minutes. The 10 minutes averaged were stored on the IBM compatible TEC MASTER hard disk. Disk backups of the data were made for each day of sampling.

5.10.2 Calibration of sensors

All the sensors were calibrated before the start of the three experimental runs of tests of the three different seasons.

5.10.2.1 Radiation sensors.

The radiation sensors were manufacturer calibrated. Their readings were compared by installing all the sensors outside close to each other. A portable Quantum/Radiometer (direct digital readout) Li-189 was used to compare computer readings with sensor readings.

5.10.2.2 Humidity sensors.

All the humidity sensors were calibrated using Lithium Chloride solution (16 % RH) and Sodium Chloride (75 % RH).

5.10.2.3 Temperature sensors.

The temperature sensors (thermocouples) were calibrated with iced water for 0° C and with boiling water for 100° C.

5.10.4 Data processing.

Each day of sampled data were processed separately with the CONVERT.EXE program. The data were then available for higher level of data processing.

One complete day of recorded data was stored as one EXCELL spreadsheet file. The total data set consisted of one hundred and twenty EXCELL spreadsheet files. EXCELL macro programs were formulated to process the recorded data for each day. These EXCELL macro programs allowed the data to be treated the same way for each day of experiment. With the EXCELL macro program the data could be manipulated in many different ways going from simple plotting of recorded data to calculation of energy term values to obtain a first evaluation of the heat transfer coefficient values.

The MACRO facilities of the EXCELL package was very useful for this purpose. A MACRO sequence could be programmed for the treatment of one sampled day of data. This MACRO was recorded and saved to be used for the exact same treatment of all the remaining sample days of data. One example of this EXCELL MACRO program sequence is shown in Appendix B (Program B1). This MACRO sheet calculates all averages, summations, ratios and coefficients necessary to have a first approximation of the various heat transfer coefficient terms. The MACRO sheet program also plots the various coefficients against the time of day.

VI. DEVELOPMENT OF HEAT TRANSFER MODELS FOR SCREENHOUSES

As established in chapter 2, no specific study has been done to determine the thermal characteristics of screenhouses. Moreover, no study attempted to model a screenhouse in terms of its energy related characteristics. Chapter 2 also confirmed the usefulness of the models and of the heat transfer characteristics determination for design purposes. This study is an attempt to tackle this problem. The second objective of this research is to derive the mathematical models that describe the heat transfer of the various configurations of the screenhouses tested in this project.

6.1 Development of a Heat Transfer Model for a Screenhouse with One Cover Layer.

The first heat transfer model considered was the case of a screenhouse with only one layer of cover. This model corresponds to three physical configurations of screenhouses tested in the experiments of this research project. These configurations were screenhouse #1 (Figure 3.1), screenhouse #2 (Figure 3.2) and screenhouse #4 (Figure 3.4) when they were not irrigated with water. The physical configurations of screenhouses were described in details in Chapter 5.

6.1.1 The cover, the inside air and the concrete floor layers lumped into a one component dynamic model.

The first approach considered was the lumped parameter analysis mainly because it is the most simple yet it has proven its efficiency. For the greenhouse case, Walker et al. (1983) explain why q_r and q_p are negligible compared to the other terms in the heat transfer equation (Eqn. 3). As there were no equipment and no furnace in the screenhouse, the terms q_e and q_f were removed.

In a screenhouse, ventilation is caused only by natural wind since there is no mechanical ventilation. The heat of infiltration which is the heat transfer through cracks and small holes has no meaning for the case of ventilation in a screenhouse because of the inherent holes of the screens. The terms q_υ and q_i are replaced by another term $q_{N\upsilon}$, representing the heat transfer by natural ventilation as described in 6.2.3 below.

6.1.1.1 <u>Effective heating of solar radiation</u>

Solar radiation plays a very important role in the energy balance of the screenhouse. For many years, researchers have tried to find a parameter that accounts for the effective heating of solar radiation in a greenhouse. Walker (1965) introduced a coefficient α which represents the conversion of solar energy into sensible heat and named it the solar absorptivity of the greenhouse. Duncan et al. (1981) suggested the notion of the heating efficiency of the solar radiation for a greenhouse and defined it as being proportional to the transmissivity τ of the greenhouse cover and the absorptivity ν of the greenhouse floor. Garzoli (1985) also used the factor α but introduced factor F1 that accounts for the reflection of internal solar radiation by the cover and factor F2 accounting for absorbed solar radiation that is used by plants in photosynthesis and stored in the floor. Albright et al. (1985) also used the heating efficiency factor defined by Duncan et al. (1981) but mentioned that Bayley (1977) did not include in this coefficient all the solar energy absorbed in the greenhouse and arrived at a considerably lower value than Duncan et al. (1981). Tantau (1989) used a coefficient ν which he called the rate of radiation transferred to sensible heat multiplied by the transmissivity τ of the greenhouse cover and the global radiation to calculate the energy input of the greenhouse.

To apply the concept of effective heating of solar radiation to the screenhouse case, the heat reflected from the floor is being considered. For radiant energy striking a material surface, Holman (1981) defines the reflectivity η as the fraction reflected, the absorptivity α as the fraction absorbed and the transmissivity τ as the fraction transmitted. The sum of these three parameters is equal to unity and is described by Eqn. 7:

$$\eta + \alpha + \tau = 1 \qquad (7)$$

The transmissivity of the concrete floor being equal to zero, its reflectivity η equals:

$$\eta = 1 - \alpha \qquad (8)$$

For the screenhouse case, the effective heating coefficient of the solar radiation is equal to the reflectivity η of the screenhouse floor. The effective solar heat gain of the inside air of the screenhouse can then be expressed as:

$$q_{Ieff} = \eta \, q_I \tag{9}$$

6.1.1.2 Effective heating of thermal (long wave) radiation

Walker et al. (1983) treat the thermal heat transfer q_t as the radiation heat of the air going through the surface, hence going out of the greenhouse. Kindelman (1980) decomposes the thermal radiation into many different elements, each one being of more or less importance in magnitudes. As for solar radiation, the concept of effective heating can be applied to thermal radiation. The effective heat gain of the screenhouse inside air (q_{teff}) is treated as the portion of the long wave radiation heat that remains in the screenhouse assuming that no energy is absorbed by the screenhouse cover. The interest is to calculate the heat energy staying in the screenhouse. q_{teff} is treated as an input to the inside air energy balance and accounts for the portion of thermal radiation that is not transmitted by the screenhouse cover as described by the following equation:

$$q_{teff} = (1 - \tau_t) \, q_{lw} \tag{10}$$

where, τ_t is the long wave (thermal) transmissivity and q_{lw} is the heat transfer of long wave radiation. The heat balance model of the screenhouse in steady state conditions can be stated as:

$$q_{Ieff} + q_{teff} - q_{Nu} +/-(q_{cd}+q_g) = 0 \tag{11}$$

In an unsteady state case, the variation of temperature within the screenhouse is described by a term accounting for the temporal variation of the thermal energy of the air in the screenhouse. This term added to Eqn. 11 gives:

$$q_{Ieff} + q_{teff} - q_{Nv} +/- (q_{cd}+q_g) = m_a C_p \frac{dTi}{dt} \qquad (12)$$

where, m_a is the mass of air inside the screenhouse and is described by:

$$m_a = \rho V \qquad (13)$$

and C_p is the specific heat of the air. Note that under steady state the derivative dT_i/dt is equal to zero. Eqn. 12 is shown pictorially in Figure 6.1.

6.1.2 Analysis of the terms involved in the lumped parameters heat balance equation of a screenhouse with one cover layer.

6.1.2.1 The solar heat gain, q_I.

The solar heat gain in a screenhouse is described by the same equation that describes the solar heat gain of a greenhouse (Walker et al. 1983).

$$q_I = \tau I A_f \qquad (14)$$

In Eqn. 14, τ is the transmittance of the cover for short wavelength radiation. Values of τ can be obtained from the literature (Bond, 1977) for different types of covering materials (e.g. plastic or glass). The case of the transmittance of greenhouse covering materials with water has been studied by Lawson (1986) and Ménard (1991). No studies have been done to determine the transmittance τ of screens on a screenhouse structure with or without a water cover. Some screen manufacturers reported radiation transmission

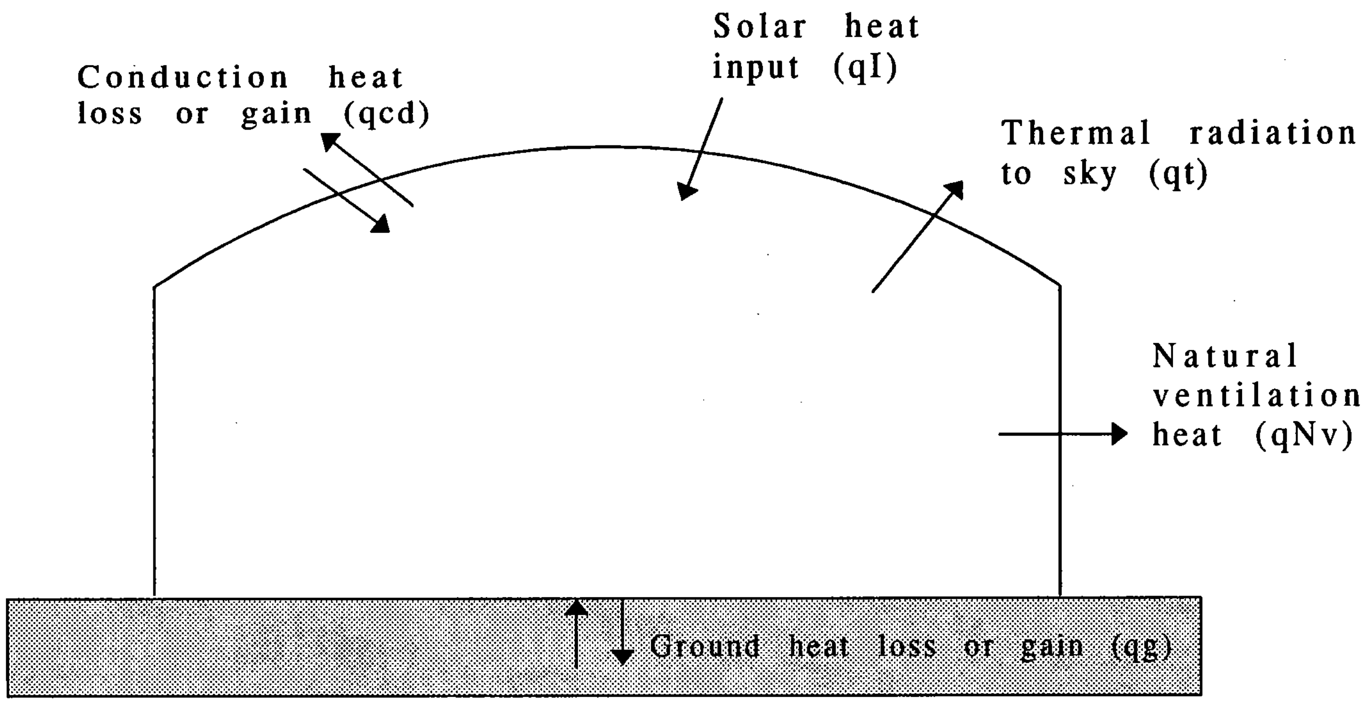

Figure 6.1: Screenhouse inside air heat exchange

values for screens in the visible light spectrum (Ross, 1994) but they have not described their method of measurement.

6.1.2.2 The heat of long wave radiation, q_{lw}

The term q_{lw} can be approximated by evaluating the radiation exchange between the surface and the sky. The sky can be considered as a black body at some equivalent sky temperature T_s, so that the actual net radiation from a surface with emissivity ε_s and surface temperature T is (Duffie and Beckman, 1991):

$$q_{lwsky} = \varepsilon_s A_f \sigma (T^4 - T_s^4) \quad (15)$$

In the previous equation, the equivalent black body sky temperature accounts that the atmosphere is not at a uniform temperature and that the atmosphere radiates only in certain wavelength bands. The atmosphere is essentially transparent in the wavelength region from 8 to 14 nm, but outside of this "window" it has absorbing bands covering much of the infrared spectrum. Several relations have been proposed to relate T_s to the ambient temperatures for clear skies. Swinbank (1963) relates sky temperature to the local air temperature. Brunt (1932) relates sky temperature to water vapour pressure, and Bliss (1961) used T_{dp}, the dew point temperature. Berdahl and Martin (1984) used extensive data from the United States to relate the effective sky temperature to the dew point temperature one hour from midnight, by the following equation:

$$T_s = T_a [\ 0.711 + 0.0056 T_{dp} + 0.000073 T_{dp}^{\ 2} + 0.013\ \cos(15t)^{1/4}] \quad (16)$$

where, T_s and T_a are expressed in degree Kelvin and T_{dp} is the dew point temperature in degree Celsius. The experimental data covered a dew point range from -20 to 30 °C. The difference between sky and air temperatures ranges from 5 °C in a hot, moist climate to 30 °C in a cold, dry climate. Clouds tend to increase the sky temperatures.

Walker et al. (1965) stated a simpler model to calculate the thermal radiation going out of the greenhouse (q_t) that uses the outside air temperature as an equivalent of the sky temperature. This model is described by Eqn. 17:

$$q_t = \tau_t A_f \sigma (\varepsilon_g (T_g + 273)^4 - \varepsilon_a (T_o + 273)^4) \quad (17)$$

where, τ_t is the long wave (or thermal) transmissivity of the covering material at inside temperature. Walker et al. (1983) observed that the heat transfer by thermal radiation directly through the greenhouse glazing to the ambient sky is normally not an important factor in the greenhouse energy balance because most glazing materials are poorly transparent or essentially opaque to long wavelength radiation. Yet, the authors also point out that thermal radiation exchange can be a significant factor when glazing such as polyethylene, which is highly transparent to thermal radiation, is used. The thermal transmissivity of the polyethylene is greatly reduced if condensed water droplets obscure the polyethylene surface due to the opacity of water to radiation in the thermal range of 20 °C to 50 °C (Walker et al., 1971). Since q_t in Eqn. 17 represents the portion of the long wave radiation that is going out of the screenhouse, the total long wave radiation is described by:

$$q_{lw} = A_f \, \sigma \, (\varepsilon_g \, (T_g+273)^4 \; - \; \varepsilon_a \, (T_o \; +273)^4) \tag{18}$$

As mentioned in section 6.1.1.2, in the screenhouse case, the interest is to calculate the effective heat gain of long wave radiation, q_{teff} (Eqn. 10).

6.1.2.3 <u>The heat of natural ventilation, $q_{N\upsilon}$</u>

The q_υ and the q_i terms defined by Walker et al. (1983) for ventilation and infiltration heat transfer are replaced by the heat transfer of natural ventilation in the case of a screenhouse and is defined as:

$$q_{N\upsilon} = N_\upsilon \; V \; \rho \; C_p \; (T_i - T_o) \tag{19}$$

where N_υ, the number of air change per unit of time, is the natural ventilation rate. The definition of N_υ is based on the definition of natural ventilation flow (Eqn. 1) through an opening defined by ASHRAE (1981), Hellickson (1983) and Choinière (1991) and is expressed as:

$$N_\upsilon = \frac{C_q \; \upsilon \; A_c}{V} \tag{20}$$

N_υ is a function of the wind speed and the temperature differences between the inside and the outside of the screenhouse and approximates, in one single term, both the wind pressure effect and the temperature difference effect.

6.1.2.4 The heat of convection-conduction, q_{cd}.

The heat of convection-conduction is the most important heat loss encountered, since greenhouse glazing is normally a thin material with inherently poor insulating properties (Walker et al., 1983). The convection-conduction heat losses of screenhouses is given by:

$$q_{cd} = U A_c (T_i - T_o) \tag{21}$$

This term is a heat loss when Ti>To. It is assumed to be always the case for a screenhouse in a warm climate. Eqn. 12 states that q_{cd} can either be an input or an output of energy but in the present case of the screenhouse in a warm climate, q_{cd} will always be considered as an output to the energy balance of the screenhouse.

The global heat transfer coefficient U depends on various factors and characteristics such as geometry of the system and heat transfer resistances (or conductance) of the materials used in the construction of the screenhouse. U also depends on air conditions such as wind speed, temperature and relative humidity of the air. Relative humidity influences U to a lesser degree than do wind speed and temperature.

6.1.2.5 The convective heat transfer to or from the ground, q_g.

The convective heat transfer to or from the ground can be described as:

$$q_g = h_g A_f (T_g - T_i) \tag{22}$$

and is a heat gain to the screenhouse when Tg>Ti. It is assumed that it is always the case for a screenhouse in a warm climate. Note that for this project, the ground layer is the concrete floor. The concrete physical attributes are utilised in this study. Walker et al. (1983) stated that for greenhouse with uninsulated floors, the ground heat transfer is generally quite small in comparison to the heat transfer through the greenhouse glazing but it can be very significant for unheated greenhouses.

The choice of material used in the fabrication of the floor of a screenhouse is important. As mentioned in chapter 5, for the purpose of uniformity, the floor of the screenhouses tested in this project were built in concrete and were not insulated. Holman (1981) lists values for convective heat transfer coefficients (h_g) for both free and forced convection. The natural wind flowing over the floor of the screenhouse is considered as a free convective situation and the value of 4.5 W/m^2 °C is taken from Holman (1981).

The lumped parameter heat transfer model for a single cover screenhouse can now be expressed as follow:

$$q_{Ieff} + q_{teff} + q_g - q_{Nv} - q_{cd} = m_a C_p \frac{dTi}{dt} \tag{23}$$

and is pictorially represented in Figure 6.2.

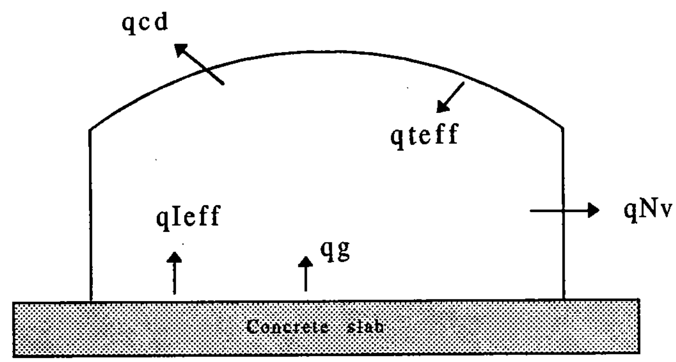

Figure 6.2: Single roof: Screenhouse inside air heat exchange (Lumped parameters)

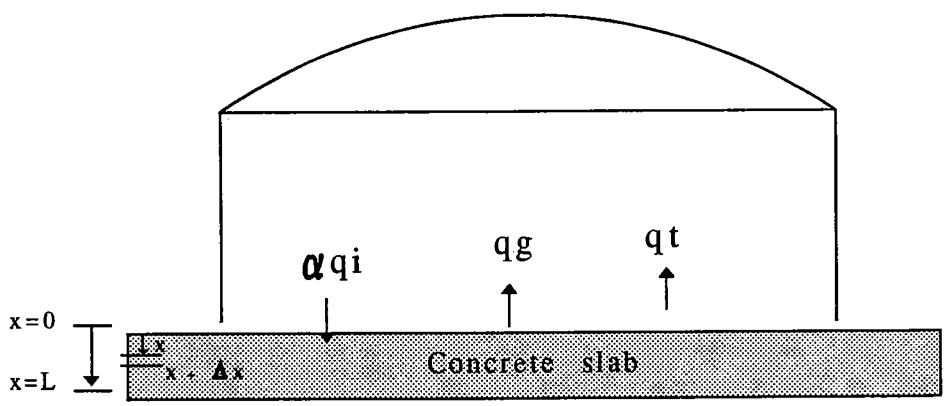

Figure 6.3: Screenhouse ground heat exchange

6.2 A Two Components Dynamic Model for a Screenhouse.

For cases where the floor is not insulated or when the surface floor temperature is not known, the thermal exchange of the floor has to be considered in a two component heat transfer model. The first component of the model is the inside air of the screenhouse. The balance of energy in the inside air layer of the screenhouse is described in Eqn. 23. The second component of the model is the ground or more precisely the floor of the screenhouse which, in the case of the experiment, is concrete. The floor can be considered as a flat plate with boundary conditions at each of its sides (Figure 6.3). The heat exchange inside the floor can be described by:

$$\rho_g \, A_f \, C_{pg} \, \frac{\partial T_g}{\partial t} = k_g \, A_f \, \frac{\partial^2 T}{\partial^2 x} \qquad (24)$$

As A_f is a constant and assuming k_g is independent of temperature and position:

$$\rho_g \, C_{pg} \, \frac{\partial T_g}{\partial t} = k_g \frac{\partial^2 T}{\partial^2 x} \qquad (25)$$

The boundary conditions for the screenhouse floor are:

BC(I): at x= L ; $T_g = T_{soil}$

and BC(II): at x= 0;

$$\alpha q_I - q_g - \tau_t q_t = -k_g A_f \frac{dT}{dx} \qquad (26)$$

When the thermal conductivity of the floor is high, the temperature within the floor block can be assumed to be uniform all over. The screenhouse floor heat transfer can therefore be expressed as:

$$\alpha q_I - q_g - \tau_t q_t = \rho_g \, C_{pg} \frac{dT_g}{dt} \qquad (27)$$

Eqn. 23 and 25 (or in the simplified case, Eqn. 23 and 27) are treated as a system of two simultaneous differential equations. The solutions of these equations lead to the temperature of the air Ti and the temperature of the ground Tg.

6.3 Development of Heat Transfer Models for Screenhouses with More than One Layer of Cover.

Screenhouses with more than one layer of cover were also tested in the experiments. Examples of such cases are screenhouse #3 (Figure 3.3) with its double roof; screenhouse #2 (Figure 3.2) and screenhouse #4 (Figure 3.4) with water irrigation which adds a supplementary layer of cover and screenhouse #3 (Figure 3.3) with water irrigation on top of its double roof.

The case of screenhouses with more than one layer of cover necessitates the elaboration of a multi-component heat transfer model with many layers of cover like the models described by Nijskens et al. (1991). The present analysis is aimed at simplifying as much as possible the interpretation of the heat transfer characteristics of the screenhouse. Using a multi-component model implies more complexity and does not necessarily improve the solutions for the system. For these reasons, the lumped parameter approach utilized in 6.1 above is still considered.

6.3.1 A screenhouse with a double roof.

Figure 6.4 shows the heat transfer terms considered for the double roof screenhouse. Eqn. 23 applies for this system assuming all conditions and assumptions described in section 6.1 are also verified. The distinction that has to be made is in the description of the solar energy and the thermal radiation input of the screenhouse. All other heat transfer terms are considered to be the same as in section 6.1.

The solar radiation has to cross two layers of cover so that q_{Ieffd}, the effective solar heat gain of the inside air of the double roof screenhouse by short wave radiation becomes:

$$q_{Ieffd} = (1 - \alpha)\, \tau_{c1}\, \tau_{c2}\, A_f\, I \qquad (28)$$

The fraction of thermal radiation that contributes to the inside air heat is the fraction reflected by the first cover layer of the screenhouse as shown on Figure 6.4, assuming no heat is absorbed by that cover layer. The fraction of thermal radiation reflected by the second cover layer is considered to heat only the air layer between the two roofs so that its heat contribution to the inside air is negligible. In the case of the double layer screenhouse, the dynamic heat transfer equation is as follows:

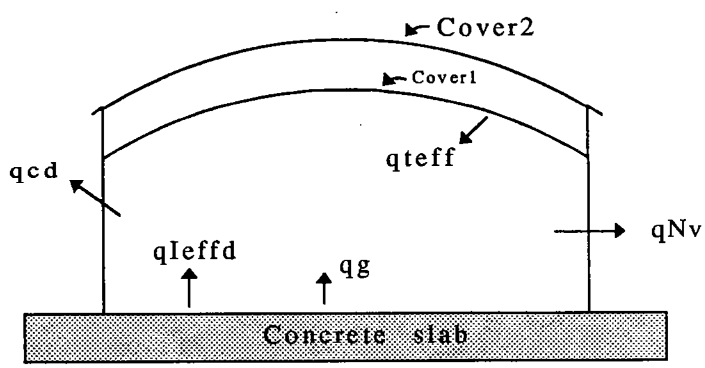

Figure 6.4: Double roof: Screenhouse inside air heat exchange (Lumped parameters).

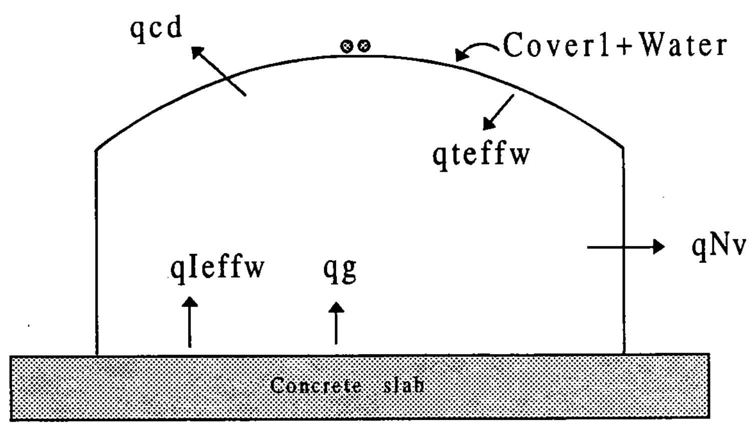

Figure 6.5: Single roof with water irrigation: Screenhouse inside air heat exchange

$$q_{Ieffd} + q_{teff} + q_g - q_{Nv} - q_{cd} = m_a C_p \frac{dTi}{dt} \qquad (29)$$

6.3.2 A single roof screenhouse with water irrigation.

Figure 6.5 shows the heat transfer terms of a single roof screenhouse with a layer of water irrigated on its cover. Using the same approach as in section 6.3.1, the effective heat gain of the inside air of the water irrigated screenhouse by short wavelength solar radiation is expressed as:

$$q_{Ieffw} = (1-\alpha)\ \tau_{c1}\ \tau_w\ A_f\ I \qquad (30)$$

Thermal radiation is reflected by both the cover of the screenhouse and the water irrigation layer. It is assumed that the absorption of long wave radiation by the water and cover layers is minimal compared to the other heat transfer terms. The effective portion of the thermal radiation heating the screenhouse inside air is hence expressed as:

$$q_{teffw} = (1-\tau_{c1}\ \tau_w)\ q_t \qquad (31)$$

The heat transfer model for this type of screenhouse is:

$$q_{Ieffw} + q_{teffw} + q_g - q_{Nv} - q_{cd} = m_a C_p \frac{dTi}{dt} \qquad (32)$$

6.3.3 A double roof screenhouse with water irrigation.

Figure 6.6 shows the heat transfer terms of a double roof screenhouse with a layer of water irrigated on its cover. The solar energy term effectively heating the inside air for this type of screenhouse can be described as:

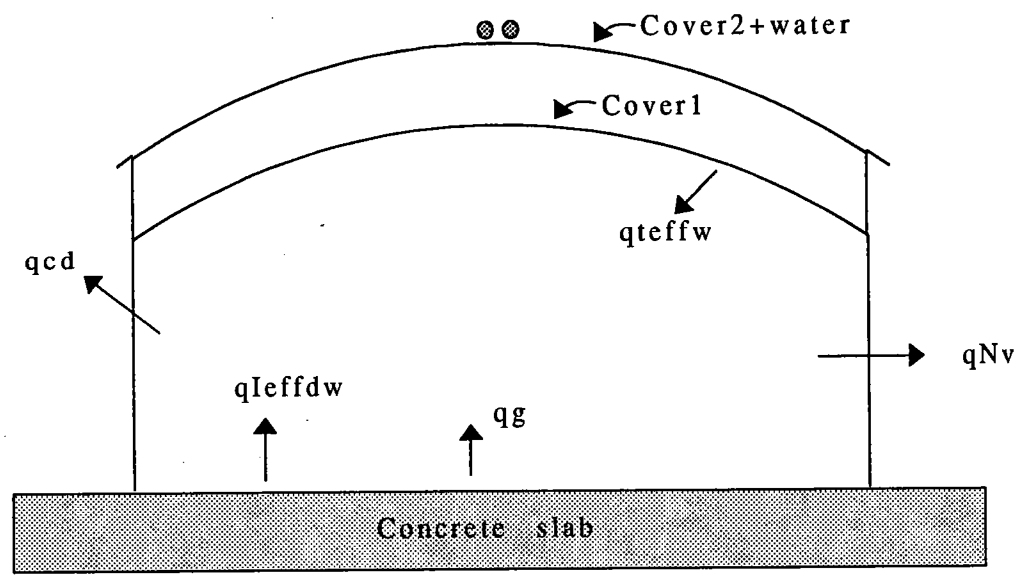

Figure 6.6: Double roof with water irrigation: Screenhouse inside air heat exchange.

$$q_{Ieffdw} = (1-\alpha)\ \tau_{c1}\ \tau_{c2}\ \tau_w\ A_f\ I \tag{33}$$

Thermal radiation is reflected by both the first layer of cover of the screenhouse and the water irrigation layer. The reflection of thermal radiation inside the screenhouse by the second cover layer is considered negligible so that Eqn. 31 can be used. It is assumed that the absorption of long wave radiation by the water and cover layers is minimal compared to the other heat transfer terms. The heat transfer model for a double roof screenhouse with water irrigation is described by:

$$q_{Ieffdw} + q_{teffw} + q_g - q_{Nv} - q_{cd} = m_a C_p \frac{dTi}{dt} \tag{34}$$

6.4 <u>Heat Transfer Characteristics Determination.</u>

As stated in chapter 4, the third objective of the research is to study the effects of the parameters measured in objective A) on 3 main screenhouse heat transfer characteristics: i) τ, the overall short wave transmissivity of the screenhouse, ii) N_v, the natural ventilation coefficient and iii) U, the global heat transfer coefficient. The values of the heat transfer characteristics are specific to each configuration of screenhouse but also vary with the climatic conditions in which the screenhouses are located.

6.4.1 Transmissivity, τ.

The light transmission in greenhouses has been studied by Critten (1986). Global τ values can be obtained from the ratio of inside over outside radiation as mentioned by Albright et al. (1985).

$$\tau = \frac{I_i}{I_o} \qquad (35)$$

τ is dependant on sun angle (Critten, 1989) but Baille et al. (1990) proposed a simple model for the estimation of greenhouse transmission which is similar to Eqn. 35.

For this research, Eqn. 35 is used to calculate the global transmissivity values using the experimentally measured inside and outside global radiation for the screenhouse configurations tested.

6.4.2 Natural ventilation coefficient, N_υ.

Eqn. 20 is used to calculate N_υ from experimental data. C_q is the air flow rate resistance coefficient of the screens. C_q is dependent on the velocity v at which the air approaches the screen. C_q versus approach air velocity curves can be obtained from the screen manufacturers. The C_q obtained from these charts can be used to calculate N_υ with the assumptions that the wind always comes perpendicular to the screens of the screenhouses.

Wind tunnel studies are appropriate to evaluate C_q coefficients from experiments (Choinière, 1991). However, C_q values can also be calculated from *in situ* experimental inside and outside wind speed measurements (Aynsley et al., 1977). In this experiment, Cq values are evaluated with the latter method.

6.4.3 Global heat transfer coefficient, U.

As demonstrated by Seginer et al. (1986), it is very useful to perform night time experiments to determine the global heat transfer coefficient because the solar radiation heat input is eliminated from the heat balance equation, implying that $q_I = 0$. In most climates, especially in warm tropical climates like the one in the Cotonou region, the night time temperatures are almost constant. Inside screenhouse night temperature data also tend to be constant. It implies that at night, dTi/dt = 0. The global heat transfer coefficients are derived for each specific screenhouse configuration tested in the experiments using the heat transfer models developed in sections 6.1 to section 6.3 above. Night time inside and outside screenhouse temperatures are used to evaluate these coefficients.

6.4.3.1 U for screenhouses with one cover layer.

Eqn. 23 is used as a basis to evaluate U for a screenhouse with one cover layer. q_{cd} is defined by Eqn. 21. Considering $q_I = 0$ and dTi/dt = 0 for night time tests:

$$U = \frac{q_{teff} + q_g - q_{Nv}}{A_{c1}(Ti - To)} \tag{36}$$

The experimental temperature data and the experimentally calculated τ and N_v values for screenhouses with one cover layer without water irrigation are used to evaluate U values in Eqn. 36.

6.4.3.2 U for double roof screenhouses.

Eqn. 29 and 21 are used as a basis for the evaluation of U for double roof screenhouse. Considering $q_I = 0$ and dTi/dt = 0 for night time tests, Eqn.

36 still applies for the calculation of U values for double roof screenhouses since $q_{Ieffd} = 0$.

The experimental temperature data and the experimentally calculated τ and N_υ values for double roof screenhouses without water irrigation are used to evaluate U values with Eqn. 36.

6.4.3.3 U for single roof screenhouses with water irrigation.

The single covered screenhouse with water irrigation heat balance was described in Eqn. 32. To solve for U, night time tests are considered ($q_I = 0$) and q_{cd} is defined by Eqn. 21. The U values for these screenhouse configurations can be evaluated with the following equation:

$$U_w = \frac{q_{teffw} + q_g - q_{N\upsilon}}{A_{c1}(Ti - To)} \tag{37}$$

The experimental temperature data and the experimentally evaluated τ an N_υ values specific to the cases of single covered screenhouses with water irrigation are used to evaluate U_w in Eqn. 37.

6.4.3.4 U for double roof screenhouses with water irrigation.

Eqn. 34 and 21 are used as a basis for the evaluation of U_w for double roof screenhouse. Considering $q_I = 0$ and $dTi/dt = 0$ for night time tests, Eqn. 37 still applies for the calculation of U_w values for double roof screenhouses since $q_{Ieffdw} = 0$.

6.4.3.5 BASIC program to calculate U-values.

A BASIC routine named UVALUES.BAS (Program B2 in Appendix B) was programmed to calculate the U-values for all the screenhouse configuration tested. For the three seasons (120 days) of experiments, a total of 480 U-values were calculated. For each day of experiment, the program accessed 1) the inside temperatures data files of screenhouses #1 to #4 separately and 2) the outside temperature data files to calculate the U-values of the four screenhouses for that day. The program was set up so that the short wave transmittance τ, the long wave transmissivity τ_t, and the N_υ coefficient values could be changed for every day and every screenhouse configuration. Night time N_υ values differ from day time N_υ. The program calculates average night time U-values using 1) 40 inside temperatures for each screenhouse and 2) 40 outside simultaneous temperature data. These data were recorded every 7 seconds but the 10 minutes averages were used from 00:00 (midnight) to 06:40 for every experimental day.

6.5 Screenhouse Heat Transfer Simulations.

The fourth objective of this research was to use computer simulations, based on the derived heat transfer models, as tools to calibrate the heat transfer models, to optimize the screenhouse heat transfer characteristics and to predict screenhouse inside temperatures in various tropical climates. The simulation programs were formulated with the heat transfer models of the configurations of the screenhouse developed in 6.1 to 6.3 above.

As a first approximation and simplification of the simulation, the outside $T_o(t)$ and the solar radiation I(t) were considered as the only two independent variables that vary with time. The dependent variable is the inside temperature of the screenhouse $T_i(t)$. Values of $T_o(t)$ and I(t) were interpolated from the measured data and served as forcing functions for the Runge-Kutta numerical integration.

Eqn. 23 was used as a basis for the development of the computer simulation of a screenhouse with one cover layer. Eqn. 23 is a first order differential equation and is solved numerically using the fourth order Runge-Kutta technique. A BASIC program, RKLUMP.BAS, was written for that purpose (Program B3 in Appendix B).

For each day of experiment, the simulation program accessed 1) the daily global radiation data file and, 2) the daily outside temperature data files to calculate the predicted inside temperature data, each 10 minutes, for a complete day for each separate screenhouse configuration. The program was set up so that the short wave transmittance τ, the long wave transmissivity τ_t, the N_υ coefficient and the U-values could be changed for every day and every screenhouse configuration. Night time N_υ values differed from day time N_υ. The RKLUMP.BAS program also accessed the measured inside temperatures data files of each screenhouses separately, for each day to allow for the comparisons between predicted and measured inside temperature values. Eqn. 29, 32 and 34 were integrated in the RKLUMP.BAS BASIC program the same way as

Eqn. 23 to predict the inside temperatures of the screenhouse with a double roof, the single layer screenhouse with water irrigation and the double roof screenhouse with water irrigation respectively.

VII. RESULTS AND DISCUSSION

An engineering design approach to data analysis was adopted. The ultimate goal was to have a comprehensive knowledge of the screenhouse heat transfer characteristics to allow for the best design of screenhouses in any tropical location. The hydrodynamic tests results that were described in section 5.4.1, the climatological results, the aerodynamic tests, and finally the simulations of the inside screenhouse climates were all performed in this perspective.

7.1 The Climatological Results

The determination of the heat transfer characteristics for the different configurations of screenhouses required climatological data (temperature, relative humidity, radiation, wind velocity, wind direction) and their counterparts inside the screenhouses as described in Chapter 5. Graphical analysis were performed with EXCELL and SAS. The statistical analyses were done with SAS. Overall, for the three seasons of tests, 25344 records of the 40 channel measurements (Table 5.3) of data were used for the analysis. Night data were not used in the graphical and statistical analyses of the climatological results. Only the data from 8:00 h until 16:00 h were analyzed because it is in that period of time that solar energy has the greatest impact on the conditions inside the screenhouses. As will be seen later, the night data were used for the calculation of U values and as input data for the simulations of the inside temperature of the screenhouse.

Frequency distributions of the climatological data were first assessed to determine whether the various screenhouse configurations had been subjected to similar conditions over the experimental periods. Graphical and statistical analyses were performed on the climatological results using four main parameters as bases of interpretation, three of which were the heat transfer characteristics targeted in this research. These four parameters were: i) the difference of temperature (DT) between the inside and the outside of the screenhouse, ii) the transmissivity (τ) of the covering materials, iii) the natural ventilation coefficient (N_{υ}) for the various configurations and iv) the global heat transfer coefficient (U) of the configurations. The effects of the screenhouse architectural structure types, the screen mesh sizes, the screen colours and the absence or presence of water cooling were examined on these four parameters. One of the issues of these analyses was to find out whether the extreme temperatures (high extremes) tended to be associated with a particular configuration or depended on outside climatic conditions.

7.1.1 Frequency distributions analysis of climatic and screenhouse interior data

Frequency distributions, over the three seasons, were plotted (Figures 7.1 to 7.8) for the following climatic variables: 1) the wind speed (Figure 7.1), 2) the wind direction (Figure 7.2), 3) the PAR solar radiation (Figure 7.3), 4) the global solar radiation (Figure 7.4), 5) the outside temperatures (Figure 7.5)

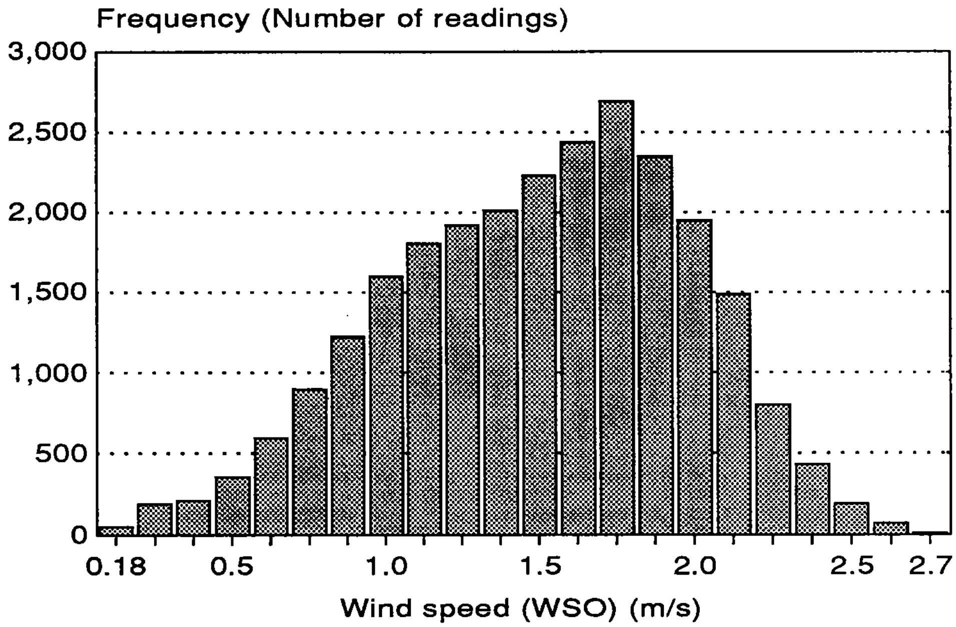

Figure 7.1 Wind speed (Frequency distribution)

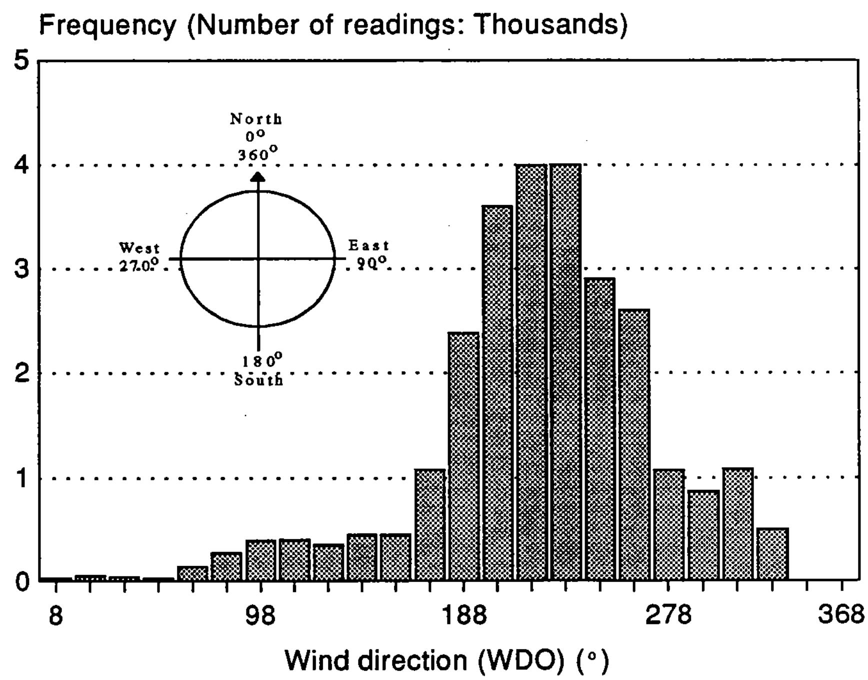

Figure 7.2 Wind direction (Frequency distribution)

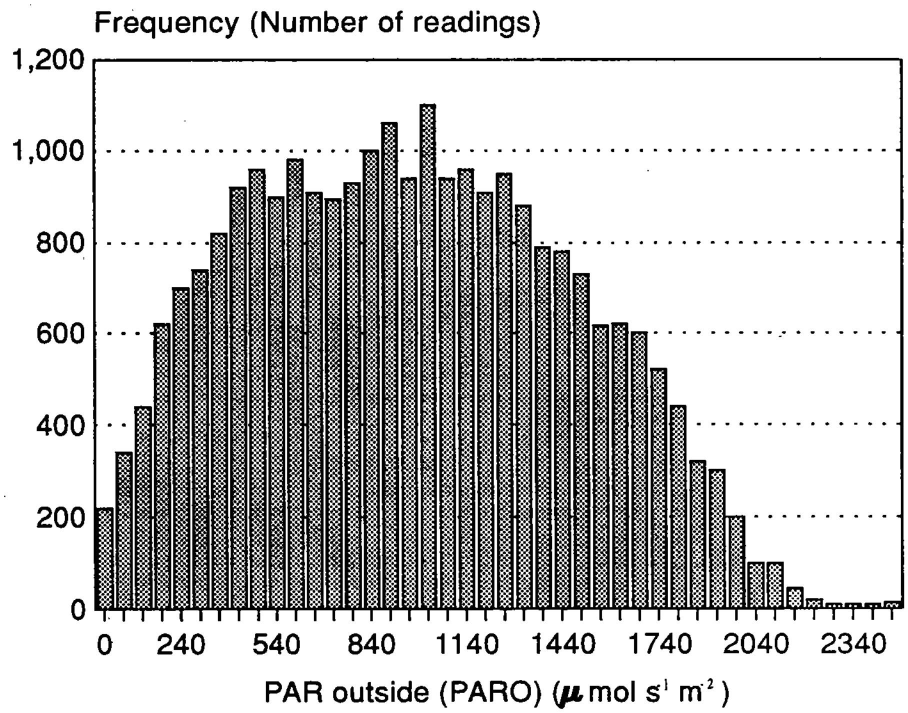

Figure 7.3 Outside PAR radiation (Frequency distribution)

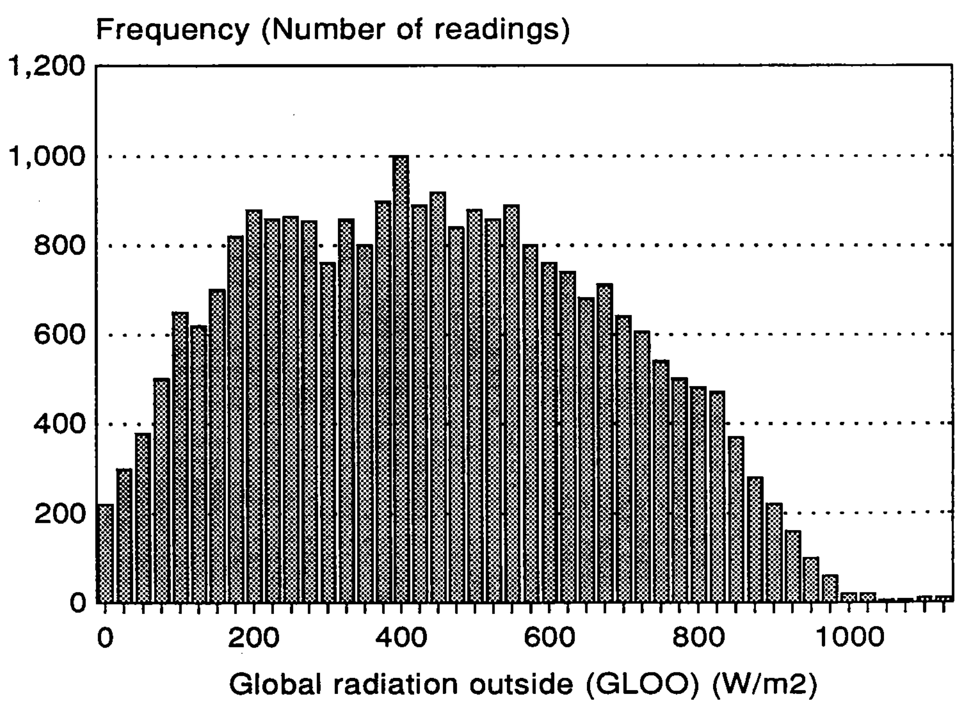

Figure 7.4 Outside Global radiation (Frequency distribution)

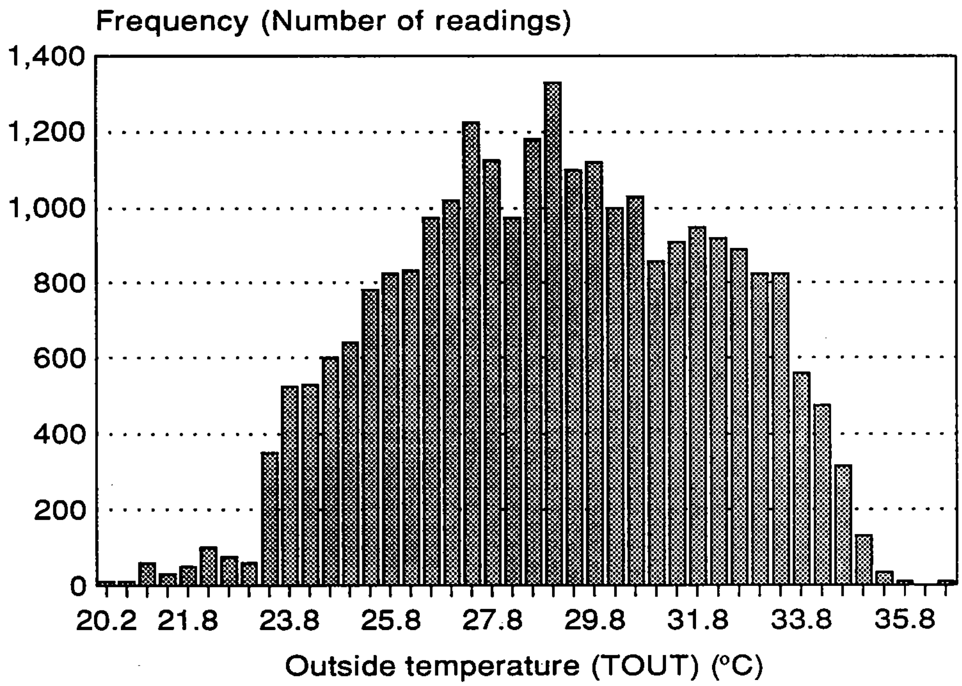

Figure 7.5 Outside temperature (Frequency distribution)

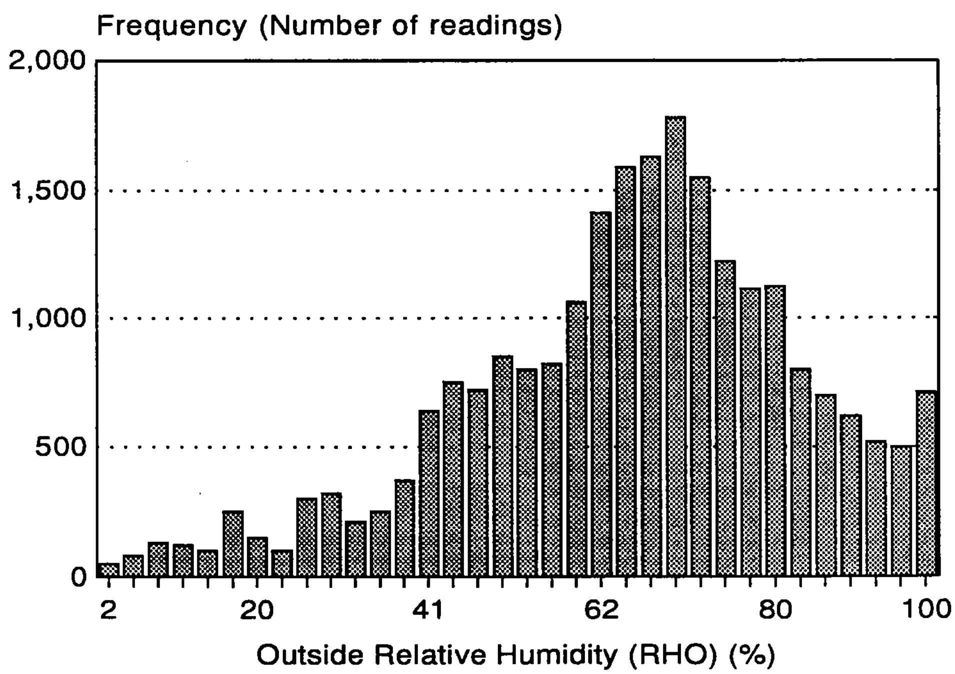

Figure 7.6 Outside Relative Humidity (Frequency distribution)

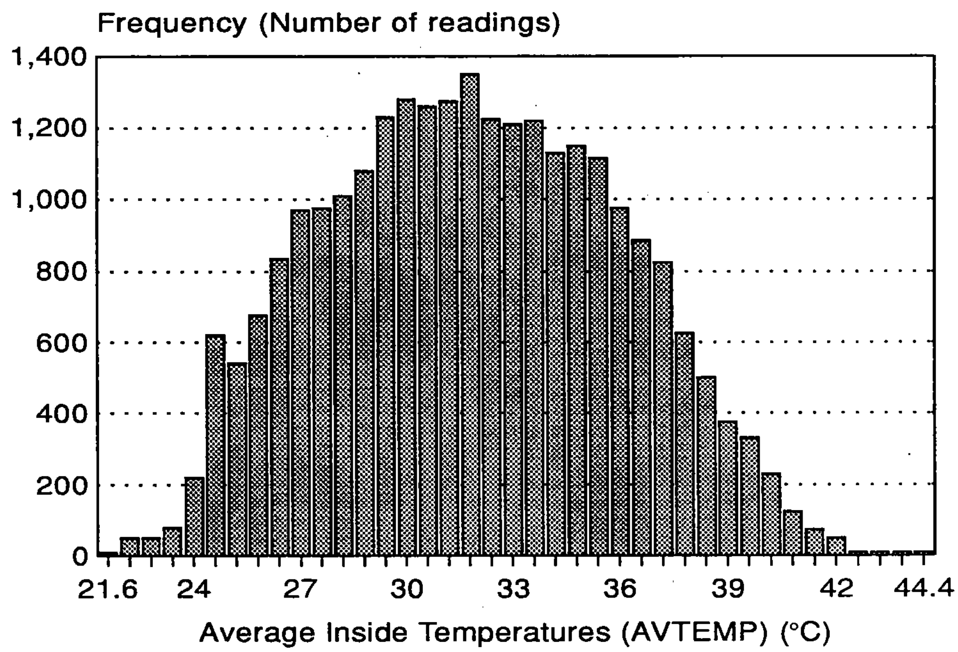

Figure 7.7 Average Inside Temperature (Frequency distribution)

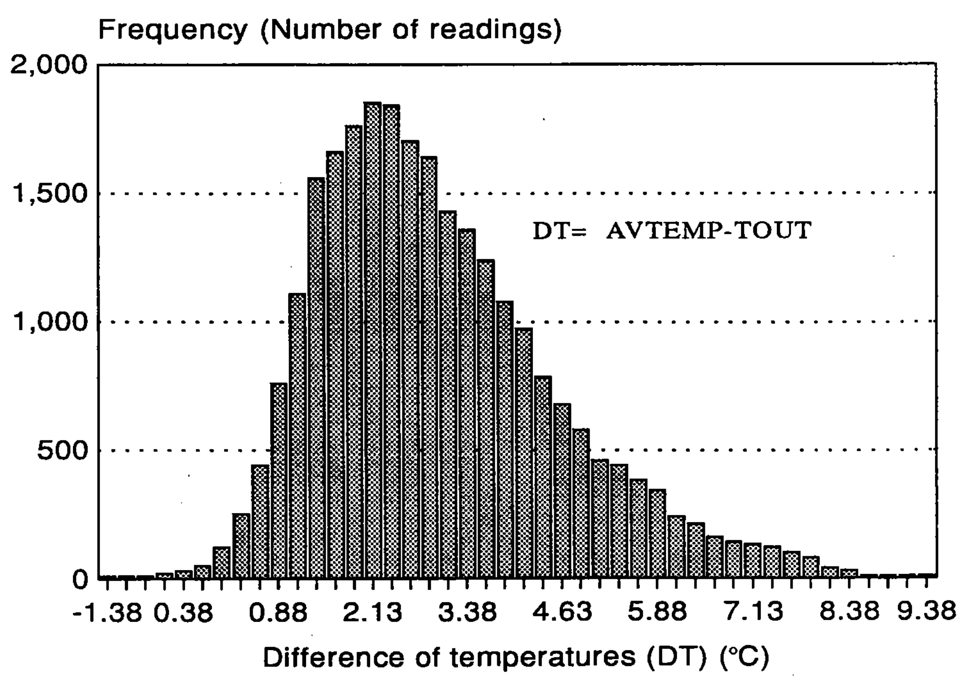

Figure 7.8 Difference of temperatures (Frequency distribution)

and 6) the outside relative humidities (Figure 7.6). Histograms were also plotted for the average inside temperatures (Figure 7.7) and DT which is the difference between AVTEMP and TOUT (Figure 7.8).

Figures 7.7 and 7.8 demonstrate the range of conditions that can be found inside the screenhouses when subjected to the outside climatic conditions of the Cotonou region. Figure 7.7 shows that average inside temperatures (AVTEMP) as high as 44.4 °C have occurred but AVTEMP was in the range of 25.2 to 37.4 °C, 90% of the time. Figure 7.8 shows that differences of temperatures between the inside and the outside of the screenhouse as high as 9.38 °C were recorded but were usually between 1 and 5 °C.

To verify if the data gathered during the three seasons (12 periods or 24 subperiods or 120 days) of data collection were comparable, the frequency graphs of the same eight parameters mentioned in the previous paragraph were plotted for the three seasons separately. The frequency graphs of the PAR solar radiation, the Global solar radiation, the wind speed and the wind direction were similar for the three experiments. One of the main differences observed was that the outside temperatures (TOUT) were skewed towards the higher temperatures (31 to 34 °C) for the dry season, during experiment #3 (Figure C1 in Appendix C). The other major difference observed was that the relative humidities were higher for the rainy season, during experiment #1 (Figure C2 in Appendix C), more evenly distributed over the whole range in the intermediate season, experiment #2 (Figure C3 in Appendix C), and skewed towards lower values in the dry season, experiment # 3 (Figure C4 in Appendix C). This has bearing on water cooling strategies. The average temperatures inside the screenhouses (AVTEMP) were warmer (34 to 38 °C) in experiment #3 and colder (29 to 32 °C) in experiment #2. The differences of temperature (DT) were greater (3 °C) in experiment #3. The DT values observed in experiment #1 and #2 were similar.

The frequency distributions of the outside climatic measurements demonstrate that the experimental data set was representative of the tropical climatic conditions found in the Cotonou region since it corresponds to the climatic conditions described in section 5.1.2.

7.1.2 Primary relationships

One of the main objectives of screenhouse design for the tropics is to minimize inside heat accumulation. As a first step of analysis, the primary relationships between the inside temperature (AVTEMP), the outside temperature (TOUT) and the difference of temperature (DT) were studied (Figure 7.9, 7.10, 7.11).

Figure 7.9 shows the 25344 average inside temperatures (AVTEMP) calculated from the average of three thermocouples readings in each screenhouses versus the corresponding outside temperatures (TOUT). The range of outside temperatures (TOUT) goes from 20 to 37 °C while the average inside temperatures (AVTEMP) ranges from 21 to 44.5 °C. Figure 7.9 shows a tendency to obtain higher average inside temperatures (AVTEMP) when

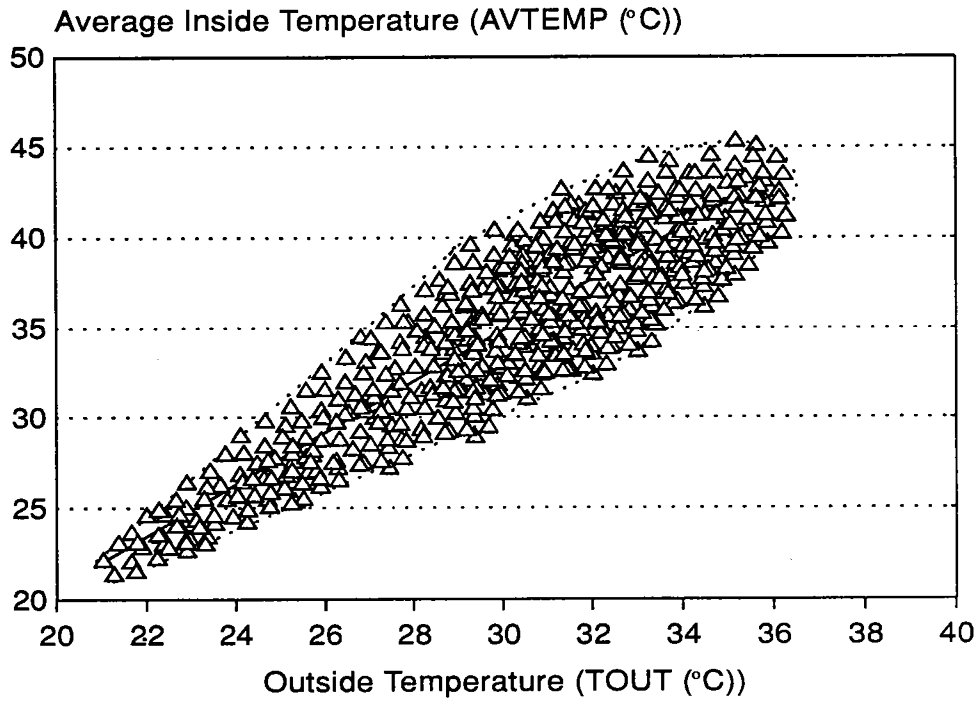

Figure 7.9 AVTEMP vs TOUT (Airplane wing domain)

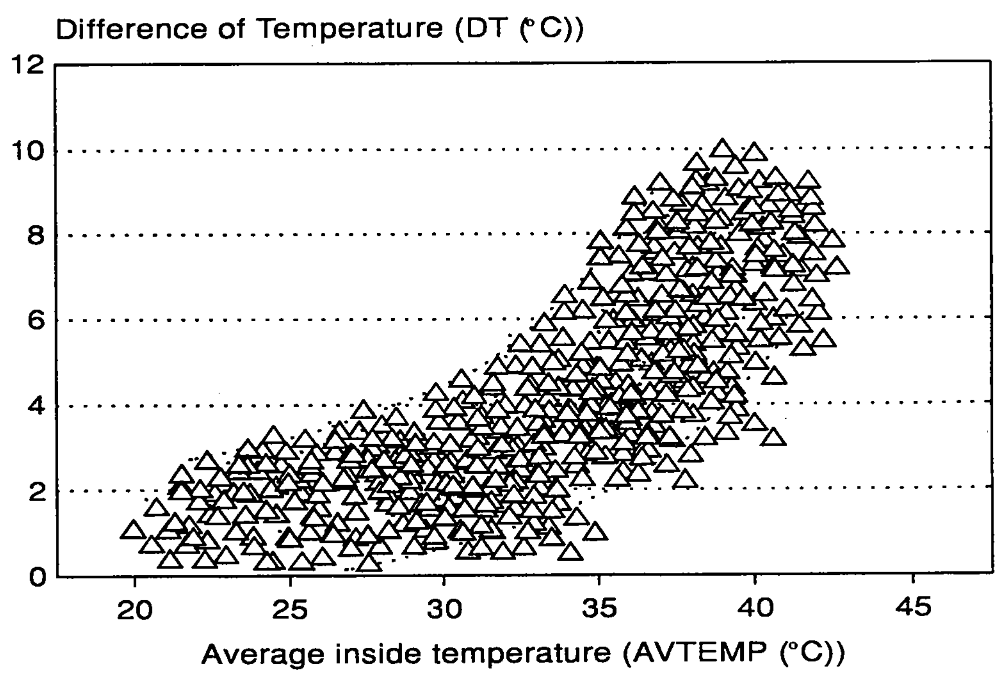

Figure 7.10 DT vs AVTEMP (Banana domain)

outside temperatures (TOUT) were rising. The scattering of average inside temperature (AVTEMP) increases with increasing outside temperatures (TOUT). The domain of data describes a cut of an airplane wing shape. It will be called the "Airplane wing domain".

Figure 7.10 shows a plot of the differences of temperature between inside and outside (DT) versus the average inside temperatures (AVTEMP). The range of difference of temperatures (DT) went from -1 to 9.6 °C when average inside temperatures (AVTEMP) were ranging from 21 to 44.5 °C. This graph shows that the differences of temperature (DT) were getting higher when the average inside temperatures (AVTEMP) were rising. The differences of temperature (DT) follow a curvilinear relationship with the corresponding average inside temperature (AVTEMP). The domain of data describes a banana shape. It is named the "Banana domain".

Figure 7.11 shows a plot of the differences of temperatures (DT) between inside and outside versus the outside temperatures (TOUT). The differences of temperature (DT) ranged from -1 to 9.6 °C when outside temperatures (TOUT) were ranging from 20 to 37 °C. Figure 7.11 shows that the difference of temperatures (DT) is more variable and tends to rise when the outside temperatures (TOUT) are higher. At this level of analysis the differences of temperature (DT) do not follow any specific relationship with the corresponding outside temperature (TOUT). The domain of data describes a pear shape and it was named the "Pear domain".

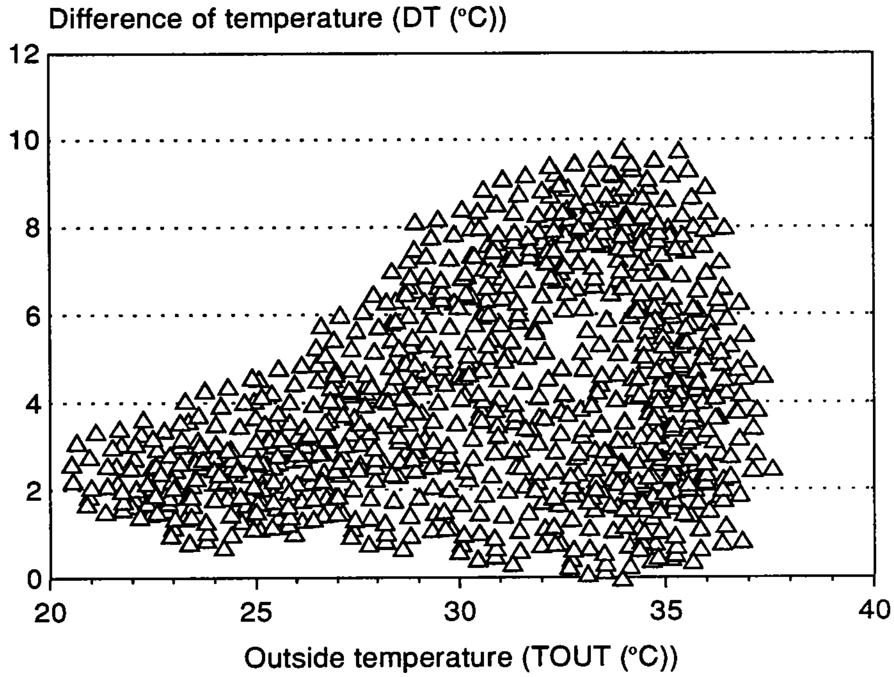

Figure 7.11 DT vs TOUT (Pear domain)

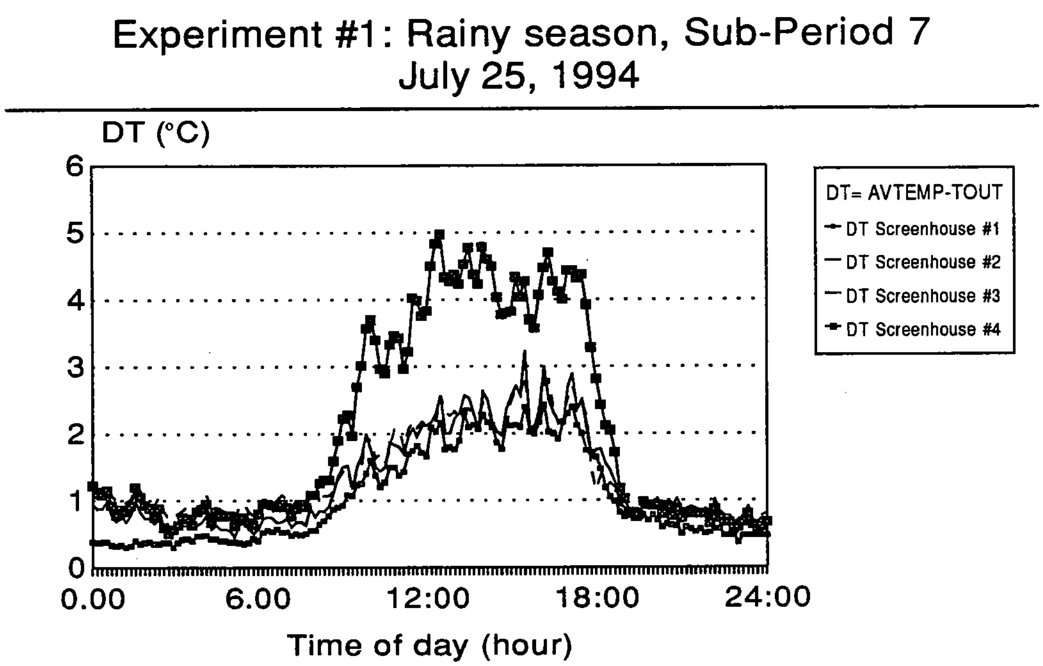

Figure 7.12: Average temperature differences (DT) vs Time

Figures 7.9 to 7.11 all show an increase in the variability of the parameter on the Y-axis when the X-axis parameter increases. The reason for this increased variability is that outside climatic factors like WSO and/or GLOO have more impact on AVTEMP as TOUT increases. The possibility of identifying definite correlations and regression coefficients with Figure 7.11 is more conspicuous because the data are more scattered and there are more possibilities for clearer subdivisions of the data set. The most useful choice is therefore to calculate regression coefficients of DT versus TOUT (Figure 7.11- The Pear Domain) for the various configuration options tested in the experiments. These regression coefficients were calculated and will be presented in section 7.2.2 below.

The primary relationship analyses were limited to graphical interpretations of the whole set of data yet they allowed to select the difference of temperatures between inside and outside the screenhouse (DT) versus the outside temperature (TOUT) as the most interesting relationship to be analyzed with more accurate graphical and statistical methods.

7.2 Difference of Temperatures (DT)

The difference between the inside and the outside temperatures of the screenhouses (DT) is a parameter giving much information about the thermal performance of the various configurations tested in the experiments.

7.2.1 Graphical analyses

Graphical outputs were done using EXCELL and permitted visual interpretations of the data sets.

7.2.1.1 Effect of screenhouse architectural structure types

Figure 7.12 shows typical average inside temperature difference curves for the 4 screenhouses. On the sample day in the rainy season (Experiment #1, Sub-Period 7: July 25, 1994), screenhouse #1 was covered with the Lumite 50 (amber) screen, screenhouse #2 was covered with the Tildenet 32 (white) screen, screenhouse #3 had the Lumite 32 (amber) screen on and screenhouse #4 was covered with the Tildenet 50 (white) screen. For this day of experiment screenhouse #3 and #4 were irrigated with water while screenhouse #1 and #2 were left dry. From this graph it is clear that there were variations of temperature within every screenhouse during that day and that the differences of temperature vary from one screenhouse to the other, screenhouse #4 having the worst cooling performance.

Figure 7.13 shows the average maximum temperatures differences recorded for each configuration tested in the three seasons of experiments. To help recognize which bar in the bar graph corresponds to which screenhouse configuration, the following example describes the proper method for identification. The first group of eight graphs on the far left are the eight maximum temperature differences between inside and outside of screenhouse #1 for the eight different combinations of screen and water that were covering

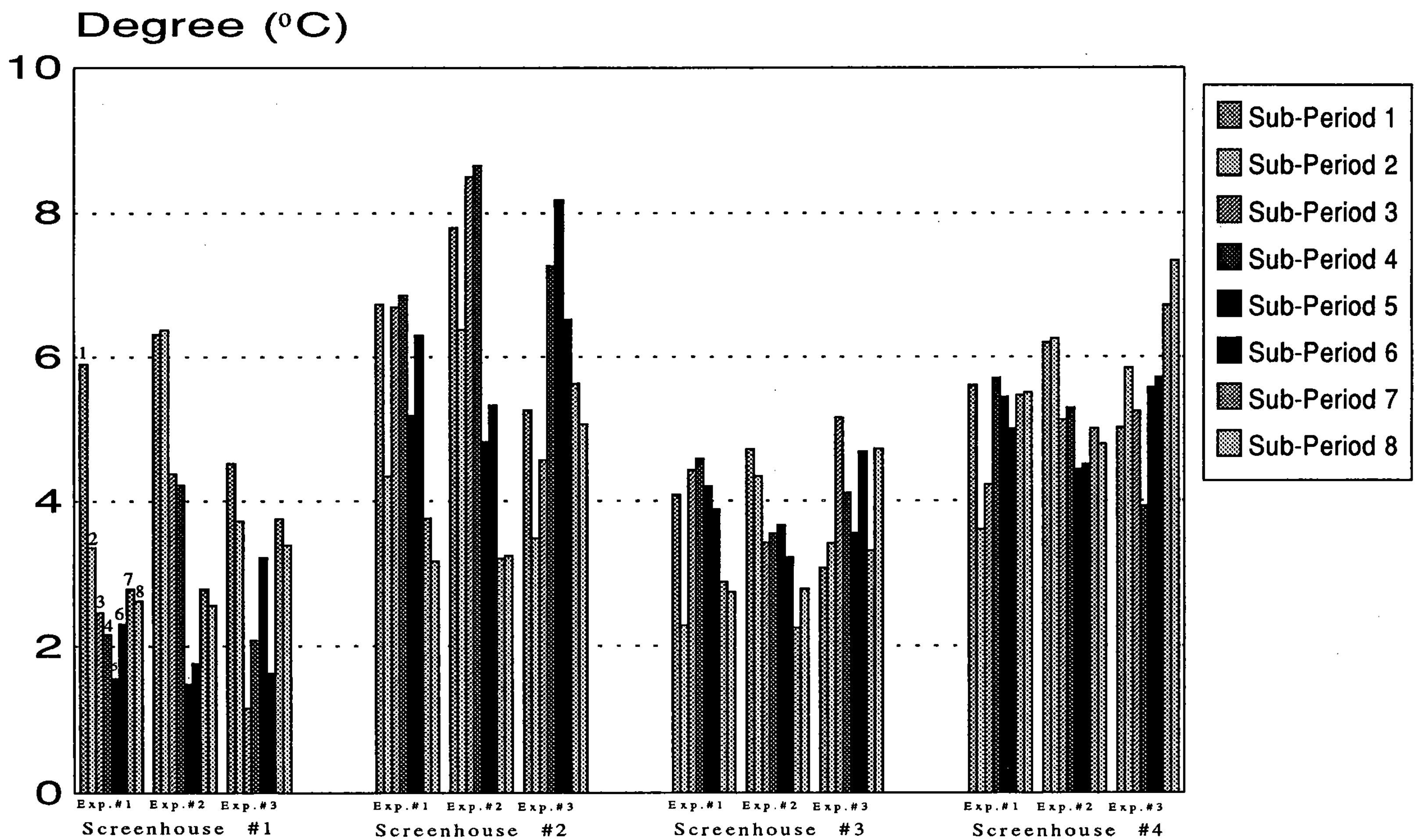

Figure 7.13 Average maximum difference of temperature (DT)

screenhouse #1 in Experiment #1. Referring to the experimental procedure table (Table 5.4), the first bar on the left of that first group corresponds to the maximum difference of temperature obtained in screenhouse #1 when screen #0 (S_0 - Tildenet 50, white, 40% opening) with no water irrigation (S_{0-0}) was covering the house. The value of one maximum difference of temperature bar on the graph is the average of the 5 maximum differences of temperature retrieved from the 5 different days of data resulting from that specific configuration tests (Example: configuration S_{0-0} on screenhouse #1 in experiment #1). The screenhouse-screen-water combinations were repeated exactly the same way for each experiments as described in Table 5.4. All the other maximum difference of temperatures bars in Figure 7.13 can be identified using the same method.

Figure 7.13 shows that there was a tendency for screenhouse #1 to be the coolest screenhouse followed by screenhouse #3 and #4. The graph shows screenhouse #2 as being the warmest. Figure 7.13 shows that the maximum differences of temperature vary quite significantly with the various screen mesh, screen colour and water state combinations. The magnitude of the maximum difference of temperatures followed the sequence of screen-water combinations quite consistently for every season of experiments. For example, the maximum difference of temperature obtained for the S_{0-0} configuration on screenhouse #1, in experiment #1 (the first bar on the left of the group of bars) is the highest of its group. It is also the highest for experiment #3 and very close to be the highest for experiment #2. This same order is followed for the other configurations tested on screenhouse #1 and on the other screenhouses. In other words, one specific screen-water configuration on one specific screenhouse responded in a quite specific way to the outside climate stimuli and this response was similar from one experiment to the other.

The comparisons between the various screenhouse-screen-water configurations responses to the outside climate stimuli were also very consistent. For example, if one specific configurations made one screenhouse react with higher inside differences of temperature compared to another screenhouse configuration, the same result was seen in the other seasons of experimental data.

In conclusion, Figure 7.13 shows that there was a significant relationship between the screenhouse structure type and the inside climate and that screenhouse #1 showed the smallest average maximum differences of temperatures (the coolest screenhouse), followed by screenhouse #3, screenhouse #4 and screenhouse #2. Screenhouse #2 showed the highest maximum differences of temperatures, hence being the warmest screenhouse. Figure 7.13 also shows that there were consistent effects of the screen mesh sizes and water irrigation states on the average maximum differences of temperatures but these effects were not quantifiable with this graph. On Figure 7.13, the colour of the screen does not show an effect on the maximum difference of temperature.

Although the graphical results gave conclusive information about the effects of the screenhouse structural types on the difference between inside and outside screenhouse temperatures (DT), it was still necessary to perform statistical analysis to quantify and classify the relations between the four screenhouse types and DT. The graphical analysis did not provide quantitative and conclusive information on the effects of the two screen mesh sizes, the effects of the two screen colours and the effects of the two water irrigation statuses on DT. These effects also had to be quantified using statistical procedures.

7.2.2 General linear model (GLM) analyses

As mentioned in section 7.1.2, between the three primary relationships sketched, the Pear domains (Figure 7.11 - DT vs TOUT (Pear domain)) is the most interesting one to analyze statistically. Also the scattering of data on this graph indicates the high probability of a better differentiation between the effects of the four parameters studied in this project: 1- the screenhouse structure types, 2- the screen mesh size, 3- the screen colour and 4- the water irrigation status. No specific quantitative relationship between DT and TOUT can be defined for the various effects with Figure 7.11 alone. Assuming that the relationships between DT vs TOUT were linear for the ranges of DT and TOUT measured, it was possible to perform the General Linear Model analysis of the data sets allowing to quantitatively differentiate between the four effects.

A General linear model analysis (GLM) was done with the 25344 records of data measured in the three seasons of experiments. The data were sorted by season of experiments (SEASON= rainy, intermediate or dry), by screenhouse structure types (SCH= 1, 2, 3 or 4), by screen mesh sizes (MESH= 32 or 50), by screen colour (COLOUR= amber or white) and by water irrigation status (WATER = 0 or 1). The model used was DT vs TOUT. Plots of data were also done using SAS graph for every different GLM analysis to visualize the effects of the four parameters.

7.2.2.1 Effect of screenhouse architectural structure types on DT

Tables 7.1, 7.2 and 7.3 summarize the GLM analysis performed on the data to observe the screenhouse architectural types effects on DT. Eight different combinations of screen mesh size, screen colour and water status were tested on each screenhouse in each season of experiments as shown in the three tables. The number of observations, the R^2 values, the estimate of the Y-intercept and the Slope values are presented for each of the 32 possibilities of screenhouse type, screen mesh size, screen colour and water irrigation status for each season of experiments.

For example, the first four lines in Table 7.1 present the GLM results when the four screenhouse types were covered with the 32 mesh size screen (MESH=32) coloured amber (COLOUR=amber) and when no water irrigation was applied (WATER=0) for the rainy season experiment (SEASON=rainy;

Table 7.1 GLM results: Experiment #1 - Rainy season - Screenhouse effect

Mesh	Color	Water	Screenhouse Number	Number of Obs.	R^2	Estimate Y-Intercept	Estimate Slope
32	Amber	0	1	311	0.978	-4.304	1.201
32	Amber	0	2	265	0.922	-8.486	1.427
32	Amber	0	3	263	0.984	-4.958	1.253
32	Amber	0	4	532	0.967	-5.307	1.274
32	Amber	1	1	266	0.975	-6.693	1.302
32	Amber	1	2	270	0.968	-2.917	1.209
32	Amber	1	3	266	0.978	-3.741	1.211
32	Amber	1	4	472	0.911	-6.456	1.340
50	Amber	0	1	266	0.982	-8.616	1.392
50	Amber	0	2	207	0.951	-16.059	1.739
50	Amber	0	3	266	0.978	-8.501	1.416
50	Amber	0	4	N/A	N/A	N/A	N/A
50	Amber	1	1	263	0.973	-7.237	1.323
50	Amber	1	2	262	0.958	-18.606	1.809
50	Amber	1	3	311	0.968	-7.892	1.405
50	Amber	1	4	N/A	N/A	N/A	N/A
32	White	0	1	207	0.991	-5.225	1.234
32	White	0	2	266	0.976	-10.174	1.467
32	White	0	3	270	0.987	-0.779	1.090
32	White	0	4	N/A	N/A	N/A	N/A
32	White	1	1	263	0.030	7.827	0.791
32	White	1	2	263	0.971	-8.088	1.365
32	White	1	3	265	0.931	-1.093	1.115
32	White	1	4	N/A	N/A	N/A	N/A
50	White	0	1	265	0.897	-9.231	1.423
50	White	0	2	311	0.959	-17.514	1.785
50	White	0	3	263	0.040	5.716	0.918
50	White	0	4	529	0.958	-10.948	1.525
50	White	1	1	270	0.967	-2.396	1.163
50	White	1	2	266	0.957	-18.346	1.830
50	White	1	3	207	0.950	-7.246	1.377
50	White	1	4	577	0.956	-11.551	1.560

Table 7.2 GLM results: Experiment #2 - Intermediate season (Rainy/dry) - Screenhouse effect

Mesh	Color	Water	Screenhouse Number	Number of obs.	R^2	Estimate Y-Intercept	Estimate Slope
32	Amber	0	1	319	0.053	20.388	0.283
32	Amber	0	2	261	0.925	-12.761	1.586
32	Amber	0	3	260	0.972	-3.149	1.186
32	Amber	0	4	523	0.549	-3.539	1.229
32	Amber	1	1	262	0.965	-0.527	1.063
32	Amber	1	2	263	0.962	-3.607	1.259
32	Amber	1	3	236	0.963	-2.822	1.155
32	Amber	1	4	474	0.060	22.424	0.364
50	Amber	0	1	236	0.986	-4.708	1.239
50	Amber	0	2	213	0.025	40.871	-0.253
50	Amber	0	3	262	0.966	-3.998	1.230
50	Amber	0	4	N/A	N/A	N/A	N/A
50	Amber	1	1	260	0.968	-4.702	1.235
50	Amber	1	2	260	0.200	4.444	1.029
50	Amber	1	3	319	0.051	21.950	0.260
50	Amber	1	4	N/A	N/A	N/A	N/A
32	White	0	1	213	0.095	43.910	-0.462
32	White	0	2	236	0.975	-6.516	1.307
32	White	0	3	263	0.967	2.715	1.019
32	White	0	4	N/A	N/A	N/A	N/A
32	White	1	1	260	0.142	8.112	0.814
32	White	1	2	260	0.966	-5.617	1.275
32	White	1	3	261	0.886	-1.605	1.160
32	White	1	4	N/A	N/A	N/A	N/A
50	White	0	1	261	0.942	-7.710	1.395
50	White	0	2	319	0.156	14.659	0.565
50	White	0	3	260	0.099	11.805	0.662
50	White	0	4	522	0.943	-7.630	1.392
50	White	1	1	263	0.973	-4.713	1.295
50	White	1	2	262	0.897	-8.401	1.427
50	White	1	3	213	0.125	44.799	-0.501
50	White	1	4	555	0.207	13.312	0.613

Table 7.3 GLM results: Experiment #3 - Dry season - Screenhouse effect

Mesh	Color	Water	Screenhouse Number	Number of Obs.	R^2	Estimate Y-Intercept	Estimate Slope
32	Amber	0	1	324	0.991	-2.891	1.163
32	Amber	0	2	263	0.978	-2.593	1.214
32	Amber	0	3	269	0.964	-4.883	1.267
32	Amber	0	4	540	0.958	-3.164	1.222
32	Amber	1	1	270	0.964	0.017	1.028
32	Amber	1	2	270	0.922	0.821	1.047
32	Amber	1	3	270	0.935	-0.895	1.101
32	Amber	1	4	479	0.928	-1.330	1.142
50	Amber	0	1	270	0.970	-5.494	1.257
50	Amber	0	2	216	0.968	-11.890	1.530
50	Amber	0	3	270	0.970	-3.327	1.215
50	Amber	0	4	N/A	N/A	N/A	N/A
50	Amber	1	1	269	0.963	-6.651	1.292
50	Amber	1	2	270	0.953	-1.576	1.142
50	Amber	1	3	324	0.924	0.815	1.055
50	Amber	1	4	N/A	N/A	N/A	N/A
32	White	0	1	216	0.989	-1.849	1.099
32	White	0	2	270	0.939	-5.198	1.286
32	White	0	3	270	0.986	-0.066	1.087
32	White	0	4	N/A	N/A	N/A	N/A
32	White	1	1	270	0.981	1.419	0.970
32	White	1	2	269	0.953	-6.840	1.322
32	White	1	3	263	0.969	1.543	1.025
32	White	1	4	N/A	N/A	N/A	N/A
50	White	0	1	263	0.987	-3.870	1.241
50	White	0	2	324	0.970	-9.684	1.492
50	White	0	3	270	0.985	-3.999	1.254
50	White	0	4	539	0.918	-4.947	1.296
50	White	1	1	270	0.927	-1.928	1.138
50	White	1	2	270	0.952	-9.065	1.425
50	White	1	3	216	0.972	-1.537	1.134
50	White	1	4	594	0.938	-7.499	1.365

experiment #1). Figure 7.14 shows graphically the linear relationship obtained with the regression coefficients of the GLM analysis, between the four screenhouse types on DT vs TOUT set for that same example.

Figure 7.14 shows that the screenhouse structures have a significant effect on the average inside temperatures. The graph also shows screenhouse #1 as being the coolest (smallest slope) and screenhouse #2 as being the warmest (highest slope). The slopes of the DT vs TOUT line for screenhouse #3 and #4 were between the slope of the DT vs TOUT line of screenhouse #1 and #2. The first four lines in Table 7.1 present the same results with the DT vs TOUT slope of: screenhouse #1 equal to 1.201, screenhouse #2 equal to 1.427, screenhouse #3 equal to 1.253 and screenhouse #4 equal to 1.274 for that same configuration. The R^2 values for this same example indicated that a high percentage of the variability was explainable by the linear relationships. The lowest R^2 value for this example was 0.922 for screenhouse #2.

The Y-intercept results at TOUT= 0 °C are misleading since data were recorded in the range of TOUT= 20 °C to 35 °C as depicted in Figures 7.11 and 7.14. Note that in the range of TOUT lower than 20 °C, the basic assumption that DT vs TOUT is linear would not hold since DT tends to zero even at 20 °C. An extrapolation of the experimental data in the range of TOUT lower than 20 °C leads to the hypothesis that the DT vs TOUT function would be close to asymptotic. It is expected that for TOUT lower than 20 °C, AVTEMP would be equal or lower than TOUT. In other words, DT values would tend to zero as

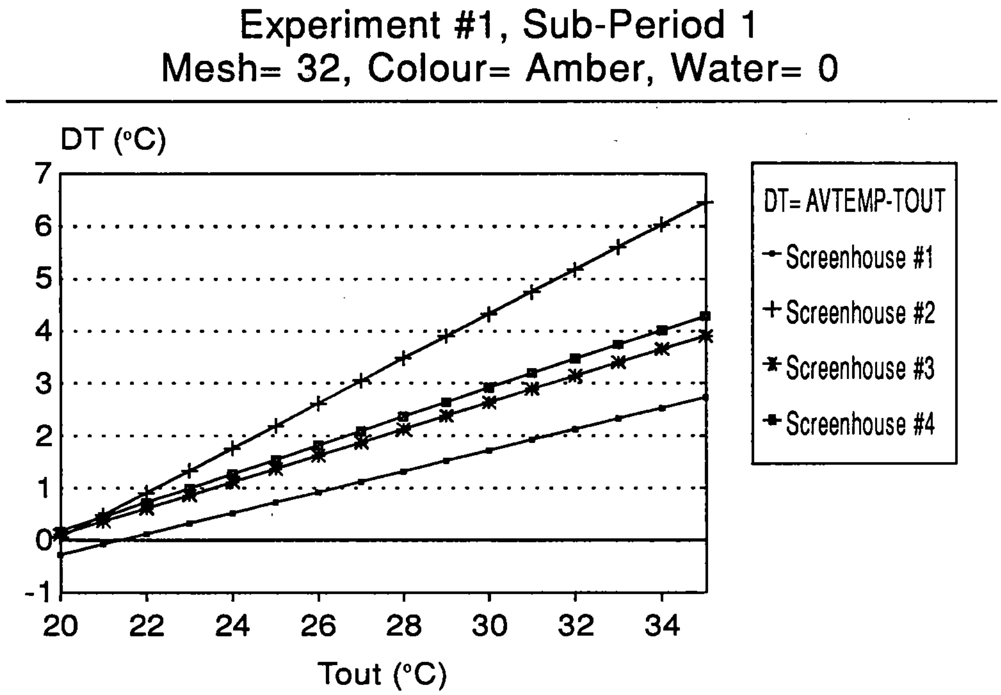

Figure 7.14 DT vs TOUT - Screenhouse effect

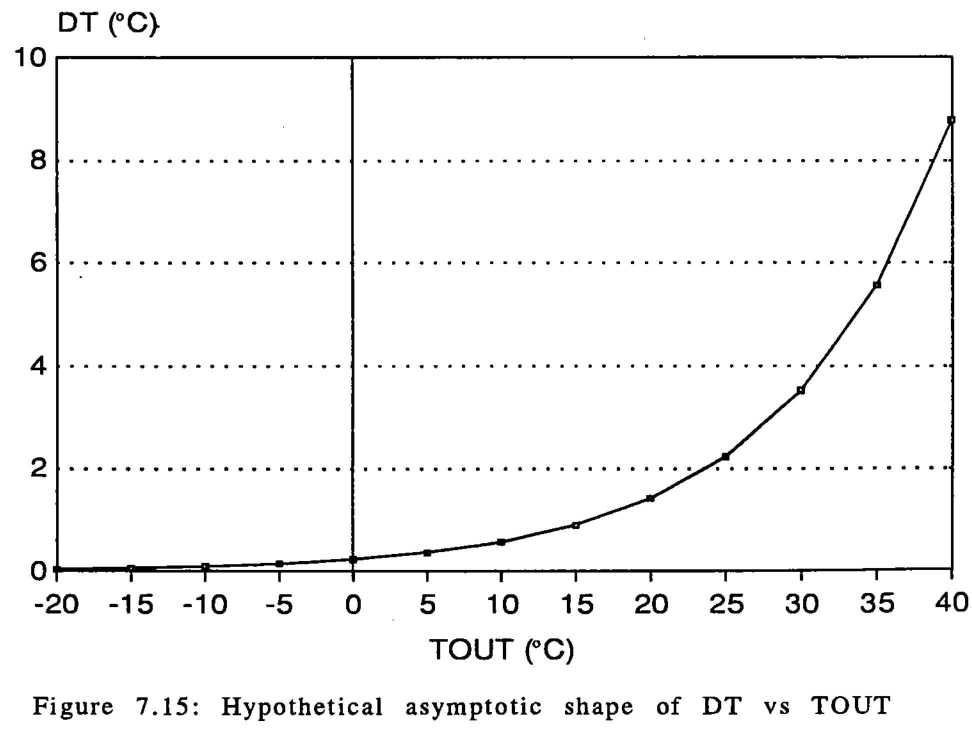

Figure 7.15: Hypothetical asymptotic shape of DT vs TOUT

mentioned above. Figure 7.15 shows the hypothetical DT vs TOUT curve for a large range of TOUT. This hypothetical curve would need to be tested against measured data in the range lower than 20 °C, taking into account the climatic factor involved.

The F-values of the regression procedure showed that the slopes of the DT vs TOUT were all significantly different from zero at the 0.001 level in all cases. The slopes of the DT curves were always positive, showing a tendency for the screenhouses to get warmer with higher outside temperatures.

The regression analysis leads to the conclusion that the screenhouse architectural structure influences DT. Screenhouse #1 turned out to be the coolest screenhouse, having the smallest slope in regression. Screenhouse #2 was the warmest screenhouse. Screenhouses #3 and #4 showed DT vs TOUT slopes between screenhouse #1 and screenhouse #2. It was assumed that the DT vs TOUT function would be asymptotic (Figure 7.15) in the TOUT range lower than 20 °C. This assumption needs to be verified in future studies since the TOUT data range in the present project was in the 20 °C to 35 °C range.

7.2.2.2 Effect of mesh size on DT

Tables 7.4, 7.5 and 7.6 examine the effects of the screen mesh sizes on DT versus TOUT for all the possible configurations in the three experiments. The R^2 values, the Y-intercept values and the slope values of the DT vs TOUT curve are presented for each case. The two mesh sizes examined were: mesh

Table 7.4 GLM results: Experiment #1 - Rainy season - Mesh size effect

Screenh. Number	Color	Water	Mesh	Number of Obs.	R^2	Estimate Y-Intercept	Estimate Slope
1	Amber	0	32	311	0.978	-4.304	1.201
1	Amber	0	50	266	0.982	-8.616	1.392
1	White	0	32	207	0.991	-5.225	1.234
1	White	0	50	265	0.897	-9.231	1.423
1	Amber	1	32	266	0.975	-6.693	1.302
1	Amber	1	50	263	0.973	-7.237	1.323
1	White	1	32	263	0.030	7.827	0.791
1	White	1	50	270	0.967	-2.396	1.163
2	Amber	0	32	265	0.922	-8.486	1.427
2	Amber	0	50	207	0.951	-16.059	1.739
2	White	0	32	266	0.976	-10.174	1.467
2	White	0	50	311	0.959	-17.514	1.785
2	Amber	1	32	270	0.968	-2.917	1.209
2	Amber	1	50	262	0.958	-18.606	1.809
2	White	1	32	263	0.971	-8.088	1.365
2	White	1	50	266	0.957	-18.346	1.830
3	Amber	0	32	263	0.984	-4.958	1.253
3	Amber	0	50	266	0.978	-8.501	1.416
3	Amber	1	32	266	0.978	-3.741	1.211
3	Amber	1	50	311	0.968	-7.892	1.405
3	White	0	32	270	0.987	-0.779	1.090
3	White	0	50	263	0.040	5.716	0.918
3	White	1	32	265	0.931	-1.093	1.115
3	White	1	50	207	0.950	-7.246	1.377
4	Amber	0	32	532	0.967	-5.307	1.274
4	Amber	1	32	472	0.911	-6.456	1.340
4	White	0	50	529	0.958	-10.948	1.525
4	White	1	50	577	0.956	-11.551	1.560

Table 7.5 GLM results: Experiment #2 - Intermediate season (Rainy-dry) - Mesh size effect

Screenh. Number	Color	Water	Mesh	Number of Obs.	R^2	Estimate Y-Intercept	Estimate Slope
1	Amber	0	32	319	0.053	20.388	0.283
1	Amber	0	50	236	0.986	-4.708	1.239
1	White	0	32	213	0.095	43.910	-0.462
1	White	0	50	261	0.942	-7.710	1.395
1	Amber	1	32	262	0.965	-0.527	1.063
1	Amber	1	50	260	0.968	-4.702	1.235
1	White	1	32	260	0.142	8.112	0.814
1	White	1	50	263	0.973	-4.713	1.295
2	Amber	0	32	261	0.925	-12.761	1.586
2	Amber	0	50	213	0.025	40.871	-0.253
2	White	0	32	236	0.975	-6.516	1.307
2	White	0	50	319	0.156	14.659	0.565
2	Amber	1	32	263	0.962	-3.607	1.259
2	Amber	1	50	260	0.200	4.444	1.029
2	White	1	32	260	0.966	-5.617	1.275
2	White	1	50	262	0.897	-8.401	1.427
3	Amber	0	32	260	0.972	-3.149	1.186
3	Amber	0	50	262	0.966	-3.998	1.230
3	White	0	32	263	0.967	2.715	1.019
3	White	0	50	260	0.099	11.805	0.662
3	Amber	1	32	236	0.963	-2.822	1.155
3	Amber	1	50	319	0.051	21.950	0.260
3	White	1	32	261	0.886	-1.605	1.160
3	White	1	50	213	0.125	44.799	-0.501
4	Amber	0	32	523	0.549	-3.539	1.229
4	Amber	1	32	474	0.060	22.424	0.364
4	White	0	50	522	0.943	-7.630	1.392
4	White	1	50	555	0.207	13.312	0.613

Table 7.6 GLM results: Experiment #3 - Dry season - Mesh size effect

Screenh. Number	Color	Water	Mesh	Number of Obs.	R^2	Estimate Y-Intercept	Estimate Slope
1	Amber	0	32	324	0.991	-2.891	1.163
1	Amber	0	50	270	0.970	-5.494	1.257
1	White	0	32	216	0.989	-1.849	1.099
1	White	0	50	263	0.987	-3.870	1.241
1	Amber	1	32	270	0.964	0.017	1.028
1	Amber	1	50	269	0.963	-6.651	1.292
1	White	1	32	270	0.981	1.419	0.970
1	White	1	50	270	0.927	-1.928	1.138
2	Amber	0	32	263	0.978	-2.593	1.214
2	Amber	0	50	216	0.968	-11.890	1.530
2	White	0	32	270	0.939	-5.198	1.286
2	White	0	50	324	0.970	-9.684	1.492
2	Amber	1	32	270	0.922	0.821	1.047
2	Amber	1	50	270	0.953	-1.576	1.142
2	White	1	32	269	0.953	-6.840	1.322
2	White	1	50	270	0.952	-9.065	1.425
3	Amber	0	32	269	0.964	-4.883	1.267
3	Amber	0	50	270	0.970	-3.327	1.215
3	White	0	32	270	0.986	-0.066	1.087
3	White	0	50	270	0.985	-3.999	1.254
3	Amber	1	32	270	0.935	-0.895	1.101
3	Amber	1	50	324	0.924	0.815	1.055
3	White	1	32	263	0.969	1.543	1.025
3	White	1	50	216	0.972	-1.537	1.134
4	Amber	0	32	540	0.958	-3.164	1.222
4	Amber	1	32	479	0.928	-1.330	1.142
4	White	0	50	539	0.918	-4.947	1.296
4	White	1	50	594	0.938	-7.499	1.365

32 and mesh 50. In all cases where there was a good linear fit of the data (ie. the R^2 values were high), the 50 mesh screen (the smallest hole sizes) resulted in a higher DT values for the same TOUT, than did the 32 mesh screen (the largest hole sizes). As an example, the first two lines of Table 7.4 show that the slope of the DT vs TOUT curve for screenhouse #1 covered with the 32 mesh amber screen and without water irrigation was 1.201 where the 50 mesh amber screen was 1.392 in the same conditions. Figure 7.16 is the graphical representation of that example. For the same reasons explained in section 7.2.2.1, the Y-intercept values in tables 7.4, 7.5 and 7.6 are misleading and should be interpreted in the same way.

The 50 mesh screens resulted in higher DT values in all cases. This leads to the conclusion that higher inside screenhouse temperatures were expected when the screen mesh size was higher or in other words, when the screen hole sizes were smaller. The physical reasoning of these results is that smaller hole sizes of the covering screen restricted the movement of air across the screen and hence reduced ventilation. The effect of the hole sizes on the natural ventilation coefficient will be studied in section 7.4 below.

7.2.2.3 Effect of colour on DT

Tables 7.7, 7.8 and 7.9 present the R^2 values, the Y-intercept values and the slopes of the DT vs TOUT curves in terms of the effects of the screen colours for each configurations tested in the three experiments. The slopes

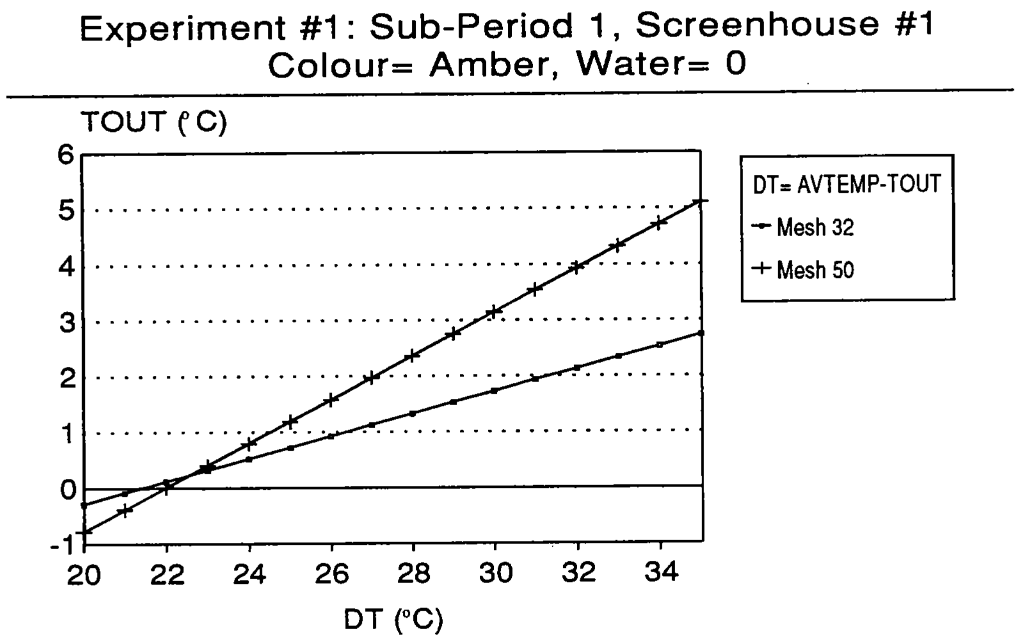

Figure 7.16 DT vs TOUT - Mesh size effect

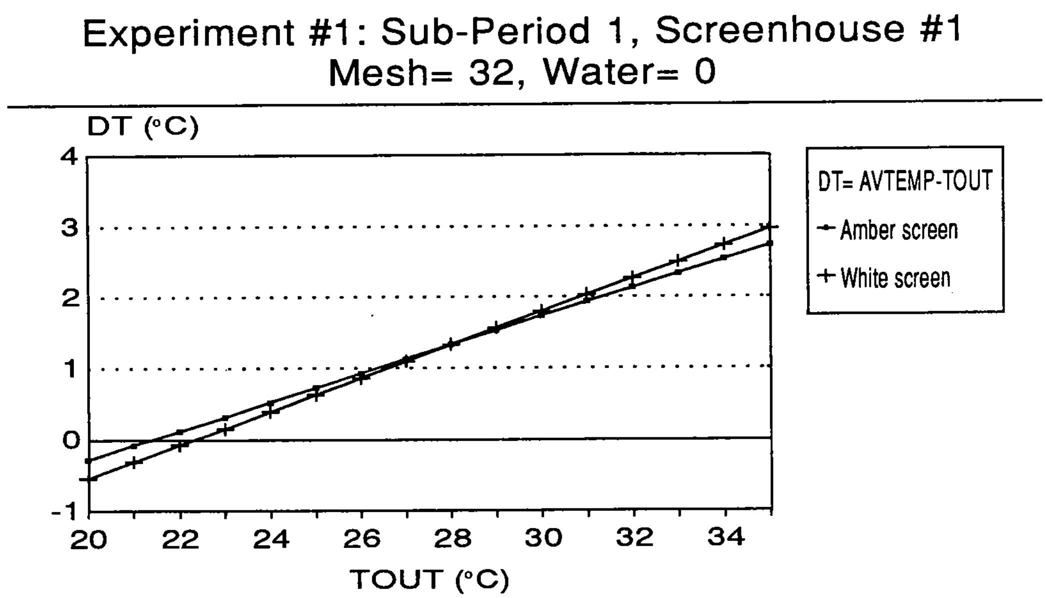

Figure 7.17 DT vs Tout - Colour effect

Table 7.7 GLM Results: Experiment #1 - Rainy season - Colour effect

Screenh. Number	Color	Water	Mesh	Number of Obs.	R^2	Estimate Y-Intercept	Estimate Slope
1	Amber	0	32	311	0.978	-4.304	1.201
1	White	0	32	207	0.991	-5.225	1.234
1	Amber	1	32	266	0.975	-6.693	1.302
1	White	1	32	263	0.030	7.827	0.791
1	Amber	0	50	266	0.982	-8.616	1.392
1	White	0	50	265	0.897	-9.231	1.423
1	Amber	1	50	263	0.973	-7.237	1.323
1	White	1	50	270	0.967	-2.396	1.163
2	Amber	0	32	265	0.922	-8.486	1.427
2	White	0	32	266	0.976	-10.174	1.467
2	Amber	0	50	207	0.951	-16.059	1.739
2	White	0	50	311	0.959	-17.514	1.785
2	Amber	1	32	270	0.968	-2.917	1.209
2	White	1	32	263	0.971	-8.088	1.365
2	Amber	1	50	262	0.958	-18.606	1.809
2	White	1	50	266	0.957	-18.346	1.830
3	Amber	0	32	263	0.984	-4.958	1.253
3	White	0	32	270	0.987	-0.779	1.090
3	Amber	0	50	266	0.978	-8.501	1.416
3	White	0	50	263	0.040	5.716	0.918
3	Amber	1	32	266	0.978	-3.741	1.211
3	White	1	32	265	0.931	-1.093	1.115
3	Amber	1	50	311	0.968	-7.892	1.405
3	White	1	50	207	0.950	-7.246	1.377
4	Amber	0	32	532	0.967	-5.307	1.274
4	Amber	1	32	472	0.911	-6.456	1.340
4	White	0	50	529	0.958	-10.948	1.525
4	White	1	50	577	0.956	-11.551	1.560

Table 7.8 GLM results: Experiment #2 - Intermediate season (Rainy-dry) - Colour effect

Screenh. Number	Color	Water	Mesh	Number of Obs.	R^2	Estimate Y-Intercept	Estimate Slope
1	Amber	0	32	319	0.053	20.388	0.283
1	White	0	32	213	0.095	43.910	-0.462
1	Amber	0	50	236	0.986	-4.708	1.239
1	White	0	50	261	0.942	-7.710	1.395
1	Amber	1	32	262	0.965	-0.527	1.063
1	White	1	32	260	0.142	8.112	0.814
1	Amber	1	50	260	0.968	-4.702	1.235
1	White	1	50	263	0.973	-4.713	1.295
2	Amber	0	32	261	0.925	-12.761	1.586
2	White	0	32	236	0.975	-6.516	1.307
2	Amber	0	50	213	0.025	40.871	-0.253
2	White	0	50	319	0.156	14.659	0.565
2	Amber	1	32	263	0.962	-3.607	1.259
2	White	1	32	260	0.966	-5.617	1.275
2	Amber	1	50	260	0.200	4.444	1.029
2	White	1	50	262	0.897	-8.401	1.427
3	Amber	0	32	260	0.972	-3.149	1.186
3	White	0	32	263	0.967	2.715	1.019
3	Amber	0	50	262	0.966	-3.998	1.230
3	White	0	50	260	0.099	11.805	0.662
3	Amber	1	32	236	0.963	-2.822	1.155
3	White	1	32	261	0.886	-1.605	1.160
3	Amber	1	50	319	0.051	21.950	0.260
3	White	1	50	213	0.125	44.799	-0.501
4	Amber	0	32	523	0.549	-3.539	1.229
4	Amber	1	32	474	0.060	22.424	0.364
4	White	0	50	522	0.943	-7.630	1.392
4	White	1	50	555	0.207	13.312	0.613

Table 7.9 GLM results: Experiment #3 - Dry season - Colour effect

Screenh. Number	Color	Water	Mesh	Number of Obs.	R^2	Estimate Y-Intercept	Estimate Slope
1	Amber	0	32	324	0.991	-2.891	1.163
1	White	0	32	216	0.989	-1.849	1.099
1	Amber	0	50	270	0.970	-5.494	1.257
1	White	0	50	263	0.987	-3.870	1.241
1	Amber	1	32	270	0.964	0.017	1.028
1	White	1	32	270	0.981	1.419	0.970
1	Amber	1	50	269	0.963	-6.651	1.292
1	White	1	50	270	0.927	-1.928	1.138
2	Amber	0	32	263	0.978	-2.593	1.214
2	White	0	32	270	0.939	-5.198	1.286
2	Amber	0	50	216	0.968	-11.890	1.530
2	White	0	50	324	0.970	-9.684	1.492
2	Amber	1	32	270	0.922	0.821	1.047
2	White	1	32	269	0.953	-6.840	1.322
2	Amber	1	50	270	0.953	-1.576	1.142
2	White	1	50	270	0.952	-9.065	1.425
3	Amber	0	32	269	0.964	-4.883	1.267
3	White	0	32	270	0.986	-0.066	1.087
3	Amber	0	50	270	0.970	-3.327	1.215
3	White	0	50	270	0.985	-3.999	1.254
3	Amber	1	32	270	0.935	-0.895	1.101
3	White	1	32	263	0.969	1.543	1.025
3	Amber	1	50	324	0.924	0.815	1.055
3	White	1	50	216	0.972	-1.537	1.134
4	Amber	0	32	540	0.958	-3.164	1.222
4	Amber	1	32	479	0.928	-1.330	1.142
4	White	0	50	539	0.918	-4.947	1.296
4	White	1	50	594	0.938	-7.499	1.365

were very similar in all cases, demonstrating a small effect of the screen colour on the screenhouse inside climates. The GLM analysis also showed that the differences between the slopes of the DT vs TOUT curves were rarely significant for the two colours.

Figure 7.17 shows a comparison between the slope of the white and amber screens of 32 mesh size on screenhouse #1 without water irrigation (same example as the first two lines in Table 7.17). The DT vs TOUT slopes of the two configurations were almost identical.

The colour of the screens during the experiments were affected by deposits of red laterite which was abundant in the local water system. The laterite would stain the screen with a reddish colour. The stains were more visible on the white screens. Filters were used at the inlet of the water irrigation system to remove as much of the laterite as possible. Even with the filters, the screens would still get stained reddish. The screens were washed after every period of experiments (10 days). Even with these red stains, the DT vs TOUT values did not exhibit a significant difference between the effects of the white and amber screens, proving that colour was not a significant factor affecting the inside screenhouse climate.

7.2.2.4 Effect of water irrigation on DT

Tables 7.10, 7.11 and 7.12 present the effect of water irrigation status on the DT vs TOUT curves. Figure 7.18 is a sample plot of the water irrigation

Table 7.10 GLM results: Experiment #1 - Rainy season - Water effect

Screenh. Number	Color	Water	Mesh	Number of Obs.	R^2	Estimate Y-Intercept	Estimate Slope
1	Amber	0	32	311	0.978	-4.304	1.201
1	Amber	1	32	266	0.975	-6.693	1.302
1	White	0	32	207	0.991	-5.225	1.234
1	White	1	32	263	0.030	7.827	0.791
1	Amber	0	50	266	0.982	-8.616	1.392
1	Amber	1	50	263	0.973	-7.237	1.323
1	White	0	50	265	0.897	-9.231	1.423
1	White	1	50	270	0.967	-2.396	1.163
2	Amber	0	32	265	0.922	-8.486	1.427
2	Amber	1	32	270	0.968	-2.917	1.209
2	White	0	32	266	0.976	-10.174	1.467
2	White	1	32	263	0.971	-8.088	1.365
2	Amber	0	50	207	0.951	-16.059	1.739
2	Amber	1	50	262	0.958	-18.606	1.809
2	White	0	50	311	0.959	-17.514	1.785
2	White	1	50	266	0.957	-18.346	1.830
3	Amber	0	32	263	0.984	-4.958	1.253
3	Amber	1	32	266	0.978	-3.741	1.211
3	White	0	32	270	0.987	-0.779	1.090
3	White	1	32	265	0.931	-1.093	1.115
3	Amber	0	50	266	0.978	-8.501	1.416
3	Amber	1	50	311	0.968	-7.892	1.405
3	White	0	50	263	0.040	5.716	0.918
3	White	1	50	207	0.950	-7.246	1.377
4	Amber	0	32	532	0.967	-5.307	1.274
4	Amber	1	32	472	0.911	-6.456	1.340
4	White	0	50	529	0.958	-10.948	1.525
4	White	1	50	577	0.956	-11.551	1.560

Table 7.11 GLM results: Experiment #2 - Intermediate season (Rainy-dry) - Water effect

Screenh. Number	Color	Water	Mesh	Number of Obs.	R^2	Estimate Y-Intercept	Estimate Slope
1	Amber	0	32	319	0.053	20.388	0.283
1	Amber	1	32	262	0.965	-0.527	1.063
1	White	0	32	213	0.095	43.910	-0.462
1	White	1	32	260	0.142	8.112	0.814
1	Amber	0	50	236	0.986	-4.708	1.239
1	Amber	1	50	260	0.968	-4.702	1.235
1	White	0	50	261	0.942	-7.710	1.395
1	White	1	50	263	0.973	-4.713	1.295
2	Amber	0	32	261	0.925	-12.761	1.586
2	Amber	1	32	263	0.962	-3.607	1.259
2	White	0	32	236	0.975	-6.516	1.307
2	White	1	32	260	0.966	-5.617	1.275
2	Amber	0	50	213	0.025	40.871	-0.253
2	Amber	1	50	260	0.200	4.444	1.029
2	White	0	50	319	0.156	14.659	0.565
2	White	1	50	262	0.897	-8.401	1.427
3	Amber	0	32	260	0.972	-3.149	1.186
3	Amber	1	32	236	0.963	-2.822	1.155
3	Amber	0	50	262	0.966	-3.998	1.230
3	Amber	1	50	319	0.051	21.950	0.260
3	White	0	32	263	0.967	2.715	1.019
3	White	1	32	261	0.886	-1.605	1.160
3	White	0	50	260	0.099	11.805	0.662
3	White	1	50	213	0.125	44.799	-0.501
4	Amber	0	32	523	0.549	-3.539	1.229
4	Amber	1	32	474	0.060	22.424	0.364
4	White	0	50	522	0.943	-7.630	1.392
4	White	1	50	555	0.207	13.312	0.613

Table 7.12 GLM results: Experiment #3 - Dry season - Water effect

Screenh. Number	Color	Water	Mesh	Number of Obs.	R^2	Estimate Y-Intercept	Estimate Slope
1	Amber	0	32	324	0.991	-2.891	1.163
1	Amber	1	32	270	0.964	0.017	1.028
1	White	0	32	216	0.989	-1.849	1.099
1	White	1	32	270	0.981	1.419	0.970
1	Amber	0	50	270	0.970	-5.494	1.257
1	Amber	1	50	269	0.963	-6.651	1.292
1	White	0	50	263	0.987	-3.870	1.241
1	White	1	50	270	0.927	-1.928	1.138
2	Amber	0	32	263	0.978	-2.593	1.214
2	Amber	1	32	270	0.922	0.821	1.047
2	White	0	32	270	0.939	-5.198	1.286
2	White	1	32	269	0.953	-6.840	1.322
2	Amber	0	50	216	0.968	-11.890	1.530
2	Amber	1	50	270	0.953	-1.576	1.142
2	White	0	50	324	0.970	-9.684	1.492
2	White	1	50	270	0.952	-9.065	1.425
3	Amber	0	32	269	0.964	-4.883	1.267
3	Amber	1	32	270	0.935	-0.895	1.101
3	White	0	32	270	0.986	-0.066	1.087
3	White	1	32	263	0.969	1.543	1.025
3	Amber	0	50	270	0.970	-3.327	1.215
3	Amber	1	50	324	0.924	0.815	1.055
3	White	0	50	270	0.985	-3.999	1.254
3	White	1	50	216	0.972	-1.537	1.134
4	Amber	0	32	540	0.958	-3.164	1.222
4	Amber	1	32	479	0.928	-1.330	1.142
4	White	0	50	539	0.918	-4.947	1.296
4	White	1	50	594	0.938	-7.499	1.365

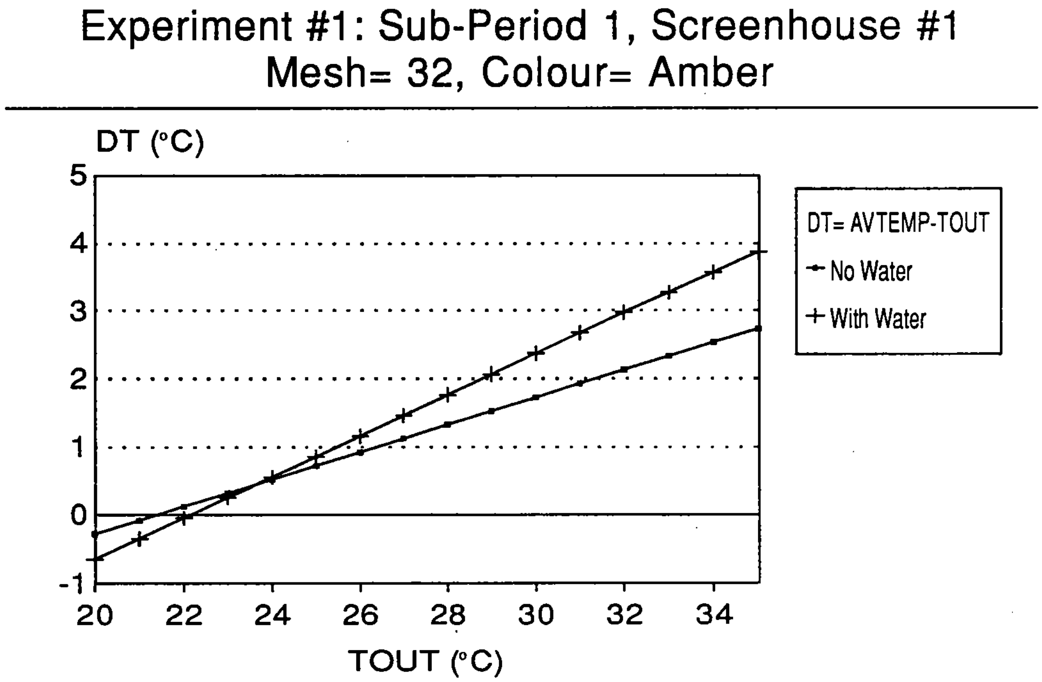

Figure 7.18 DT vs TOUT - Water effect

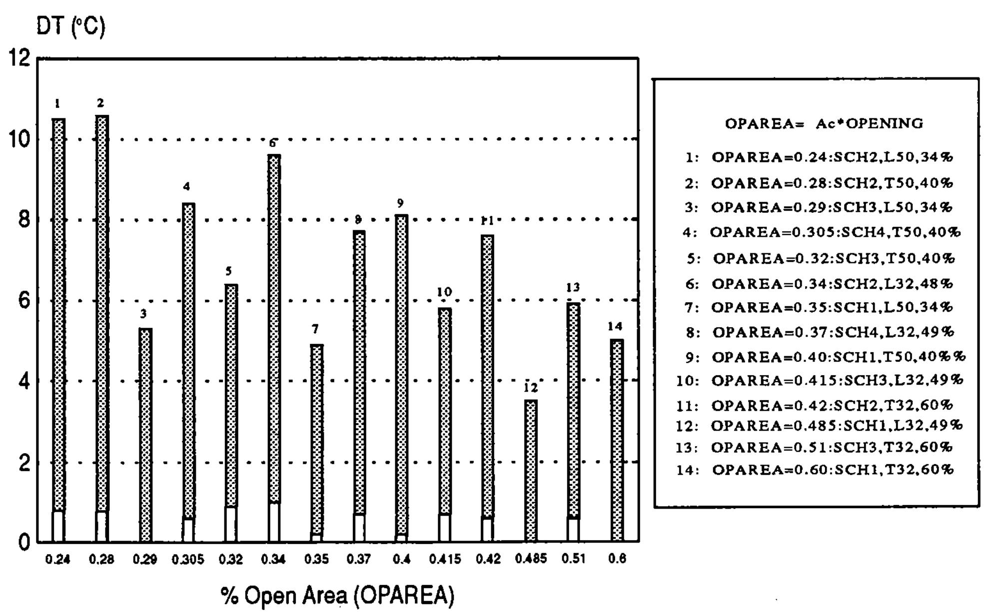

Figure 7.19 DT vs OPAREA

effect on DT for screenhouse #1 covered with the Lumite 32 mesh Amber screen in experiment #1. Although the regression analysis showed DT vs TOUT slopes to be significantly different in more cases than for the colour effect case, the water irrigation effect was not always as expected. The initial hypothesis was that water irrigation would cause evaporative cooling hence lowering DT. The DT vs TOUT slopes did not always lower slope when water irrigation was applied on the screenhouse, contradicting the initial hypothesis. This can be explained by a few reasons. First, it was noticed that the water curtain flowing on the screens and the capacity of the screen to attract water inside its holes, blocked the movement of air through the screenhouse. This reduced the natural ventilation capacity of the screenhouse and led to a counter-cooling effect. Measurements of temperature of the screen with and without water irrigation demonstrated clearly that evaporative cooling was taking place at the screen wall surface, especially in dry conditions, but the inside air temperature measurements did not show these effects as clearly.

The high relative humidity conditions encountered in the three seasons of experiments did not favour the occurrence of evaporative cooling. Yet, the water irrigation had a higher cooling effect in the rainy season than in the two other season of tests as demonstrated by the highest slope values obtained in Table 7.10. This can be explained by the fact that in the dry season, the relative humidity values were still quite high (between 60% and 78%, 90% of the time) and the outside temperatures were much higher most of the time than in the two other seasons. The water cooling was more efficient when outside temperatures were relatively lower, like in the rainy season, even if the ambient relative humidity was high.

Another reason why the water irrigation did not show as much effect on DT as expected was related to the temperature of the water used to irrigate during the experiments. The temperature of water was measured in the irrigation hose during the experiment and was usually around 29 °C to 30 °C. These temperatures were very close to the measured ambient temperature (TOUT) and cooler water would necessarily demonstrate a greater cooling effect.

Hypothesis 4) in section 3.3) stated: "Water cooling is an energy efficient method to cool screenhouses in humid tropical climate". The measurement of temperatures of screens and water at the screen surface and the regression results on DT vs TOUT have succeeded to prove two points: 1) there was an evaporative cooling effect at the screen surface and 2) the highest water cooling effect on DT vs TOUT was recorded in the rainy season. These results were obtained even when the water temperatures, used for irrigating the screenhouses, were high. These results prove that there is potential for the use of water evaporative techniques for cooling in humid tropical conditions and demonstrate the validity of hypothesis 4). Whether the water cooling is efficient or not in reaching a specific cooling objective (eg. in this research, the objective was to cool the inside screenhouse air as much as possible), much depends on the physical configuration of the evaporative cooling apparatus. In this research, the apparatus was the screen which held water well, but this set up was not cooling efficiently since the water itself was blocking the wind which is responsible for both the evaporative cooling and the natural ventilation cooling effect.

To conclude, water irrigation had a significant effect on the DT vs TOUT slopes but this effect was not always a cooling effect. Water irrigation on the screens created a wall that blocked the air movements in and out of the screenhouse and counteracted the desired water cooling effects. Evaporative cooling effects were observed at the screen surface. High relative humidity conditions did not favour evaporative cooling yet the highest cooling effects were still observed in the rainy season. The evaporative cooling techniques have potential in humid tropical conditions but the physical configurations need further design to achieve higher cooling efficiency.

7.2.2.5 DT vs OPAREA

The total % free open area of the various configuration of screenhouses tested in the experiments was calculated and used as an experimental parameter called OPAREA. OPAREA was calculated using Eqn. 39.

$$OPAREA = A_c * OPENING \qquad \textbf{(39)}$$

The OPAREA parameter quantifies the % total free open area of a specific screenhouse-screen configuration and it was calculated by multiplying the total area of cover (A_c) by the size of opening of the screen (OPENING) covering the screenhouse. There were fourteen resulting values of OPAREA for the experiment, one for each screenhouse-screen configuration. Screenhouses #1, #2 and #3 have four OPAREA values because they were covered with four screens each and screenhouse #4 has two OPAREA values because screenhouse #4 was tested with only two screens.

The advantage of using the fourteen resulting OPAREA values as experimental parameters was that they quantify the overall open surface area of the screenhouse. As described in Eqn. 20, the area of opening of a building is essential to calculate the Natural Ventilation coefficient, N_{υ}.

The DT values obtained for the three experiments were plotted against OPAREA in Figure 7.19. This graph shows the range of differences of temperature obtained for the fourteen total % free open area (OPAREA) tested. The graph shows that screenhouse #1 with the Lumite 32 (amber, 48.5% opening, OPAREA=0.47, position 12) gives the smaller differences of temperature range, followed very closely by screenhouse #1 with the Tildenet 32 (white, 60.1% opening, OPAREA=0.6, position 14) screen. The higher differences of temperature ranges were obtained with screenhouse #2 with the Lumite 50 (amber, 34.9% opening, OPAREA=0.24, position 1) and the Tildenet 50 (white, 40.5% opening, OPAREA=0.28, position 2) screens. This was a clear indication that the total % free opening area (OPAREA) plays an important role on the inside temperature performance of the screenhouse. The highest OPAREA gave the lowest range of DT while the lowest OPAREA gave the largest DT range. Yet, it can also be said that generally screenhouses #1 and #3 have the lowest ranges even if in some cases, as for OPAREA=0.29 (screenhouse #3, Lumite 50, amber, 34% opening, position 3) and OPAREA = 0.32 (screenhouse #3, Tildenet 50, white, 40% opening, position 5), the OPAREA values were not the highest. This also indicates that the architectural structure plays a role too.

In conclusion, the graphical and regression analyses of the difference of temperature (DT) parameter in the experimentally measured range both lead to the following statements: Screenhouse #1 was the coolest screenhouse, followed by #3 and #4. The warmest was screenhouse #2. When the high mesh size screens (smaller size of holes) were used, the highest DT vs TOUT slopes were obtained. Water irrigation did not always have the expected cooling effects on DT but these effects were still significant. The screen colour had the smallest effect on DT vs TOUT slopes.

7.3 Transmissivity (τ)

Figure 7.20 shows typical Global and PAR (Photosynthetically Active Radiation) transmissivity curves for two screenhouses studied on July 25, 1994 (Sub-Period 7, Experiment #1, rainy season). Global and PAR transmissivity were both defined by Eqn. 36 using the global radiation or the PAR radiation values respectively for the calculation. The global transmissivity values were hence obtained by dividing the inside radiation values by the outside radiation values measured simultaneously.

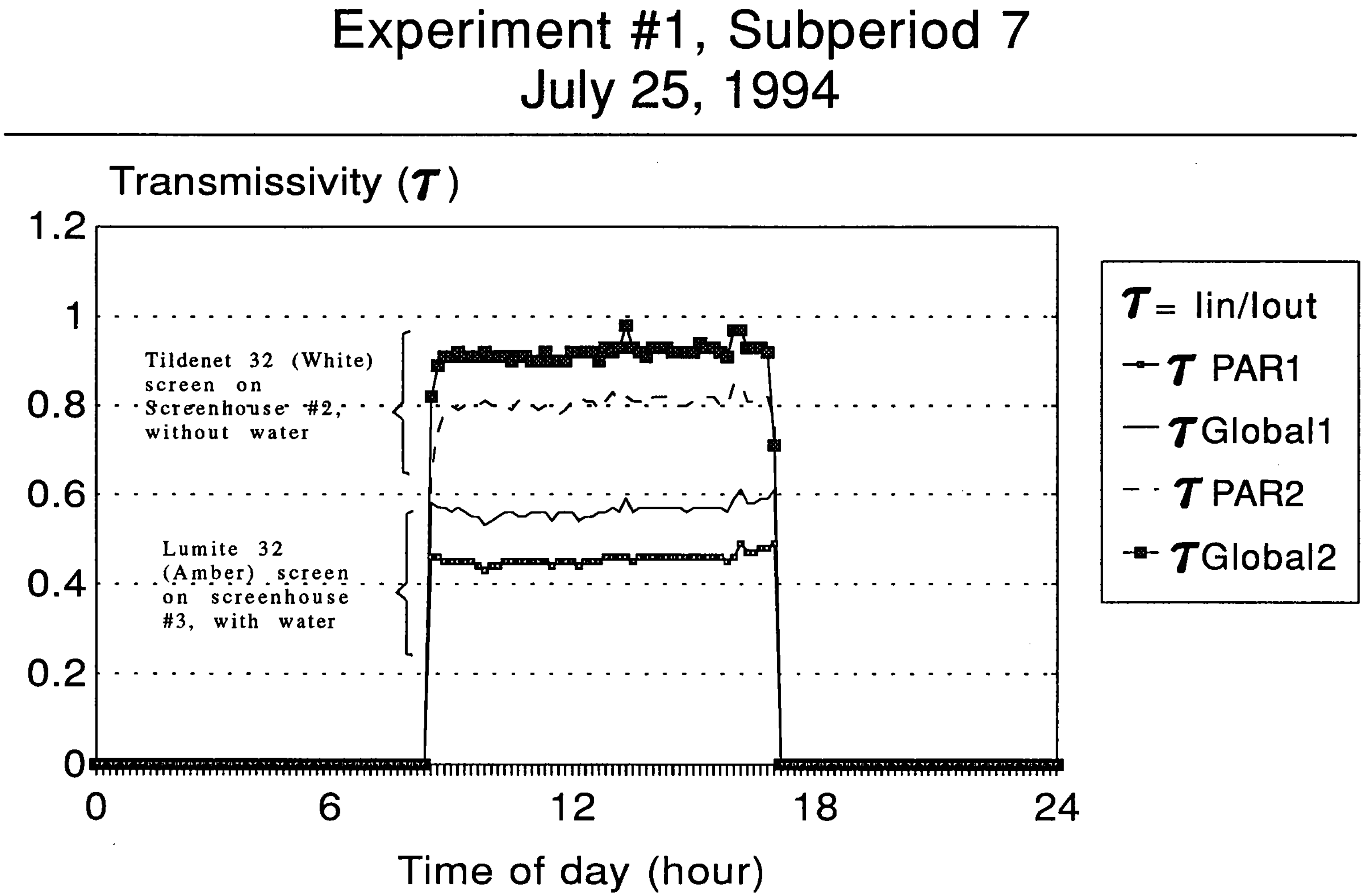

Figure 7.19: Transmissivity values (τ)

On July 25 1994, the first pair of radiation sensors (PAR and Global) was installed in screenhouse #3 while the second pair was measuring radiations in screenhouse #2. Screenhouse #3 was equipped with the Lumite 32 (amber) screen and was on the irrigation mode. Screenhouse #2 wore the Tildenet 32 (white) screen and was not irrigated.

Figure 7.20 shows that during the course of one day, the transmissivity values do not vary much. Similar graphs were plotted for each day of the experiments and the transmissivity values were always constant during one day. On July 25, screenhouse #3 showed lower values of transmissivity than screenhouse #2 for both PAR and global radiation. The PAR transmissivity values were lower than the global values. This was observed for every day of experiments.

The effects of the structure types, of the screen colours, of the screen mesh sizes and of the water irrigation status on the global transmissivity values were analyzed in the next section. Global radiation was chosen for this analysis because it is the factor utilised for calculation of radiative heat transfer.

7.3.1 Effect of screenhouse architectural structure types on global τ

The average global transmissivities for every subperiod of experiments (5 days) and for every screenhouse were calculated and plotted in Figure 7.21. Since Figure 7.21 is the same type of bar graph as Figure 7.13 that was presented in section 7.2.1.1, the same method of identification presented in

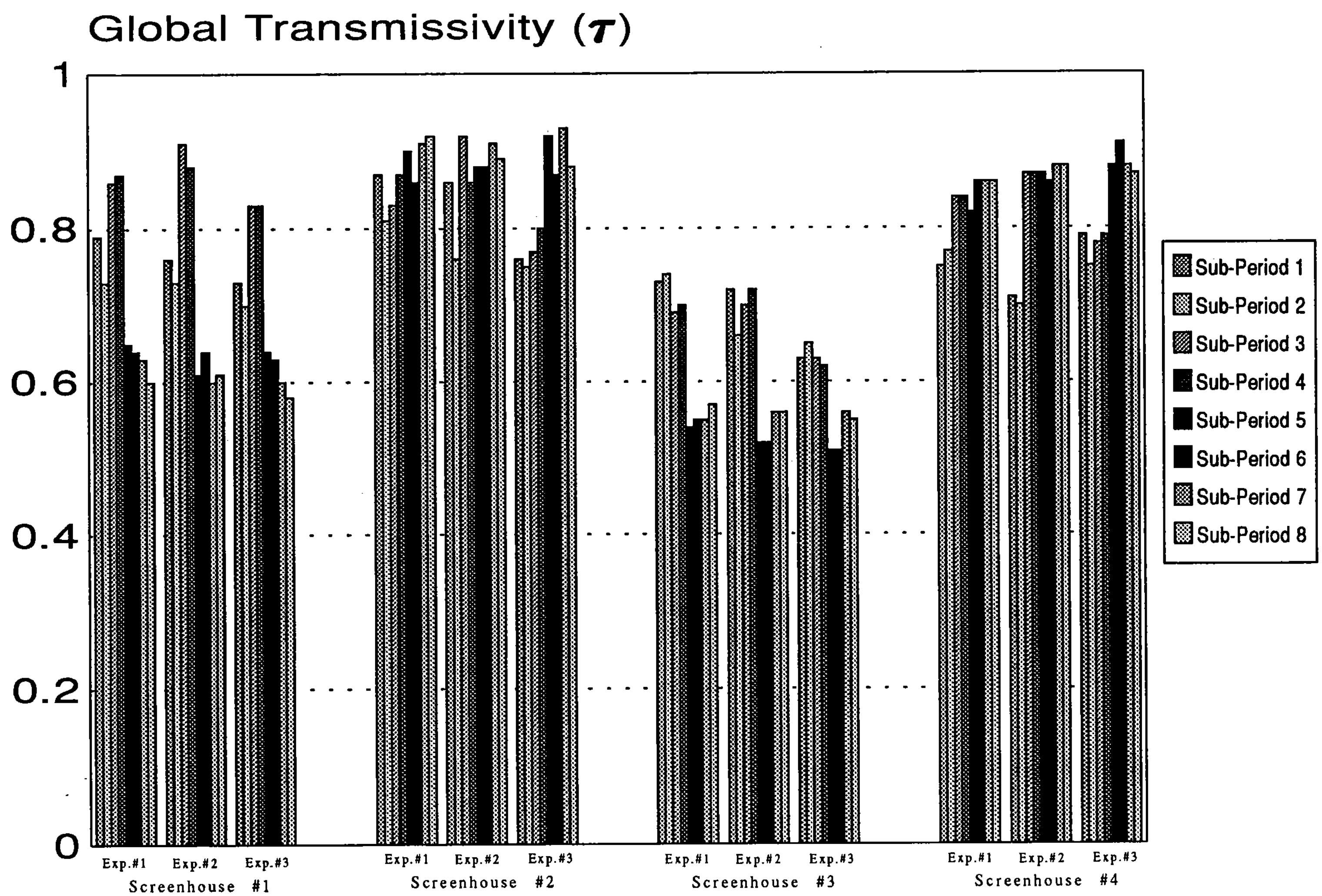

Fig 7.21 Average Global Transmissivity (τ)

that section was used to identify which bar in the graph corresponds to which configuration.

Figure 7.21 shows that over all the experiments, the global transmissivity values were influenced differently in each of the screenhouses. Screenhouse #3 showed the lowest global transmissivity values followed by screenhouse #1 and #4. Screenhouse #2 demonstrated the highest transmissivity. The latter is explained by the fact that Teflon is very transparent to solar radiation and was covering screenhouse #2 and #4 constantly for all the experiments. Screenhouse #4 exhibits lower values than screenhouse #2 because the percentage of area covered by the Teflon for screenhouse #4 was lower than for screenhouse #2, and was thus more influenced by the screen colour. Also, the tunnel shape of screenhouse #4 was allowing the screens to be higher on the ends of the screenhouse, thus permitting more light to cross the screens from the sides. It was also the reason for the more distinct change of the global transmissivity values when the colours change on screenhouse #4 compared to #2.

Light has to cross two layers, one of Teflon and one of screen, before getting into screenhouse #3. This is why it demonstrates the lower transmissivity values. For screenhouse #1, light has to cross only one screen layer apparently being less transparent than Teflon alone because it shows lower global transmissivity values than screenhouse #3 and #4.

7.3.2 Effect of colour on global τ

Figure 7.21 shows very distinct differences in the transmissivity values obtained for the different colours of screens used on screenhouse #1 and screenhouse #3. Referring to Table 5.4, it can be seen that screenhouse #1 was covered with the white screens for the first two periods of testing (P1:S_0 and P2:S_3; on Figure 7.21: the first four bars for the three experiments on screenhouse #1) and with the amber screens for the last periods of tests (P3:S_2 and P4:S_1; on Figure 7.21: the four last bars on the right for the three experiments on screenhouse #1). Figure 7.21 shows that the amber screen gives significantly lower values than the white screens for screenhouse #1 in the three seasons of experiments.

The differences in transmissivity between the white and the amber screens were not as large for screenhouses #2 and #4 but were still present. This is explained by the fact that screenhouses #2 and #4 were covered by a layer of Teflon that stayed in place for all experiments, thus resulting in more constant transmissivity values. For screenhouses #1 and #3, the white screen shows the higher transmissivity values for all the cases, while the amber screen results in the lower values.

7.3.3 Effect of mesh sizes on global τ

Figure 7.21 shows that the effect of mesh size was quite small compared to the effect of colours. The colour and mesh size may have a cumulative effect but the colour effect was dominant. Results indicated that τ values were directly proportionally related to the screen hole sizes of the screens or, in other words, inversely proportional to the screen mesh sizes. The smaller screen hole sizes (the higher mesh sizes) resulted in small transmissivity values and the bigger hole sizes (the smaller mesh sizes) exhibited high transmissivity values.

7.3.4 Effect of water irrigation on global τ

Figure 7.21 shows that water irrigation had a small effect on the global transmissivity values compared to the colour effect and the screen mesh size effect. For example, the four resulting τ values for the amber screen on screenhouse #1 of experiment #1 (on Figure 7.21: the four last of the first eight bars on the left of the graph) were almost identical and do not show any effect of the water irrigation status.

7.4 Natural Ventilation Coefficient, N_υ

The effects of the four parameters (the screenhouse structure types, the screen mesh size, the screen colour and the water irrigation status) on the natural ventilation (N_υ) were studied both quantitatively and qualitatively. Most of the quantitative results on the effects of the four parameters on the natural ventilation coefficients (N_υ) were obtained from the wind speed measurements outside the screenhouses and the air velocity measurements inside the screenhouses. Wind speed measurements performed in controlled conditions using a small scale wind tunnel lead to quantification of C_υ (Air velocity coefficients) for the four screens tested. Most of the qualitative and descriptive results on N_v were obtained from the smoke tests section. The quantitative and qualitative results lead to estimations of N_v.

7.4.1 Wind speed and wind direction outside the screenhouse.

Figures 7.1 and 7.2 show the frequency distributions of the wind speeds and wind directions that occurred during the whole experimental period. Figure 7.1 shows that the maximum outside wind speed recorded was around 2.7 m/s (9.7 km/h) and that the most frequent occurrences of recorded wind speeds were ranging between 1.5 and 2 m/s (5.4 to 7.2 km/h). Thus the experimental screenhouses were subjected to relatively low wind speeds. Figure 7.2 shows that winds were mainly from South-West direction (between 180° and 270°). The wind speed and wind direction data were in concordance with the climatic characteristics of the Cotonou region described in section 5.1.2.

7.4.2 Air velocity measurements inside the screenhouse (v)

During the whole set of experiments and for all the outside conditions tested, the air velocity (v) inside the screenhouse was always low. The horizontal air velocity (v) measured inside the screenhouses ranged from zero to a maximum of 0.25 m/s for all outside conditions tested. Most often the air speed measurements were between 0.1 and 0.2 m/s.

7.4.3 Estimation of C_v using a small scale wind tunnel

A small scale wind tunnel was fabricated and used to perform air speed measurements in controlled conditions in a laboratory at IITA-Benin station

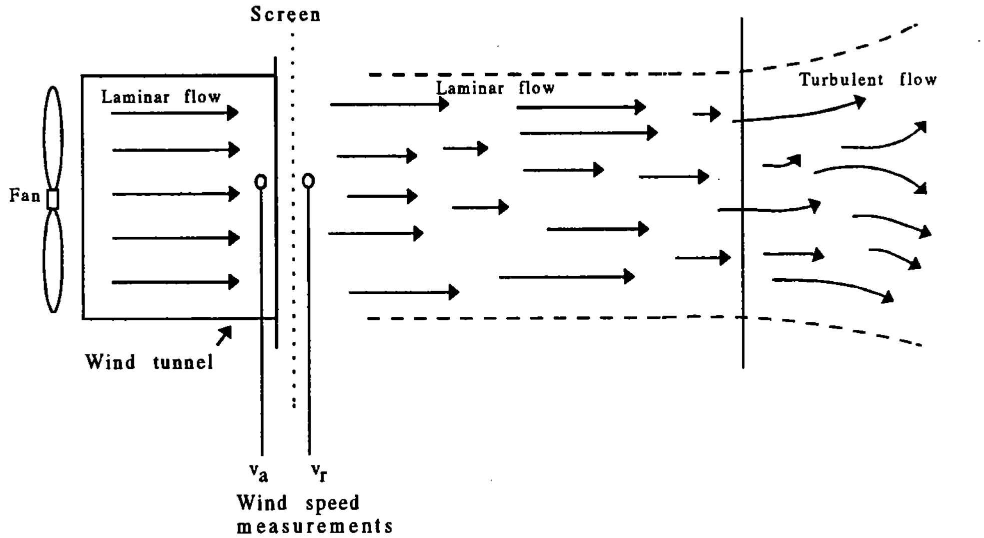

Figure 7.22 Small scale wind tunnel tests (Cv determination)

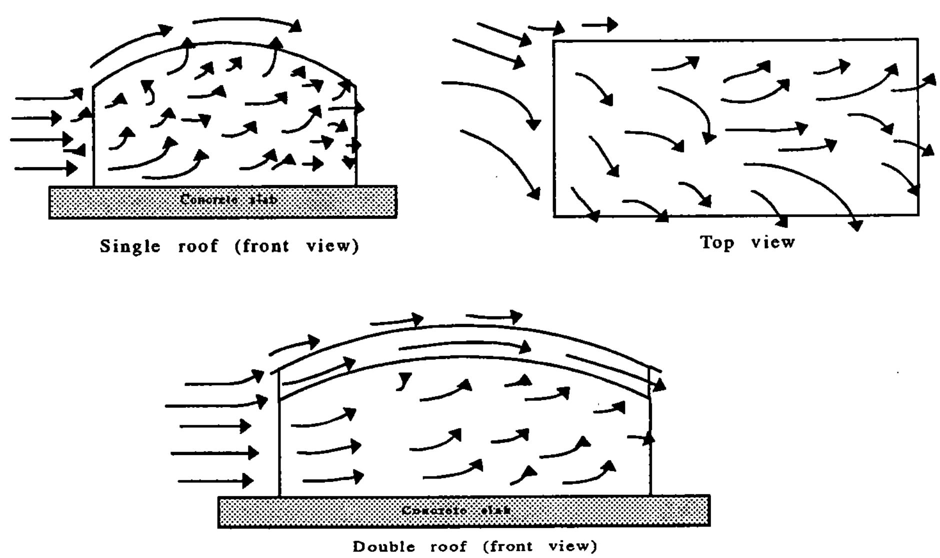

Figure 7.23 Typical air movements

to estimate the air velocity coefficient (C_{υ}). Figure 7.22 shows a sketch of the experimental set up. The wind tunnel consisted of a fan blowing in a cardboard box segmented in cells constructed with cardboard sheets. The small scale wind tunnel was calibrated to obtain laminar flow. The tested screens were placed at the air exit of the wind tunnel where laminar flow was occurring. Air velocity measurements were performed before the air had hit the screens (air approach velocity, υ_a) and after the air had crossed the screen surface (air remaining velocity, υ_r). C_{υ} was calculated using Eqn. 40.

$$C_{\upsilon} = \frac{\upsilon_r}{\upsilon_a} \quad \textbf{(40)}$$

Results showed that the air velocity coefficient (C_{υ}) was constant for one specific screen in the range of approach velocities of 0 to 2 m/s. C_{υ} is dependent on the hole size, and ranged from 0.43 to 0.73 as shown in Table 7.13.

Table 7.13- Air velocity coefficient, C_{υ}

Screen Type	Mesh	Colour	%opening	C_{υ}
S1- Lumite	50	Amber	34.9	0.43
S0- Tildenet	50	White	40.5	0.55
S2- Lumite	32	Amber	48.5	0.60
S3- Tildenet	32	White	60.1	0.73

In Eqn. 20, N_{υ} is expressed in terms of C_q:

$$N_v = \frac{C_q \; v \; A_c}{V} \qquad \textbf{(20)}$$

In the ideal case of unidirectional laminar flow C_q can be approximated by C_v. The relationship between C_v and C_q is only trivial in this ideal case, otherwise C_q differs from C_v. Assuming ideal conditions, the N_v coefficient can be approximated using the estimated C_v instead of C_q in Eqn. 20.

Wet screens were also tested with the small scale wind tunnel set up. These tests showed that a screen that has its hole interstices filled by a water film would almost completely block the air movement across the screen as long as the water film resisted in place. After a few minutes of flow of air in the screen, the water would dry out and let the air flow cross the screen with the same C_v as in Table 7.13.

7.4.4 Smoke tests

On site visual aerodynamic tests were performed using DRAGER smoke tube air movement detectors. The smoke tests were performed inside the screenhouse to visualise the nature of the air movements in screenhouses for different outside conditions and for various screenhouse configurations. Air movements were also sketched close to the screen walls and screen or teflon roofs outside the screenhouse using the smoke tubes.

7.4.4.1 Air movement inside the screenhouses

These smoke tests showed that in the conditions tested, the air movements inside the screenhouse were neither uniform nor unidirectional.

Examples of general patterns of the air movement were sketched in Figure 7.23. The side view shows the outside air coming from the west side of the screenhouse. When the air hits the screen, much of it gets deflected to the sides or over the top of the screenhouse. The air that does cross the screen surface, moves very slowly inside the screenhouse, at first following the direction in which it entered and then very rapidly swirling into eddies in many horizontal direction with a vertical component due to the inside temperature gradient. Vertical wind speed component ranging from 0 to 0.15 m/s were measured with a hot wire anemometer inside the screenhouses. These wind speeds were in the same magnitude range as the horizontal wind speed measurements. Vertical temperature gradients as high as 5 °C from close to floor to close to roof were measured inside the screenhouse. The vertical air movement component was more obvious in the screenhouse with a single layer teflon roof (screenhouse #2 and #4) but was also observed in the other two screenhouses. The general flow through the screenhouse is shown in Figure 7.23 - (Top view); however other patterns were observed from time to time. For example, there were episodes of air exiting from the same side as it had entered.

7.4.4.2 Air movement and air speed between the double layer roof

Smoke test observations and air speed measurements showed a tendency for the air to move more rapidly between the two layer roof of screenhouse #3 (Figure 7.23 - Double roof: side view). The apparent reason for this venturi-type phenomenon would be due to the constriction offered by the semi-circular shape of the roof, creating negative pressures on the perimeter of the roof area. This phenomenon appeared to help exhaust air through the first layer screen roof because of the suction it created. Air velocities as high as 3 m/s (10.8 km/h) were measured in between the two roofs of screenhouse #3, when the maximum outside wind speeds values recorded were in the range of 2.7 m/s (9.7 km/h) as mentioned in section 7.4.1 above. This also suggests that the distance between the first layer roof and the second roof has an effect on N_υ. It also suggest the idea of creating venturi effects on every side of the screenhouse surface to improve the ventilation. Yet, these specific effects were not measured in this experiment but subjects for future research.

7.4.4.3 <u>Other factors affecting air movements and air speed</u>

Other factors seem to affect the distribution of air speed and air movements inside and near the screenhouse. Such parameter were the architectural shape of the screenhouse. For example, there was a definite difference between the way the Tunnel screenhouse (screenhouse #4) deflected the incoming wind compared to the Rossel screenhouse (screenhouse #3). For example, winds blowing in the East-West axis followed over the semi-circular shape of screenhouse #4 (Tunnel shape) near its Teflon roof surface while the same winds from the same direction were blocked, diverted or crossed the screen surface of screenhouse #3.

The smoke tests also showed that there were definite effects of the wind direction on the inside and near the screenhouse air speed and air movements. The air patterns inside and near the screenhouse were quite different when the winds blew along the North-South axis than when they blew along the East-West axis.

Another parameter that also has a definite effect on the air speed and air movements was the size of holes of the screen used to cover the screenhouse. Bigger holes (smaller Mesh size) lets the air flow easily, while small holes obstruct the air flow. These effects were demonstrated quantitatively in ideal condition in section 7.4.3 above.

The smoke tests also gave an indication that roof ventilation was quite important for screenhouse with one layer screen roof (screenhouse #1 and #3). As mentioned in 7.4.4.2, the double roof seemed to accentuate the ventilation. Also, for screenhouse #1 which had only one layer of screen as a roof, there was a definite tendency for the air to exhaust across that screen roof. In screenhouse #2 and #4, the uprising air was blocked by the impermeable Teflon roof and either stayed stagnant or moved in other directions.

The air movement smoke tests were useful to qualitatively describe the air movements patterns inside and close to outside the screenhouses. The smoke tests determined that the conditions of measurements in the natural wind conditions were not ideal. A scaled model screenhouse wind tunnel study in ideal controlled wind conditions would bring more precision in the determination of N_v and air movement patterns and is suggested for further studies. One of the objectives of these further studies would be to increase N_v as much as possible by varying the structure, screen and water configurations in the best way respecting the design specifications. As in the present research, configuration parameters are interacting together on the same heat transfer characteristics. Yet, it is possible to quantify these effects.

7.4.5 Quantitative determination of N_v

The Natural ventilation coefficient N_v describes the air movement phenomena in a purely quantitative manner. In that sense, N_v is limited to a quantity. The quantity expressed by N_v is fundamental for the calculation of the heat transfer in and out of the screenhouses (Eqn. 19). It is therefore essential to have the best quantitative approximation of the N_v coefficient.

The method used to evaluate N_v in the experiment was to measure the wind speed inside the screenhouse, at a fixed location but in many directions. The inside wind speed measurements were related to the simultaneous outside wind speed and direction measurements to relate the N_v values to outside wind speed. This method proved to be quite limiting mainly because of the non-uniform and multi-directional flow of air inside and outside the screenhouse as it was described in section 7.4.4 above. Yet, these measurements showed that inside air speed were always very low (between 0 and 0.25 m/s) for outside wind speed that could be as high as 2.7 m/s (Section 7.4.2). Most often the air speed measurements inside the screenhouse ranged between 0.1 to 0.2 m/s.

In the present section, the quantitative effects of the screenhouse architectural structure types, of the screen mesh size, of the screen colour of the water on the Natural ventilation coefficient N_{υ} were evaluated.

7.4.5.1 Effect of the screenhouse architectural structure types on N_{υ}

As an example, if in an ideal case where the air was flowing uniformly and unidirectionally, and if the air was moving at 0.1 m/s from one screenhouse side to the other in a 6 m wide screenhouse, it would take 60 seconds (1 min.) for one molecule of air to cross the screenhouse in its whole width. This result gave an N_{v} being equal to 1 air change per minute. Since the smoke tests revealed that the conditions of wind measurement testing were non-ideal, a quantitatively estimated N_{υ} would necessarily be lower than the ideal N_{υ} value.

In the present case it was estimated that the ratio between the N_{υ} values in non ideal conditions and the N_{υ} values in ideal case will be 0.25. Since measurements of inside wind speeds have ranged from 0 to 0.2 m/s most of the time during the whole experimental period, for all outside condition tested, it was estimated that the N_{υ} values in these non ideal conditions were varying from 0.1 to 0.5 air change per minute. As will be seen in section 7.6, these N_{υ} values were used for the simulation of the inside temperature prediction and gave good prediction results.

7.4.5.2 Effect of the screen mesh sizes on N_υ

The effect of mesh size on N_υ was clearly demonstrated in section 7.4.3. As mentioned in that section, in the ideal case of unidirectional laminar flow C_q values can be approximated by C_υ values. The relationship between the C_υ values and the C_q values is only trivial in this ideal case, otherwise C_q values differ from C_υ values. An exact N_υ (and hence C_q) evaluation would consider all the air movement patterns of the inside screenhouse. C_υ only describes the restriction offered by the screen to the air right at the screen surface. Even if C_υ gives an approximation of the effect of mesh size for the ideal laminar case, the C_υ values were not readily usable for the evaluation of the effect of the mesh size on N_υ non ideal cases. The approximation presented in 7.4.5.1 above still holds for the evaluation of N_υ.

7.4.5.3 Effect of the screen colour on N_υ

The screen colour did not have a measurable effect on N_υ. Theoretically, since the colour of the screen had a large effect on τ values and since τ values affect the heat balance of the screenhouse to a large extent, the colour of the screen should affect the temperature gradients inside the screenhouse and hence N_υ. These effects were not detected with the measurements performed in this experiment. To quantify such an effect, wind tunnel controlled conditions are necessary. Yet these effects are expected to be quite small, the proof being that they were not measured in this experiment.

7.4.5.4 Effect of the water irrigation on N_v

Water irrigation on the screens provoked a tendency for a water film to form in the interstice of the screen hole as already mentioned in section 7.2.2.4. Also, as measured in section 7.4.1, the water film could completely block the air flow across the screens. In the experience, the water irrigation curtain was flowing quite uniformly over all the surface of the screen but was not always covering the screen surface completely at all time. Ventilation was still occurring, even if the water irrigation status was on, but to a lesser degree than when the screens were completely dry. The water curtain had direct effect on the air exchange rate and therefore on N_v. This phenomena explains the rise of temperatures inside the screenhouse when water irrigation was applied. The blocking of the air flow by the water counterbalanced the desired evaporative cooling effect.

To conclude, the quantitative measurements and the qualitative descriptions resulted in an estimated N_v coefficient ranging from 0.1 air change per minute when inside screenhouse wind speed were around 0.04 m/s (at night for example) to 0.5 air change per minute for the inside screenhouse wind speed measurements of 0.2 m/s (during normal day conditions).

7.5 Global Heat Transfer Coefficient (U)

As mentioned in section 6.4.3.5, the UVALUES.BAS (Appendix B) was used to calculate U-values with night data (from 00:00 (midnight) till 6:40) for every 120 days of experiments (Table 5.4 - 8 subperiods, 5 days in 3 seasons) using Eqn. 36 and 37 according to the configuration tested. As explained in section 6.4.3, night data are used to eliminate the effects of solar radiations. Average U-values for each Sub-period (5 days) were calculated and plotted in Figure 7.24, differentiating each screenhouse and each experiment. To recognise which bar is associated with which screenhouse-screen-water configuration, the method of identification presented in section 7.2.1.1 was utilised.

At first glance, the cause-effect relationship of the independent parameters: the screenhouse architectural types, the mesh size and the colour on the global heat transfer coefficient U, does not appear to be a simplistic, direct and straightforward one. The U-values presented in Figure 7.24 do not show the effect of water irrigation because for the night data used, no water irrigation was applied on any screenhouse.

Figure 7.24 shows U-values ranging from 0.1 to 11.1 W/m^2 °C. On the average, screenhouse #3 presented the smallest range of U-values. The U-values of the same screen on the same screenhouse but in different experiments varied. No simplistic relationships between the U-values and the structural, the screen parameters and the water status were observed. The fact that U-values were calculated for night data only suggest that varied screenhouse configuration parameters (structure, screen, water) would have little effect on the U-values since these configuration parameters have high interaction levels with solar radiation. The results of the U-values themselves

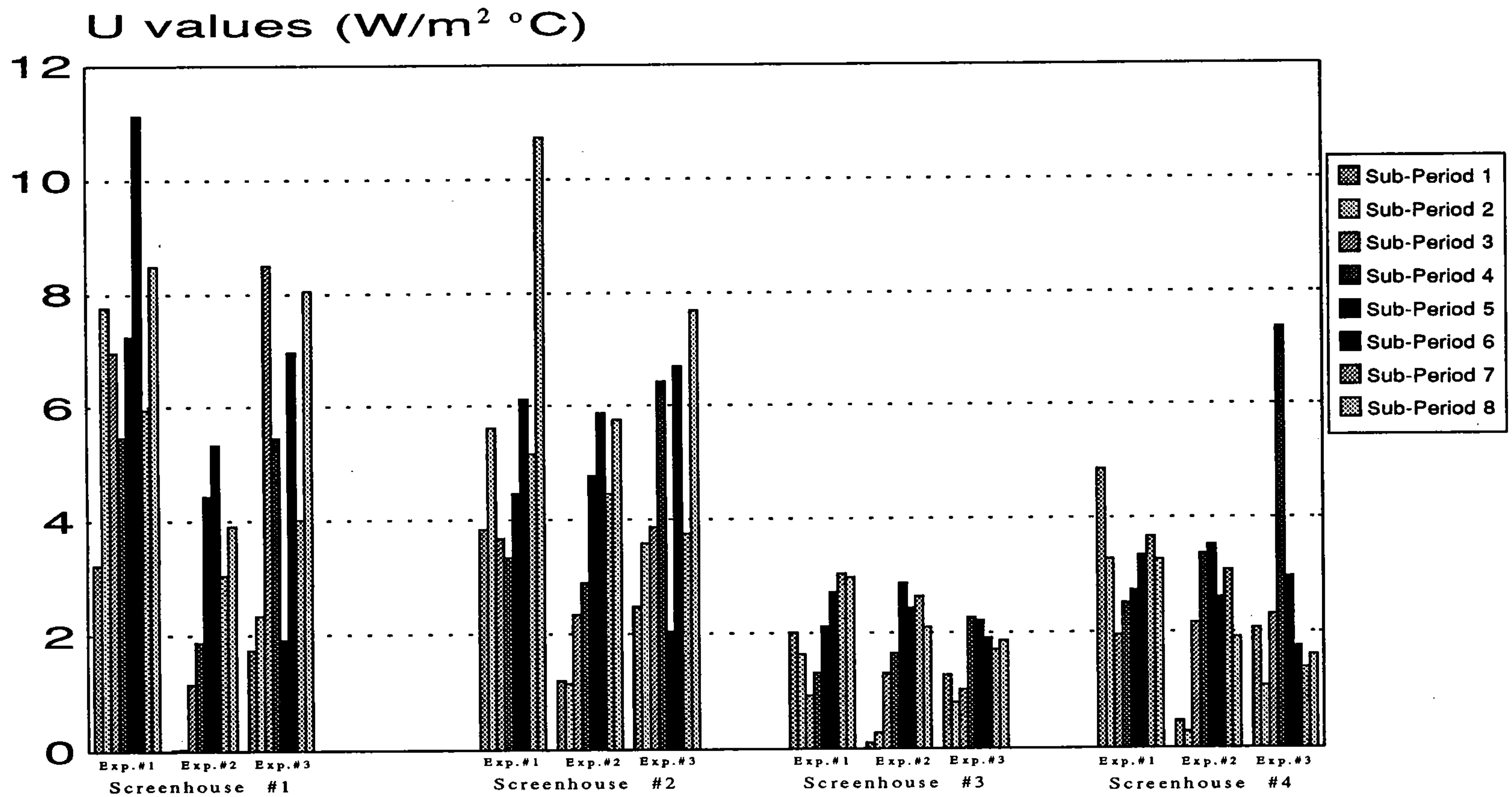

Figure 7.24 Average U-values (W/m ^{2} °C)

seem to demonstrate the assertion of the small effects of the configuration parameters on the U-values since no simple relationships between the configuration parameters and U were observed. Yet, as it will be seen in the following section 7.6, these U-values were utilised for the inside screenhouse temperature simulations and gave excellent predictions of day and night inside temperature. This proved that the calculated U-values that were obtained using night data were also valid for the heat transfer occurring during the day. This has fundamental value but more night experiments and data would determine which of the screenhouse configuration parameters have the most effect so that it would be possible to quantify the relationships between U-values and the varied configuration parameters.

7.6 Screenhouse Inside Air Temperature Simulations

Inside screenhouse air temperature simulations were run using the simulation program detailed in section 6.5 based on the screenhouse heat transfer models developed in sections 6.1 to 6.4. The simulated data were derived using the calculated heat transfer characteristics (τ, N_{υ} and U) obtained from experimental data and for every specific screenhouse configuration as described in section 6.4. The heat transfer characteristics data were analyzed in section 7.3 for the global transmissivity τ, in section 7.4 for the natural ventilation coefficient N_{υ} and in section 7.5 for the global heat transfer coefficient U. The other parameter values needed for the simulation program were either drawn from literature (ρ, Cp, σ, ε_a, m_a, ε_g, τ_t, h_g) or calculated (A (area), V (volume)) with physical data.

Each combination of screenhouse structure, screen mesh size opening, screen colour and water status was simulated using their corresponding calculated heat transfer characteristics values.

7.6.1 Sensitivity study

The interior air temperature sensitivity was evaluated in the screenhouse dynamic lumped parameter model with respect to the external climatic conditions of the screenhouse and the model parameter. It was found that the exterior air temperature (TOUT), the global solar radiation (GLOO) and the wind speed (WSO) were the most influential boundary conditions. The screenhouse characteristics act on the inside air temperature along the following decreasing order:

1. Solar absorptance of the ground (α)
2. Global transmittance of the cover (τ)
3. Global heat transfer coefficient (U)
4. Natural ventilation coefficient (N_υ)
5. Thermal or infrared transmittance of the cover (τ_t)
6. Ground to inside air convective heat transfer coefficient (hg)

The sensitivity study allows to rank the importance of the boundary conditions and of the screenhouse characteristics in terms of their influence on the inside air temperature. This analysis considerably helped the adjustment process of the model when simulated inside temperature data were compared to measured experimental data. The validation or adjustment analysis of the inside air temperature simulations was performed in terms of categories of models. Two main categories of model are described: 1) the screenhouse with one cover layer and 2) the double roof screenhouse. Each of these models were analyzed with and without water irrigation.

7.6.2 Inside air temperature simulations of screenhouses with one cover layer without water irrigation.

Eqn. 23 was used in the RKLUMP.BAS program (Appendix B) to generate the predicted T_i values of the single layer screenhouse without water irrigation. Figure 7.25 shows the simulated inside temperature results compared to the measured inside temperatures and the measured outside temperatures in screenhouse #1, for a sample day (July 25, 1994). That day screenhouse #1 was covered with the Lumite 50 screen (colour: amber, 35% open area) and was not irrigated with water.

The parameters used for the simulation showed in Figure 7.25 were: i) global transmissivity, $\tau = 0.63$ (measured), ii) infrared transmissivity, $\tau_t = 0.55$ (from literature), iii) natural ventilation coefficient, $N_\upsilon = 0.5$ (calculated from wind speed measurements) and iv) global heat transfer coefficient, U = 5.95 (calculated from night temperature measurements).

Figure 7.25 shows that the simulated inside temperature values were very similar both in magnitude and in trends to the measured inside temperature values. Even if the global heat transfer coefficient was calculated

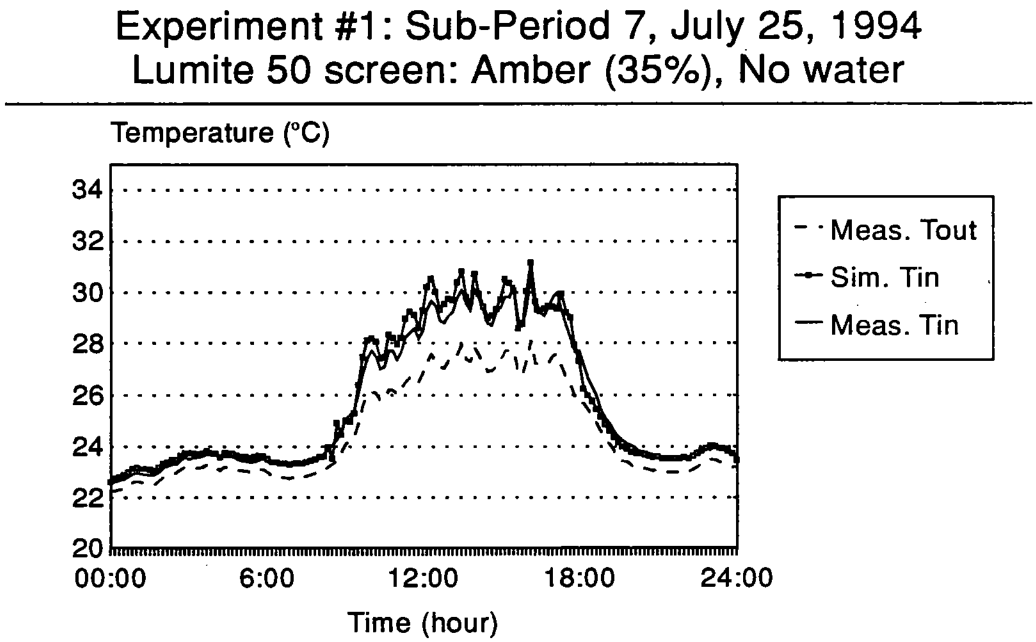

Figure 7.25: Inside air temperature simulation: Screenhouse #1 Single roof without water irrigation

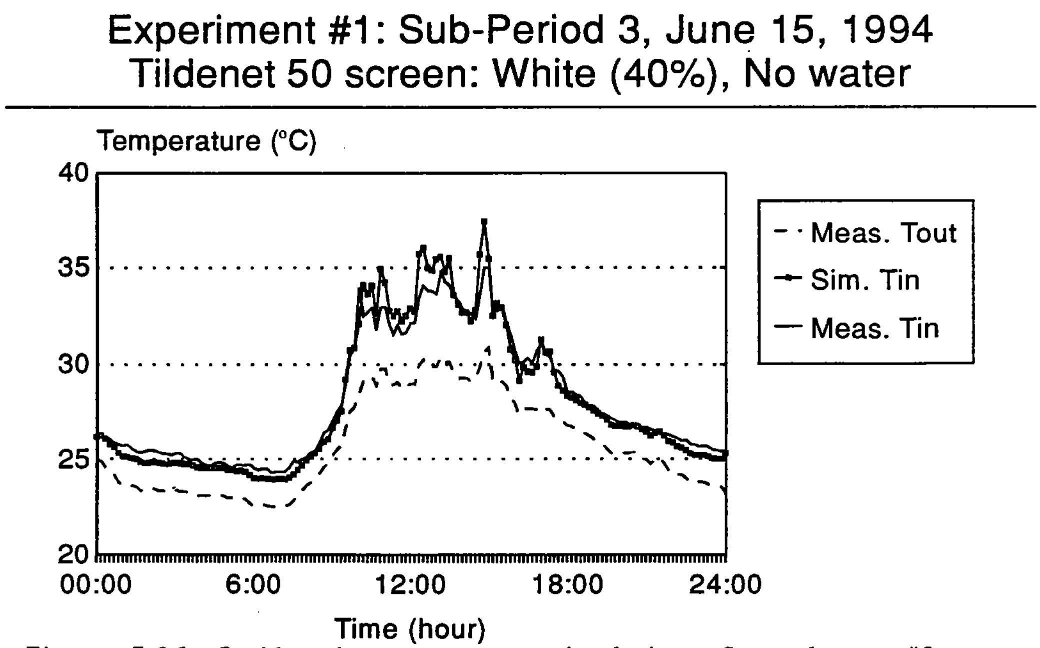

Figure 7.26: Inside air temperature simulation: Screenhouse #3 Double roof without water irrigation

only with the night temperature data, the simulation program predicted the night and day inside temperature values within one °C difference of the measured data. For that specific day, the simulation program achieved very good results.

Many other simulations of inside temperature of single layer screenhouses (#1, #2 and #4), with the various types of screens and without water irrigation for different days of experiments were performed. Some examples are presented in Appendix D. The parameters (τ, τ_t, N_υ, U) were specific to each day of experiments and they described the specific screenhouse architecture, screen mesh size and screen colour for that day. As mentioned, U was obtained using only the night temperature data from 00:00 hr (midnight) till 6:40 hr for the specific day of interest. All these inside temperature simulations gave results that were very similar to the results obtained for screenhouse #1 on July 25, 1994.

The simulation model, with the calculated parameter values, predicted the inside temperature for all the simulated days taking into account the changes of architectural structure types, the changes of screen mesh sizes and the screen colour changes. These predicted temperature values were always very similar (within one °C compared to the inside temperature measured during the experiments on site, at IITA Cotonou).

It can be said that the simplified lumped parameter (one component) dynamic model described by Eqn. 23 is a very good approximation of the heat transfer occurring in a single layer screenhouse, without water irrigation for all the 3 screenhouse architectural configurations and the 4 screen types tested.

The simulation results suggest that Eqn. 23 can be used as a design tool for single layer screenhouses in various tropical locations. Eqn. 23 can be used to predict inside temperature of various single layered screenhouses without water irrigation configurations with other screen types than the one used in the experiments and for other locations than Cotonou. All the above results have showed that it was possible to predict the parameter values τ, τ_t, N_υ and U for the various screenhouse types, screen mesh and colour combinations. With a set of one day of meteorological data (global solar radiation, outside ambient temperature, wind speed and wind direction data), RKLUMP.BAS programmed with Eqn. 23 will predict the inside temperature of a single layer screenhouse without water irrigation at that location. Ambient relative humidity could also be measured to give more information to the designer but was not essential to the prediction program.

It is expected that Eqn. 23 will be able to predict the inside temperatures of single layer screenhouse without water irrigation for other climates than the tropical ones but tests are needed for these other climatic locations before the model can be validated.

7.6.3 Inside air temperature simulations of the double roof screenhouse without water irrigation

Figure 7.26 shows the simulated inside temperatures compared to the measured inside temperatures and the measured outside temperatures for screenhouse #3 without water irrigation, for one sample day (June 15, 1994). Eqn. 29 was used to generate the simulated inside temperature data for the double roof case. Figure 7.26 shows that the simulated inside temperatures were very similar both in magnitude and in trends to the measured inside temperature values. For that day, Eqn. 29 was able to predict within one °C the inside temperature of the double roof screenhouse without water irrigation. Many other simulations were performed for the double roof case without water irrigation with very similar results.

7.6.4 Inside air temperature simulations of one cover layer screenhouses with water irrigation

Eqn. 32 was used to generate the simulated inside air temperature values of single layered screenhouses with water irrigation and the result was shown in Figure 7.27. As for the two previous screenhouse configuration cases, the simulated values were very close in magnitude and in trends to the measured inside temperature values.

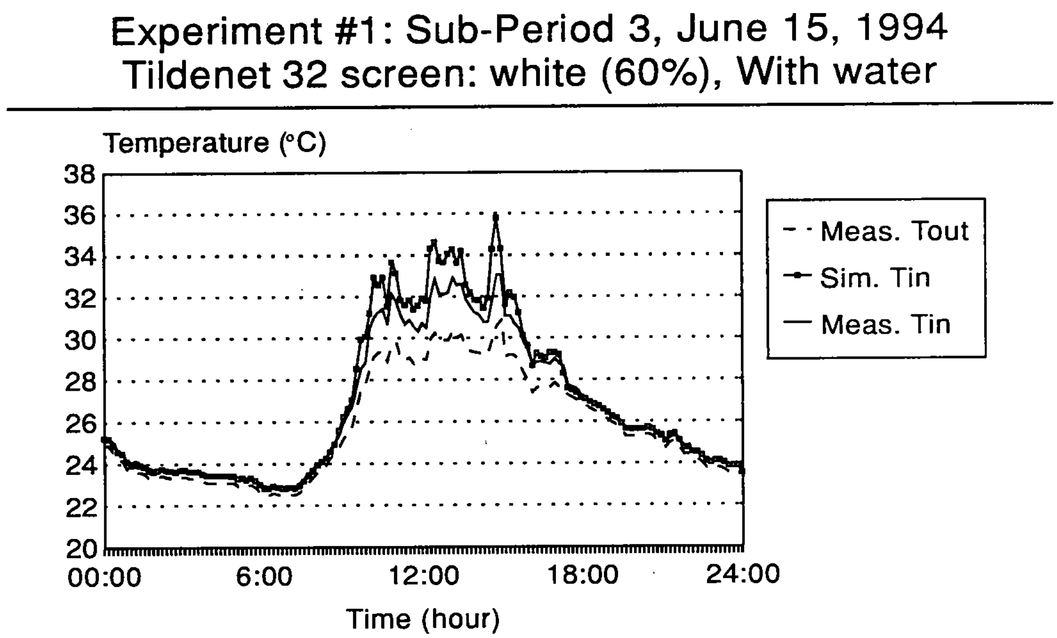

Figure 7.27: Inside air temperature simulation: Screenhouse #1 Single roof with water irrigation

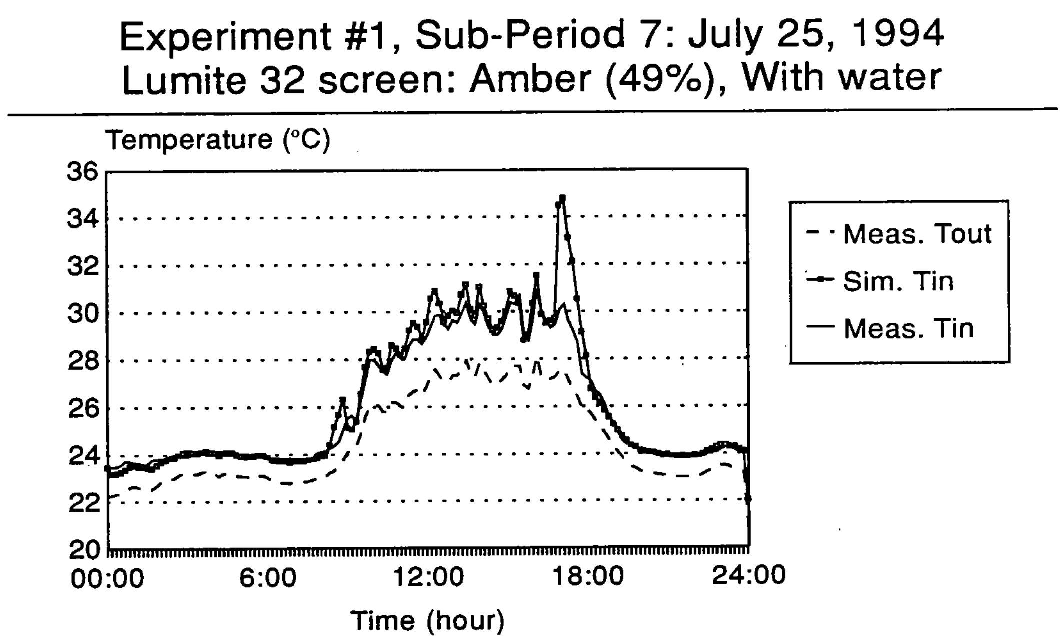

Figure 7.28: Inside air temperature simulation: Screenhouse #3 Double roof with water irrgation

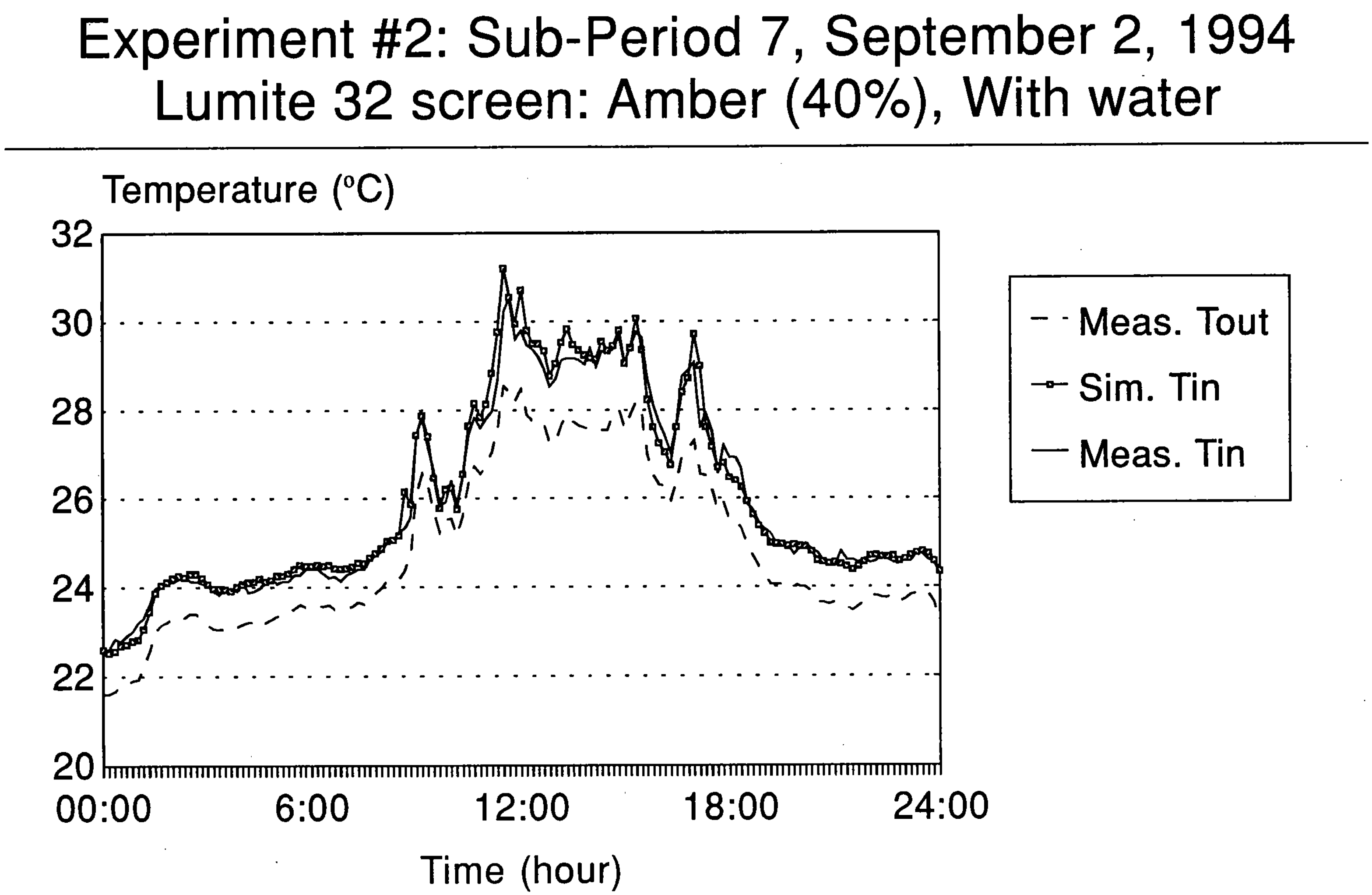

Figure 7.29: Inside air temperature simulation: Screenhouse #3 Double roof with water irrigation

7.6.5 Inside air temperature simulations of the double roof screenhouse with water irrigation

The simulated inside air temperatures (Figures 7.28 and 7.29) were generated with Eqn. 34 for the double roof screenhouse including water irrigation. Results show that predicted and measured values were always within one °C.

To conclude, the simulation results were very good. The predicted inside temperature values were within one °C difference from the measured values which was within the experimental error of the thermocouples temperatures measurements.

The proper choice of heat transfer characteristics (τ, τ_t, N_υ, U) is essential to achieve good simulation results. These heat transfer characteristics were chosen from the calculated values obtained from the experiments.

7.6.6 Screenhouse design procedure

The engineering design approach was followed for data analysis. The logical conclusion to this approach is the development of a screenhouse design procedure. This section presents such a procedure in seven simple steps. Note that the choice of the location of the screenhouse also has to consider and follow some basic design parameter indicators and principles such as, for example, the direction of main winds and/or the soils physical characteristics of the physical construction site and/or the proximity to other buildings and wind barriers. These parameters are outside the scope of the present design procedure since the latter is to determine the design characteristics specific to screenhouse parameters.

1: After the location of the screenhouse has been chosen, a minimum of one complete day of meteorological data (temperature, wind speed, wind direction, radiation, humidity (optional)) recorded at minimally one hour intervals during the day is necessary for the inside air temperature prediction program. 2: The screen hole size is chosen according to the desired level of containment. 3: The colour of the screen is chosen in terms of the desired light levels. 4: The screenhouse structure type configuration is chosen in terms of meteorological (for example: necessity of rain protection), plant and/or insects material protection considerations (sensitivity of plants and insect to light levels or other environmental parameters). 5: The next design step is to calculate the U-value of the chosen screenhouse with the UVALUE.BAS program using the night temperature data recorded above and using the heat transfer characteristics values (τ, N_v and the other simulation parameters) corresponding to the above choices of screenhouse-screen configuration. 6: When the U-value is calculated, it can be introduced in the RKLUMP.BAS program along with the other corresponding simulation parameter values (τ, N_v, etc.) to predict the inside air temperature of the screenhouse for the sample day of recorded data. 7: If the inside air temperature data does not correspond to specifications, repeat procedure from step 2 to 7 until the specifications are satisfied. If specification cannot be satisfied, it might mean that the location has to be changed or that other structures than screenhouse may have to be considered.

The main objectives of the research were achieved by defining the relationships between four screenhouse physical parameters (structure types, screen mesh sizes, screen colours and water irrigation statuses) on the four main screenhouse heat transfer characteristics (DT, τ, N_{υ}, and U). The quantification of these relationships was used to validate the screenhouse heat transfer models that were developed in this project. The prediction of the inside screenhouse air temperatures using the simulation programs showed results that were within one °C of difference with the measured data for all the screenhouse configurations tested in the three seasons of experiments. These results allow to utilize the simulation programs for designing screenhouses in tropical locations similar to those found in the Cotonou region.

VIII. SUMMARY AND CONCLUSIONS

The focus of the study reported in this thesis was the investigation of the issues pertaining to heat transfer characteristics of screenhouse configurations in West-African tropical climatic conditions. The four main heat transfer characteristics studied were the difference of temperature between the inside and the outside of the screenhouse (DT), the transmissivity of the screenhouse cover (τ), the natural ventilation coefficient (N_υ) and the global heat transfer coefficient (U). The main target of the field experiments was to study the effects of the architectural structure types, of the screen mesh size, of the screen colour and of the water irrigation on the four main heat transfer coefficients. The heat transfer coefficients obtained for the screenhouse configurations tested were introduced into the screenhouse heat transfer models developed in this thesis to validate both the values of the heat transfer characteristics and the models themselves. Simulations of inside screenhouse temperature were performed and compared to the experimentally measured data. The conclusions drawn on the basis of these studies can be summarized as follows:

1. The hydrodynamic tests demonstrated that it was possible to obtain a uniform flow of water over the screen without water crossing the screen surface even when the screen was not completely vertical. The maximum critical angle of the screen-water flow from vertical was found to be 20°. The water curtain had to be oriented in the same direction as

the angle of the screen before water touches the screen to increase the critical angle of the water-screen from vertical to its maximum.

2. The frequency distribution analysis of the climatological results showed that the data gathered during the three sets of experiments were representative of the climatic conditions of the Cotonou region and that these climatic conditions are comparable from one season to the other. The main difference observed between the climatic data of the different seasons was the higher relative humidity values in the rainy season and the higher outside temperature values in the dry season.

3. The graphical and GLM analyses on the difference between the inside and outside temperatures of the screenhouse (DT) showed that screenhouse #1 was the coolest screenhouse and that screenhouse #2 was the warmest for all the conditions tested. The values of DT for screenhouse #3 and #4 were always in between the DT values of screenhouses #1 and #3. Most of the time, screenhouse #3 was slightly cooler (lower DT values) than screenhouse #4.

4. The analysis of the screen mesh size effects on DT showed that the 50 screen mesh size (smallest hole size) resulted in higher DT values and that it was significantly different from the 32 screen mesh size. The colour of the screens did not demonstrate significant effects on DT values. The water irrigation had a significant effect on DT values but the result was not always a cooling effect. The water irrigation was

blocking the air movement across the screen surface, reducing ventilation and therefore resulting in higher DT values when water irrigation was applied. Measurement of screen-water temperature at the surface of the screen and in the irrigation hose indicated that evaporative cooling was occurring at the screen surface. The highest water cooling effects on DT vs TOUT slopes were observed in the rainy seasons. The results prove that there is potential for evaporative cooling techniques in humid tropical conditions but more design efforts are needed on the physical configurations to achieve higher efficiency.

5. Figure 7.19 which pictures the range of DT values obtained in all the experiments in relation to the fourteen OPAREA values calculated with Eqn. 39 shows that there are definite relationships between the total % free open area of a screenhouse and the difference of temperature between inside and outside the screenhouse (DT). The determination of these specific relationships should be one of the primary objectives of future studies on screenhouse heat transfer performances.

6. The graphical analyses on the Global transmissivity (τ) values showed that, over all the experiments, screenhouse #3 demonstrated the lowest τ values. The resulting τ values in screenhouse #1 were higher than the τ values in screenhouse #3 but lower than the τ values in screenhouse #4. Screenhouse #2 resulted in the highest τ values.

7. The colour of the screen had a significant effect on the τ values. The white screen always showed the highest τ values while the amber screen always showed the lowest τ values. The effect of the screen mesh size on τ values was significant but to a lesser degree than the effect of the colour of the screen. The resulting τ were directly proportional to the screen hole sizes or inversely proportional to the screen mesh sizes. The water irrigation status did not demonstrate a significant effect on the Global transmissivity (τ) values.

8. The wind speed measurement and the air movement analyses demonstrated that the screenhouse architectural structure type had a significant effect on the natural ventilation coefficient (N_υ). The results suggested that the distance between the first layer roof and the double roof affects, to a significant level, the results of N_υ. These analyses also showed that the screen mesh size had a significant effect on N_υ. The smaller the mesh size, the more restriction to air movement, therefore the smaller N_υ. The measurement of C_υ in controlled conditions showed the same tendency. The water irrigation status also had a significant effect on N_υ. The water curtain on the screen and the capacity of the screen to retain a water film in the interstice of the screen hole were blocking the air movement across the screen surface, therefore reducing N_υ significantly. The colour of the screen did not have an effect on N_υ. N_υ was estimated to range from 0.1 to 0.5 air change per minute for

inside screenhouse wind speed measurements ranging from 0.04 m/s to 0.2 m/s.

The wind speed measurements and air movement analysis showed a significant effect of the roof ventilation on N_{υ}. The first layer of the roof of screenhouses #1 and #3 was always screen covered and demonstrated higher N_{υ} values than screenhouse #4 and #1 for which the first layer roof was always covered with Teflon. The results on DT values, concluded in paragraph 3 of this section, are consistent with the affirmation that the screenhouse with a first layer screen roof showed high ventilation rates therefore lower inside air temperature than a screenhouse with a first layer Teflon roof which showed higher inside temperature values. Figure 7.19 also implies that N_{υ} could be closely related to OPAREA but more studies are needed to determine those relationships.

9. U-values were calculated with the developed UVALUE.BAS program using night data only to eliminate the effects of solar radiation. The resulting U values obtained over all the experiments ranged from 0.1 to 11.1 W/m^2 °C. On the average, screenhouse #3 presented the smallest range of U-values. No simplistic relationship was observed between the U-values versus the structural, the screen and the water parameters that were varied during the experiment. More night experimental studies would specify these relationships.

10. The interior air temperature sensitivity study on the lumped parameter models developed in the project showed that the exterior air temperature, the global solar radiation and the wind speed were the most influential boundary conditions. The sensitivity study also revealed that the screenhouse characteristics were acting on the inside air temperature along the following decreasing order: 1) the solar absorptance of the ground (α), 2) the global transmittance of the cover (τ), 3) the global heat transfer coefficient (U), 4) natural ventilation coefficient (N_v), 5) the infrared transmittance of the cover (τ_t), 6) the ground inside air convective heat transfer coefficient (hg).

11. The inside screenhouse air temperature were predicted using the RKLUMP.BAS program for all the configuration models tested, with the corresponding heat transfer characteristics, and the results of the temperature predictions were within one °C from the measured values which was within the experimental measurement error of the thermocouples.

IX. CONTRIBUTIONS TO KNOWLEDGE

This thesis made an original contribution to knowledge by providing basic and applied information on the heat transfer characteristics of screenhouse configurations in a tropical climate. The knowledge gained is of practical value. The contributions to knowledge are summarized below:

1. Linear regression coefficients relating the difference of temperature (DT) as a function of the outside temperature (TOUT) considering the effects of the screenhouse architectural structural types, the effects of the screen mesh sizes, the effects of the screen colours and the effects of a water irrigation curtain in tropical climate conditions were quantified.
2. The concept of the natural ventilation coefficient N_v for screenhouses was introduced and N_v was quantified.
3. Heat transfer models were developed to simulate the inside air temperature of screenhouses with specific configuration parameters as a function of external meteorological data and heat transfer characteristics of these screenhouse configurations. These models can be used as tools to design screenhouses in tropical locations.
4. The Global heat transfer coefficients, U, were calculated using night experimental data for all the configurations tested. These U-values were used in the inside air temperature simulation program and produced excellent prediction results for both night and day conditions.

X. RECOMMENDATIONS FOR FURTHER RESEARCH

Further studies could be performed to obtain more precision in the determination of the N_v coefficients of different configurations of screenhouses in a scaled model screenhouse wind tunnel study. Measurements of ventilation static pressures and the use of ventilation determination techniques such as the smoke decay method would increase the accuracy of the N_v coefficient. N_v should be related to OPAREA and the latter could be related to DT. The influence of the proximity of other buildings and/or wind barriers on N_v could also be defined. Techniques to increase N_v would be one objective of the study. The study could also quantify the effect of colour on N_v.

Further studies could concentrate on quantifying the water evaporative cooling efficiency for different design of water evaporative apparatus that would be implementable on screenhouses and on other tropical buildings.

Further night experimental research work is needed to quantify the relationships between the varied screenhouse configuration parameters and the Global heat transfer coefficients (U).

Studies of screenhouse heat transfer performance in different climates than the tropical climates found in the Cotonou region would broaden and validate the scope of application of the developed heat transfer mathematical models. In particular, studies of the screenhouse heat transfer performance in dry (desert) climate area and also in cold climates would increase the extent of application of the models.

The effects of plant growth on screenhouse heat transfer characteristics and vice versa the effects of screenhouse heat transfer characteristics on plant growth should be part of future studies aiming at improving the heat transfer performance of tropical containment facilities in general, including the screenhouse designs.

XI. REFERENCES

Albright LD, Seginer I, Marsh LS, Oko A, 1985. In situ thermal calibration of unventilated greenhouses. Journal of Agricultural Engineering Research 31: 265 -281.

Albright LD, 1983. Modelling thermal mass effects in commercial greenhouses. Acta Horticulturae 148: 359-365.

Arbel A, Segal I, Yekutieli O and Zamir N, 1990. Natural ventilation of greenhouses in desert climate. Acta Horticulturae 281: 167-174.

ASHRAE, 1981. ASHRAE Handbook, Fundamentals. Am. Soc. of Heating, Refrigerating and Air Conditioning Eng. Atlantic, GA 30329, 4th edition.

Aynsley RM, Melbourne W and Vickery BJ, 1977. Architectural Aerodynamics. Applied science publishers LTD, London. ISBN: 0 85334 698 4 : 254 pages.

Baille M and Baille A, 1990. A simple model for the estimation of greenhouse transmission: influence of structures and internal equipment. Acta Horticulturae 281: 35-46.

Bayley BJ, 1977. The calculation of glasshouse fuel requirements using degree-day data corrected for solar heat gain. Dept. Note. No. DN/G/798/04013, National Institute of Agricultural Engineering, Silsoe.

Bean A, Alperi RW, Federer CA, 1975. A method for characterising shelterbelt porosity. Agricultural Meteorology 14: 417-429.

Beard JT, Ribando RJ, Adams RR and Arthur JH, 1989. Thermal performance of a heated plate with open-channel infrared radiation shields. Transactions of the ASME Journal of Solar Engineering Volume 111: p233-236.

Berdahl P and Martin M, 1984. Emissivity of Clear Skies. Solar Energy, 32: 5.

Besancenot JP, 1992. Stress et pathologies liées aux types de temps d'harmattan dans la région du golfe du Bénin. Risques pathologiques, rythmes et paroxysmes climatiques. John Libbey Eurotext, Paris p. 271-278.

Bethke JA, 1990. Screening greenhouses for insect size. (Editor prepared article). Growers Talks, December: p102.

Bliss RW. 1961. Atmospheric Radiation Near the Surface of the Ground. Solar Energy, 5: 105.

Bond, TE, Godbey LC and Zornig HF, 1977. Solar, long wavelength, and photosynthetic energy transmission of greenhouse covering materials. Proceedings, A Conference on Solar Energy for Heating Greenhouses and Greenhouse-Residential Combinations, Cleveland and Wooster, Ohio, March 20-23, pp. 234-255.

Brochier JF, 1979. Cultures maraîchères sous abri et hydroponie en climat tropical humide/ Protected vegetable crops and hydroponics in humid tropical climates. Plasticulture 42: 27-39.

Brunt D, 1932. Notes on Radiation in the Atmosphere. Quarterly, J. Royal Meteorological Soc., 58: 389.

Chandra P, Singh JK and Majumbar G, 1990. Prediction of the cooling pad temperature in a fan-pad cooling system used in greenhouse. Proceedings of the 11th International Congress on the use of Plastics in Agriculture, New Delhi, India, 1990, F41 - F48.

Chiapale JP, 1981. La serre solaire INRA-CEA: Résultats physiques. Acta Horticulturae 115: 387 - 400.

Choinière Y, 1991. Wind induced natural ventilation of low-rise buildings for livestock housing by the pressure difference method and concentration decay method. M.Sc. Thesis, Civil Engineering department, University of Ottawa, Canada.

Cochran WG and Cox GM, 1957. Experimental designs. Wiley publication, New York, London, 2nd edition.

Critten DL, 1989. Light transmission into greenhouses. Acta Horticulturae 245: 377-383.

Critten DL, 1986. A general analysis of light transmission in greenhouse. Journal of Agricultural engineering research 33: 289-302.

Daunitch HJ, 1975. Problems of desert greenhouses. Acta Horticulturae 51: 51-60.

Desmarais G, 1992. Greenhouses, screenhouses and biological containment facilities at IITA and for African national programs. Report presented to the Plant Health Management Division of the International Institute of Tropical Agriculture, Nigeria, August 1992, (unpublished).

Duffie and Beckman, 1991. Solar Engineering of Thermal Processes. Second Edition John Wiley & Sons. Inc. New York.

Duncan GA, Loewer OJ, Colliver DG, 1981. Simulation of energy flows in a greenhouse: Magnitude and conservation potential. ASAE transactions 24(4): 197-201.

FAO, 1990. Protected cultivation in the Mediterranean climate. FAO Plant Production and Protection Paper No. 90. Food and Agriculture Organization of the United Nations, Rome, 1990.

Fontes MR, 1975. Controlled-environment agriculture in desert regions. Acta Horticulturae 51: 49 -50.

Gale J, 1981. Controlled environment agriculture for hot desert regions. Symposium of the British Ecological Society. Oxford: Blackwell Scientific Publications. 1981. (21st Pete: 21st what?), 391 - 402.

Garzoli KV, 1989. Cooling greenhouses in tropical and sub-tropical climates. Acta Horticulturae 257: 93-100.

Garzoli K, 1985. A simple greenhouse climate model. Acta Horticulturae 174: 393-400.

Hayashi Y, Takimoto A, Matsuda O and Kitagawa, 1990. Study on mist cooling for heat exchanger (Development of high performance mist-cooled heat transfer tubes). Japanese Society of Mechanical Engineering International Journal, Series II, 33, No. 2: 333-339.

Hellickson MA, Hinckle CN and Jedele DG, 1983. Natural ventilation. Chapter 5 of Ventilation of Agricultural structures. ASAE Monograph Number 6: 81-102.

Herren HR and Yaninek JS, 1989. Biological Control : A Sustainable Solution to Crop Pest Problems in Africa, eds. 1989. IITA, Ibadan, Nigeria.ISBN 978-131-039-1. 210 pages.

Hindeleh AM, Al-Haj Abdalla M and Braik NS, 1990. Crystallinity enhances light transmissivity through low-density polyethylene sheets. Journal of Materials Science, 25: 1808-1812.

Holman JP, 1981. Heat transfer. McGraw-Hill Book Company. 5th edition.

IDRC, 1993. Green technologies for development: transfer, trade and cooperation. Ottawa, Ontario, Canada. International Development Research Centre (IDRC) publication.

IDRC and AUCC, 1992. International cooperation in agricultural research. A guidebook for Canadian researchers. A co-publication of the International Development Research Centre and the Association of Universities and Colleges of Canada. Ottawa, Ontario, Canada.

IDRC, 1991. Empowerment through knowledge: the strategy of the International Development Research Centre. Ottawa, Ontario, Canada.

IITA, 1990, 1991, 1992, 1993. International Institute of Tropical Agriculture Annual Reports, ISSN 0331-4340, Oyo Road, PMB 5320, Ibadan, Nigeria.

Jaubourg J, 1988. Les filets brise-vent (essai en cours). CEMAGREF, BTMEA No 29, mai 1988.

Kempthorne O, 1975. The design and analysis of experiments. Krieger Publishing Company, Huntington, New York, U.S.A. pp.631.

Kindelman M, 1980. Dynamic modelling of greenhouse environment. Transactions of the ASAE, 1980:1232-1239.

Kozai H, Imura H, Ikeda Y, 1991. The permeability of screen wicks. Japanese Society of Mechanical Engineering International Journal, Series II, 34, No. 2: 212-219.

Kurosaki Y and Viskanta R, 1978. Heat transfer in a solar radiation absorbing fluid layer flowing over a substrate. Heat Transfer Laboratory, School of Mechanical Engineering, Purdue University West Lafayette, Indiana.

Lacroix R et Zanghi JC, 1990. Etude comparative de la structure des modèles de transfert d'énergie et de masse dans les serres. Canadian Agricultural Engineering 32: 269 - 284.

Lacroix R, 1988. Une étude comparative de la structure des modèles de transfert d'énergie et de masse dans les serres de production. Thèse de M. Sc., Université du Québec à Montréal, Montréal, Québec, Canada, 119pp.

Larousse, 1992. Larousse, Mémo. Encyclopédie générale, visuelle et thématique. 1372 p. ISBN 2-03-152230-2.

Lawson C, 1986. A study of thin water films for greenhouse applications. Project report. Agricultural Engineering Department, Macdonald College, McGill University, Montreal, Canada.

Lewandowski WM, Bieszk H, Cieslinski, 1991. Influence of cylindrical screens on free convection heat transfer from a horizontal plate. Technical University of Gdansk, Poland. International Journal of Heat and Fluid Flow, 12: p93-94.

Mannan KD and Cheema LS, 1979. Year-round studies on natural cooling and heating of greenhouses in Northern India. Punjab Agricultural University, Ludhiana, India, 141004. Proceeding of the International Solar Energy Society, Volume 2.

Matsuda O, Takimoto A and Hayashi Y, 1986. Study on mist cooling for heat exchangers (Collision of droplet and film formation on a horizontal cylinder) (in Japanese). Trans. Jpn. Soc. Mech. Eng., 52(482,B): 3545

Mead R, 1984. Confounded experiments are simple, efficient and misunderstood. Experimental agriculture 38(20), pp. 185-201.

Ménard O, 1991. A solar climate control system using a water film flow to conserve energy in greenhouses. Master thesis. Agricultural Engineering Department, Macdonald Campus, McGill University, Montreal, Canada.

Ng KL, 1990. Dewatering performance of vibrating screens. Proceeding of the Institute of Mechanical Engineers, Volume 34: 73-79.

Nijskens J, de Halleux D and Deltour J, 1991. Sensitivity study of a greenhouse climate dynamic model. Bulletin de Recherche Agronomique, Gembloux 26(3):389-410.

Pruzan DA, Torrence KE and Avedisian CT, 1990. Two-phase flow and dryout in a screen wick saturated with a fluid mixture. International Journal of Heat and Mass Transfer 33(4): 675-681.

Rault PA, 1990. A tunnel greenhouse adapted to the tropical lowland climate. Institut de Recherche Agronomiques tropicales. IRAT/CIRAD, Martinique, French West Indies.

Rault PA, 1988. Protected crops in humid tropical regions. How could we avoid or reduce excessive temperatures? How could we select the cladding materials and the greenhouse design? Institut de Recherches Agronomiques tropicales. IRAT/CIRAD, Martinique, French West Indies.

Roberts WJ, Vasvary L and Kania S, 1995. Screening for insect control in mechanically ventilated greenhouses. NABEC 95 paper: 9509.

Ross DS, 1995. Status of selection procedures for greenhouse insect screening. NABEC 95 paper: 9512.

Ross DS and Gill SA, 1994. Insect screening for greenhouses. Agricultural Engineering FACTS 186, October. University of Maryland, Cooperative Extension Service, 21 pp.

Rossel HW and Ferguson JM, 1979. A new and economical screenhouse for virus research in tropical areas. FAO, Plant Protection Bulletin 27(3): 74-76.

Seginer I and Kantz D, 1986. In-situ determination of transfer coefficients for heat and water vapour in a small greenhouse. J. Agric. Eng. Res. 35: 39-54.

Strauch KH and Von Zabeltitz C, 1989. Closed system greenhouses with integrated solar desalination for arid regions. Acta Horticulturae 257: 115-125.

Su, CC and Huang, CC, 1991. Experimental studies of flow through single gauges. International Journal of Heat and Fluid Flow 12(3): 273-278.

Swinbank, WC. 1963. Long- wave Radiation from Clear Skies. Quarterly, J. Royal Meteorological Soc., 89, 339.

Tantau HJ, 1989. Models for greenhouse climate control. Acta Horticulturae 245: 397-404.

Thimijan RW, Heins RD. 1983. Photometric, Radiometric and Quantum Light Units of Measures: A review of procedures of Interconversion. Hortscience, Vol. 18(6), December.

Tillie M, 1988. Efficacité des filets brise-vent utilisés sur les bâtiments d'élevage bovins. CEMAGREF,BTMEAN No 29, mai 1998.

Ueda T, Hisai O, Wardana NG and Mizomoto M, 1992. Structure of grid turbulence through a heated screen. JSME International Journal, Series II, Vol 35(2): 266-272.

Von Zabeltitz C, 1988. L'adaptation des serres aux climats plus chauds/ Greenhouse design for warmer climates. Plasticulture 80:39-50.

Von Zabeltitz C, 1990. Appropriate greenhouse constructions for mild climates. Proceedings of the 11th International Congress on the Use of Plastics in Agriculture, New Delhi, India, 1990, F117 -F126.

Walker JN, Aldrich RA and Short TH, 1983. Quantity of air flow for greenhouse structures. Chapter 11 of Ventilation of Agricultural structures. ASAE Monograph Number 6: 257-277.

Walker JN, Walton LR, 1971. Effect of condensation on greenhouse heat requirements. Transaction of the ASAE 14(2):282-284.

Walker JN, 1965. Predicting temperatures in ventilated greenhouses. Transaction of the ASAE 8(3):445-448.

Williamson, MR and Wong, F, 1984. Shade house structures: an alternative approach. Research Extension Series of the College of Tropical Agricultural and Human Resources, Hawaii. No. 41, 14pp.

Zeroni M, Gale J, Kopel R, Levi S, 1990. Agrotechniques for a closed greenhouse with a radiant filtering roof. Proceedings of international symposium on applied technology of greenhouse, Beijing, China; Knowledge Publishing House (1991).

Zhang Z, Bejan A, Lage JL, 1991. Natural convection in a vertical enclosure with internal permeable screen. Transactions of the ASME Journal of Heat Transfer 113: 381-383.

APPENDIX A.

SCREEN TYPES

SCREEN #0 (S0)

**TILDENET, MESH 50, WHITE,
40.5 % FREE OPEN AREA (FOA)**

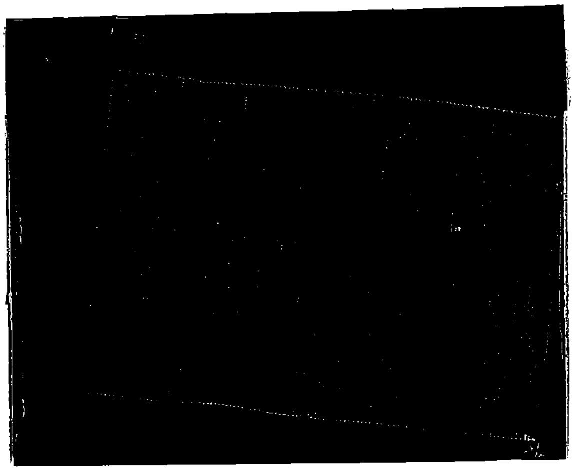

SCREEN #1 (S1)

**LUMITE, MESH 50, AMBER,
34.9 % FOA**

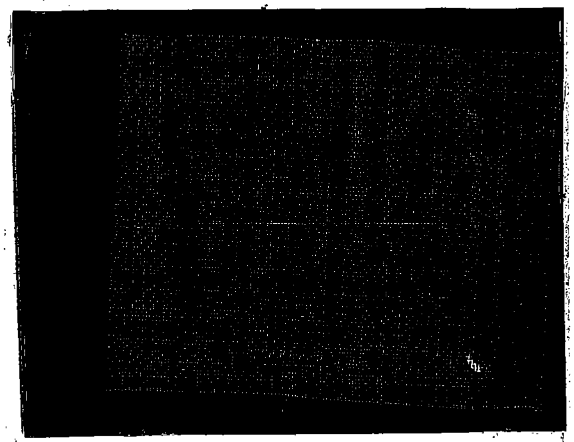

SCREEN #2 (S2)

**LUMITE, MESH 32, AMBER
48.5 % FOA**

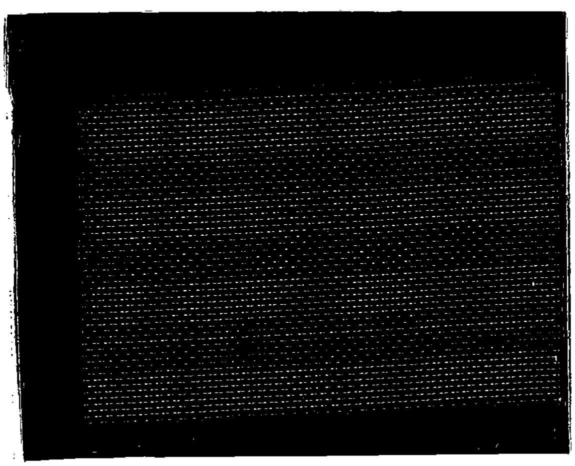

SCREEN #3 (S3)

**TILDENET, MESH 32, WHITE
60.1 % FOA**

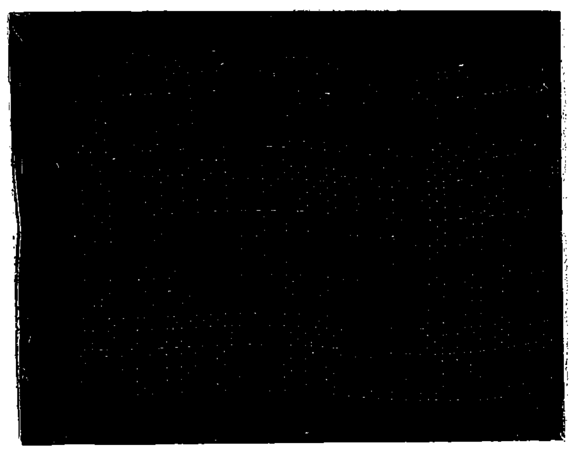

APPENDIX B.

Appendix B1 - EXCELL MACRO Program sequence

Name of program: AVFORCING (e)

Function: **Calculates the average of the forcing function parameters (Ex: TOUT, GLOO)**

Coding sequence:

```
avforcing (e)
=ARRANGE.ALL(2)
"=HSCROLL(148,TRUE)"
"=SELECT(""C148:C163"")"
=EDIT.DELETE(1)
"=HSCROLL(2,TRUE)"
"=SELECT(""R1C7"")"
"=FORMULA(""gloout"")"
"=SELECT(""R1C8"")"
"=FORMULA(""glout"")"
"=SELECT(""C8"")"
=COPY()
=NEW(1)
=PASTE()
"=SELECT(""R1"")"
=EDIT.DELETE(2)
"=SAVE.AS(""C:\PHD\SIMULI\GLO0329.TXT"",3,,FALSE)"
=CLOSE()
"=SELECT(""C17"")"
=INSERT(1)
"=SELECT(""R1C17"")"
"=FORMULA(""tout"")"
"=SELECT(""R2C17"")"
"=FORMULA(""=RC[-3]+RC[-1]/2"")"
"=SELECT(""R2C17"")"
"=FORMULA(""=(RC[-3]+RC[-1])/2"")"
=COPY()
"=SELECT(""R3C17:R145C17"")"
=PASTE()
=VLINE(-1)
"=SELECT(""C17"")"
=COPY()
=NEW(1)
"=PASTE.SPECIAL(3,1,FALSE,FALSE)"
"=SELECT(""R1"")"
=EDIT.DELETE(2)
"=SAVE.AS(""C:\PHD\SIMULI\TOUT0329.TXT"",3,,FALSE)"
=CLOSE()
=HLINE(26)
"=SELECT(""C42"")"
=INSERT(1)
"=SELECT(""R1C42"")"
"=FORMULA(""tin1"")"
"=SELECT(""R2C42"")"
"=FORMULA(""=(RC[-5]+RC[-3]+RC[-1])/3"")"
=COPY()
"=SELECT(""R3C42:R145C42"")"
=PASTE()
```

```
"=SELECT(""C42"")"
=COPY()
=NEW(1)
"=PASTE.SPECIAL(3,1,FALSE,FALSE)"
"=SELECT(""R1"")"
=EDIT.DELETE(2)
"=SAVE.AS(""C:\PHD\SIMULI\TI10329.TXT"",3,,FALSE)"
=CLOSE()
=HLINE(12)
"=SELECT(""C55"",""R2C55"")"
=INSERT(1)
"=SELECT(""R1C55"")"
"=FORMULA(""tin2"")"
"=SELECT(""R2C55"")"
"=FORMULA(""=(RC[-5]+RC[-3]+RC[-1])/3"")"
=COPY()
"=SELECT(""R3C55:R145C55"")"
=PASTE()
"=SELECT(""C55"")"
=COPY()
=NEW(1)
"=PASTE.SPECIAL(3,1,FALSE,FALSE)"
"=SELECT(""R1"")"
=EDIT.DELETE(2)
"=SAVE.AS(""C:\PHD\SIMULI\TI20329.TXT"",3,,FALSE)"
=CLOSE()
"=SELECT(""C68"",""R2C68"")"
=INSERT(1)
=VLINE(-1)
"=SELECT(""R1C68"")"
"=FORMULA(""tin3"")"
"=SELECT(""R2C68"")"
"=FORMULA(""=(RC[-5]+RC[-3]+RC[-1])/3"")"
=COPY()
"=SELECT(""R3C68:R145C68"")"
=PASTE()
=VLINE(-1)
"=SELECT(""C68"")"
=COPY()
=NEW(1)
"=PASTE.SPECIAL(3,1,FALSE,FALSE)"
"=SELECT(""R1"")"
=EDIT.DELETE(2)
"=SAVE.AS(""C:\PHD\SIMULI\TI30329.TXT"",3,,FALSE)"
=CLOSE()
=HLINE(13)
"=SELECT(""C81"")"
=INSERT(1)
"=SELECT(""R1C81"")"
"=FORMULA(""tin4"")"
"=SELECT(""R2C81"")"
"=FORMULA(""=(RC[-5]+RC[-3]+RC[-1])/3"")"
=COPY()
"=SELECT(""R3C81:R145C81"")"
=PASTE()
=VLINE(-1)
```

```
"=SELECT(""C81"")"
=COPY()
=NEW(1)
"=PASTE.SPECIAL(3,1,FALSE,FALSE)"
"=SELECT(""R1"")"
=EDIT.DELETE(2)
"=SAVE.AS(""C:\PHD\SIMULI\TI40329.TXT"",3,,FALSE)"
=CLOSE()
"=HSCROLL(1,TRUE)"
=HLINE(14)
"=SELECT(""R1C21"")"
"=FORMULA(""tg"")"
"=SELECT(""C21"")"
=COPY()
=NEW(1)
=PASTE()
"=SELECT(""R1"")"
=EDIT.DELETE(2)
"=SAVE.AS(""C:\PHD\SIMULI\TG0329.TXT"",3,,FALSE)"
=CLOSE()
=HLINE(-7)
"=SELECT(""C10"")"
=COPY()
=NEW(1)
=PASTE()
"=SELECT(""R1"")"
=EDIT.DELETE(2)
=VLINE(43)
"=VSCROLL(2,TRUE)"
"=SELECT(""R2C3"")"
"=FORMULA(""=MAX(R[48]C[-2]:R[98]C[-2])"")"
"=SELECT(""R3C3"")"
"=FORMULA(""=AVERAGE(R[47]C[-2]:R[97]C[-2])"")"
"=SELECT(""R4C3"")"
"=FORMULA(""=MIN(R[46]C[-2]:R[96]C[-2])"")"
"=SELECT(""R3C4"")"
"=FORMULA(""=STDEV(R[47]C[-3]:R[97]C[-3])"")"
"=SELECT(""R8C3"")"
"=FORMULA(""=AVERAGE(R[-6]C[-2]:R[22]C[-2])"")"
"=SELECT(""R2C3:R4C4"")"
"=FORMAT.NUMBER(""0.00"")"
"=SELECT(""C1"",""R2C1"")"
"=NEW(2,1)"
=RETURN()
```

Appendix B2 - UVALUE.BAS BASIC Program sequence

Name of program: UVALUE.BAS

Function: **Calculates the U-values of a specific screenhouse configuration**

Coding sequence:

```
'
'
' Open files
'
OPEN "c:\phd\simuli\s0323" FOR OUTPUT AS #1
OPEN "c:\phd\simuli\glo0323.txt" FOR INPUT AS #2
OPEN "c:\phd\simuli\tout0323.txt" FOR INPUT AS #3
OPEN "c:\phd\simuli\ti10323.txt" FOR INPUT AS #4
OPEN "c:\phd\simuli\tg0323.txt" FOR INPUT AS #5
OPEN "c:\phd\simuli\u0323.txt" FOR OUTPUT AS #6
OPEN "c:\phd\simuli\ti20323.txt" FOR INPUT AS #7
OPEN "c:\phd\simuli\ti30323.txt" FOR INPUT AS #8
OPEN "c:\phd\simuli\ti40323.txt" FOR INPUT AS #9
'
' Dimension matrix and vectors
'
DIM glout(150), tout(150), tin(150), ti1(150), ti2(150), ti3(150), ti4(150)
DIM tg(150), uu1(150), uu2(150), uu3(150), uu4(150)
FOR k = 1 TO 100
INPUT #2, glout(k)
INPUT #3, tout(k)
INPUT #4, ti1(k)
INPUT #5, tg(k)
INPUT #7, ti2(k)
INPUT #8, ti3(k)
INPUT #9, ti4(k)
'PRINT k, glout(k), tout(k)
NEXT k
CLS
'
' Input constants
'
' Input "transmissivity, U, Nv, hg"; trans,u,nv,hg
'
trans = .89
towt1 = .58
towt3 = .55
towt2 = .256
towt4 = .256
u = 43
nv1 = .1
nv2 = .1
nv3 = .1
nv4 = .1
hg = 4.5
'
' Calculate coefficients
'
```

```
A123 = 24 * trans
A4 = 32 * trans
B123 = 84 * u
B4 = 135 * u
C1 = 86 * 1.15 * 1 * nv1 * 16.667
C2 = 86 * 1.15 * 1 * nv2 * 16.667
C3 = 86 * 1.15 * 1 * nv3 * 16.667
C4 = 176 * 1.15 * 1 * nv4 * 16.667
CC = 24 * hg
D123 = 24 * 5.64E-08
D4 = 32 * 5.64E-08
E = 302
'
' Prepare for printing
'
CLS
PRINT "k    time    glosim    tosim   tinsim  tin    U    "
'
' Input initial conditions
'
'INPUT "iniTime,iniTin"; x0, Y0
x0 = 0: y0 = tin(1)
'
' Set initial conditions
'
k = 0
x = 0
i = glout(1)
t = tout(1)
ti(1) = tin(1)
y = y0
'
' Print initial conditions
'
PRINT USING "####.## "; k; x; i; t; tin(1)
PRINT #1, USING "###.##,"; k; x; i; t; tin(1)

'
' Input stepsize, steps to print and simulation time
'
'INPUT "Step-size"; h
h = .016666667#
'INPUT "Number of steps before printing"; NN
NN = 10
'INPUT "Number of hours to run"; xx
xx = 24
'
' Initialise
'
n = 0
k = 1
x = x0: y = y0
'
' Calculate  U values for the 4 screenhouse evry 10 minutes (144 values)
'
10 IF k = 41 THEN 1000
```

```
GOSUB 100

' Conditions for iteration

n = n + 1
IF n < NN GOTO 10 ELSE 20
20 IF x > xx THEN 1000
'
' Printing
'
PRINT USING "####.## "; x; i; t; uu1(k); uu2(k); uu3(k); uu4(k)
'PRINT #1, USING "###.##,"; k; x; i; t; tin(k); uu(k)
'PRINT #6, USING "###.##"; uu1(k); uu2(k); uu3(k); uu4(k)
'
' Re-initialise
'
n = 0
k = k + 1
'
' Iteration
'
GOTO 10
'
' Subroutine: Equation to integrate
'
100 i = (glout(k + 1) - glout(k)) / 10 + glout(k)
IF i < 0 THEN i = 0 ELSE i = i
t = (tout(k + 1) - tout(k)) / 10 + tout(k)
'ti1(k + 1) = (ti1(k + 1) - ti1(k)) / 10 + ti1(k)
'ti2(k + 1) = (ti2(k + 1) - ti2(k)) / 10 + ti2(k)
'ti3(k + 1) = (ti3(k + 1) - ti3(k)) / 10 + ti3(k)
'ti4(k + 1) = (ti4(k + 1) - ti4(k)) / 10 + ti4(k)
'ytg = (tg(k + 1) - tg(k) / 10 + tg(k)
'
' U1
'
qi1 = A123 * i
qcd1 = B123 * (ti1(k) - tout(k))
qnv1 = C1 * (ti1(k) - tout(k))
qt11 = D123 * .88 * (ti1(k) + 2 + 273) ^ 4
qt21 = D123 * .88 * (tout(k) + 273) ^ 4
qt1 = qt11 - qt21
qg1 = hg * 24 * (ti1(k) + 2 - ti1(k))
'f = (ti1(k + 1) - ti1(k)) / h
IF (ti1(k) - tout(k)) = 0 THEN 990
uu1(k) = (-qnv1 + qg1 + (1 - towt1) * qt1) / (84 * (ti1(k) - tout(k)))
'
' U2
'
990 qi2 = A123 * i
qcd2 = B123 * (ti2(k) - tout(k))
qnv2 = C2 * (ti2(k) - tout(k))
qt12 = D123 * .88 * (ti2(k) + 2 + 273) ^ 4
qt22 = D123 * .88 * (tout(k) + 273) ^ 4
qt2 = qt12 - qt22
qg2 = hg * 24 * (ti2(k) + 2 - ti2(k))
```

```
'f = (ti1(k + 1) - ti1(k)) / h
IF (ti2(k) - tout(k)) = 0 THEN 991
uu2(k) = (-qnv2 + qg2 + (1 - towt2) * qt2) / (84 * (ti2(k) - tout(k)))
'
' U3
'
991 qi3 = A123 * i
qcd3 = B123 * (ti3(k) - tout(k))
qnv3 = C3 * (ti3(k) - tout(k))
qt13 = D123 * .88 * (ti3(k) + 2 + 273) ^ 4
qt23 = D123 * .88 * (tout(k) + 273) ^ 4
qt3 = qt13 - qt23
qg3 = hg * 24 * (ti3(k) + 2 - ti3(k))
'f = (ti1(k + 1) - ti1(k)) / h
IF (ti3(k) - tout(k)) = 0 THEN 992
uu3(k) = (-qnv3 + qg3 + (1 - towt3) * qt3) / (84 * (ti3(k) - tout(k)))
'
' U4
'
992 qi4 = A4 * i
qcd4 = B4 * (ti4(k) - tout(k))
qnv4 = C4 * (ti4(k) - tout(k))
qt14 = D4 * .88 * (ti4(k) + 2 + 273) ^ 4
qt24 = D4 * .88 * (tout(k) + 273) ^ 4
qt4 = qt14 - qt24
qg4 = hg * 32 * (ti4(k) + 2 - ti4(k))
'f = (ti1(k + 1) - ti1(k)) / h
'IF (ti4(k) - tout(k)) = 0 THEN 999
uu4(k) = (-qnv4 + qg4 + (1 - towt4) * qt4) / (135 * (ti4(k) - tout(k)))
999 RETURN
'
'  Calculate average U values for night data (first 40 U's from midnight)
'
1000 avu1 = 0: avu2 = 0: avu3 = 0: avu4 = 4
FOR j = 1 TO 40
avu1 = avu1 + uu1(j)
avu2 = avu2 + uu2(j)
avu3 = avu3 + uu3(j)
avu4 = avu4 + uu4(j)
NEXT j
avu1 = avu1 / 40
avu2 = avu2 / 40
avu3 = avu3 / 40
avu4 = avu4 / 40
PRINT USING "###.##"; avu1; avu2; avu3; avu4
PRINT #6, USING "###.##,"; avu1; avu2; avu3; avu4
CLOSE : END
```

Appendix B3 - RKLUMP.BAS BASIC Program sequence

Name of program: RKLUMP.BAS

Function: **Simulation program to predict inside screenhouse air temperatures for a specific configuration of screenhouse using the Runge Kutta numerical integration techniques. The Input parameters of the program** are the Heat transfer characteristics of the specific screenhouse configuration and the outside climate data (TOUT, GLOO)

Coding sequence:

```
'
' Open files
'
OPEN "c:\phd\simuli\s10919" FOR OUTPUT AS #1
OPEN "c:\phd\simuli\glo0919.txt" FOR INPUT AS #2
OPEN "c:\phd\simuli\tout0919.txt" FOR INPUT AS #3
OPEN "c:\phd\simuli\ti10919.txt" FOR INPUT AS #4
OPEN "c:\phd\simuli\tg0919.txt" FOR INPUT AS #5
'OPEN "c:\phd\simuli\uu0919.txt" FOR INPUT AS #6
'
' Dimension matrix and vectors
'
DIM glout(150), tout(150), tin(150), tg(150), uu(150)
FOR k = 1 TO 144
INPUT #2, glout(k)
INPUT #3, tout(k)
INPUT #4, tin(k)
INPUT #5, tg(k)
'INPUT #6, uu(k)
'PRINT k, glout(k), tout(k), uu(k)
NEXT k
CLS
'
' Input constants
'
' Input "transmissivity, U, Nv, hg"; trans,u,nv,hg
'
trans = .61
u = 2.7
towt = .62
nu = .4
nv = .1
nvday = .5
hg = 4.5
'
' Calculate coefficients
'
A = 24 * trans * nu
B = 84 * u
c = 86 * 1.15 * 1 * nv * 16.667
cday = 86 * 1.15 * 1 * nvday * 16.67
CC = 24 * hg
D = 24 * 5.64E-08
E = 302
```

```
'
' Prepare for printing
'
CLS
PRINT "Time values       Tin values"
'
' Input initial conditions
'
'INPUT "iniTime,iniTin"; x0, Y0
x0 = 0: y0 = tin(1)
'
' Set initial conditions
'
k = 0
x = 0
i = glout(1)
t = tout(1)
y = y0
'
' Print initial conditions
'
PRINT USING "####.## "; k; x; i; t; y; tin(1)
PRINT #1, USING "###.##,"; k; x; i; t; y; tin(1)

'
' Input stepsize, steps to print and simulation time
'
'INPUT "Step-size"; h
h = .016666667#
'INPUT "Number of steps before printing"; NN
NN = 10
'INPUT "Number of hours to run"; xx
xx = 24
'
' Initialise
'
n = 0
k = 1
x = x0: y = y0
'
' Calculate first term of Runge-Kutta
'
10 xt = x: yt = y
GOSUB 100
k1 = f: ' PRINT k1
'
' Calculate second term of Runge-Kutta
'
xt = x + (h / 2): yt = y + k1 * (h / 2)
GOSUB 100
k2 = f: ' PRINT k2
'
' Calculate third term of Runge-Kutta
'
yt = y + k2 * (h / 2)
GOSUB 100
```

```
k3 = f: ' PRINT k3
'
' Calculate fourth term of Runge-Kutta
'
xt = x + h: yt = y + k3 * h
GOSUB 100
k4 = f: ' PRINT k4
'
' Calculate result of Runge-Kutta integration
x = x + h: y = y + (h / 6) * (k1 + 2 * k2 + 2 * k3 + k4)
'
' Conditions for iteration
'
n = n + 1
IF n < NN GOTO 10 ELSE 20
20 IF x > xx THEN 1000
'
' Printing
'
PRINT USING "####.## "; k; x; i; t; y; tin(k); delt; deltat; qnv
PRINT #1, USING "###.##,"; k; x; i; t; y; tin(k); delt; deltat
'PRINT "qi="; qi; "qcd="; qcd; "qnv="; qnv; "qt="; qt; "qg="; qg
'IF k = 1 THEN STOP
'
' Re-initialise
n = 0
k = k + 1
'
' Iteration
'
GOTO 10
'
' Subroutine: Equation to integrate
'
100 i = (glout(k + 1) - glout(k)) / 10 + glout(k)
IF i < 0 THEN i = 0 ELSE i = i
t = (tout(k + 1) - tout(k)) / 10 + tout(k)
ti = (tin(k + 1) - tin(k)) / 10 + tin(k)
yt1 = (tg(k + 1) - tg(k)) / 10 + tg(k)
qi = A * i
delt = yt - t
deltat = tin(k) - t
qcd = B * (yt - t)
IF (k > 40) AND (k < 110) THEN qnv = cday * (yt - t): GOTO 400 ELSE qnv = c * (yt - t)
400 qt1 = D * .88 * (yt + 2 + 273) ^ 4
qt2 = D * .88 * (t + 273) ^ 4
'IF i <= 0 THEN qg = hg * 24 * (4) ELSE qg = 0
qg = hg * 24 * (yt + 2 - yt)
qt = qt1 - qt2
f = (qi - qcd - qnv + qg + (1 - towt) * qt) / 27.47
uu = (qi - f * 27.47 - qnv - qt + qg) / (84 * (yt - t))
'PRINT #1, USING "###.##,"; k; x; i; t; y; tin(k); delt; deltat; uu; 2
'PRINT #1, "qi="; qi; "qcd="; qcd; "qnv="; qnv; "qt="; qt; "qg="; qg; "f="; f
'IF k = 2 THEN STOP
RETURN
1000 CLOSE : END
```

APPENDIX C.

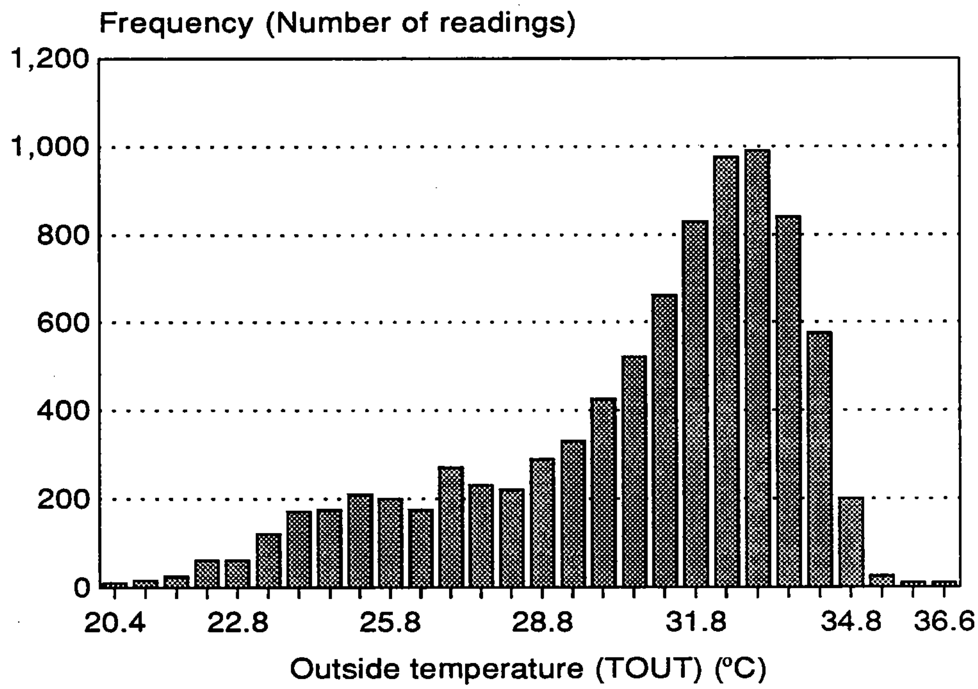

Figure C1. Outside temperature (Frequency distribution) - Experiment #3 - Dry season

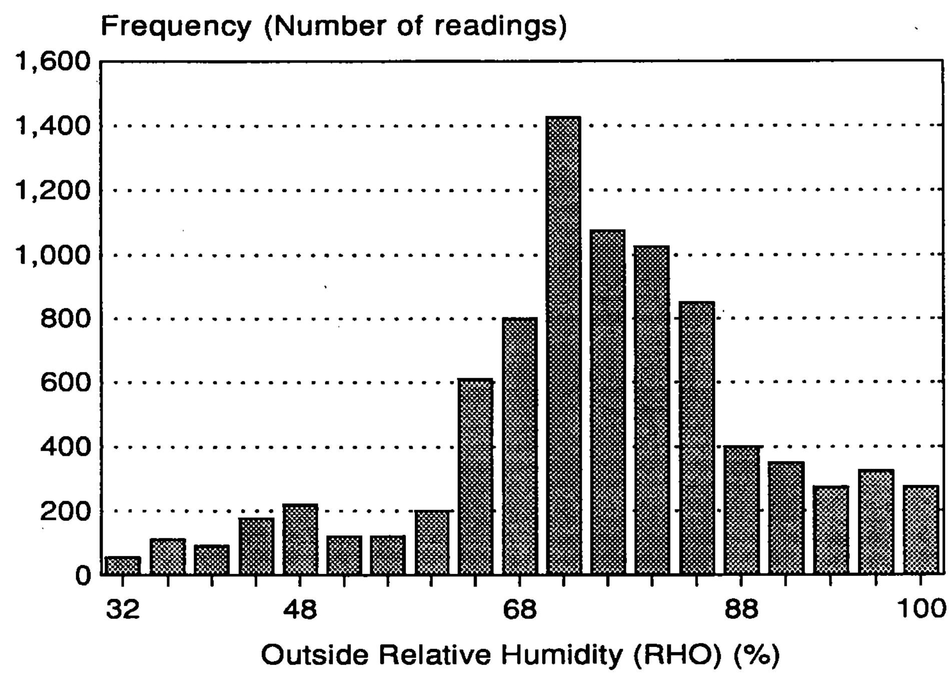

Figure C2. Outside Relative Humidity (Frequency distribution): Experiment #1 - Rainy season

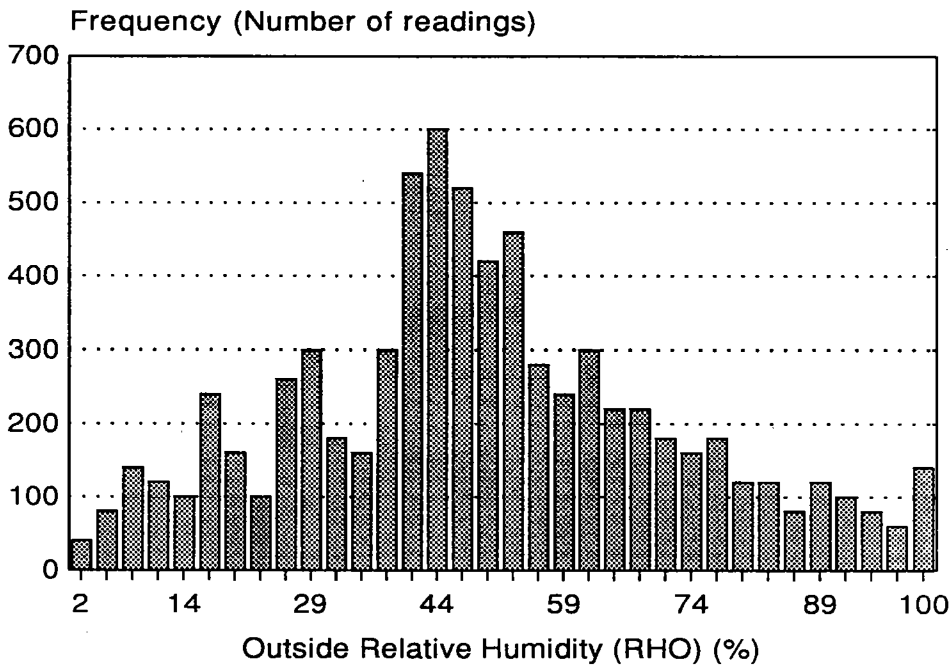

Figure C3. Outside Relative Humidity (Frequency distribution): Experiment #2 - Intermediate (Rainy/Dry) season

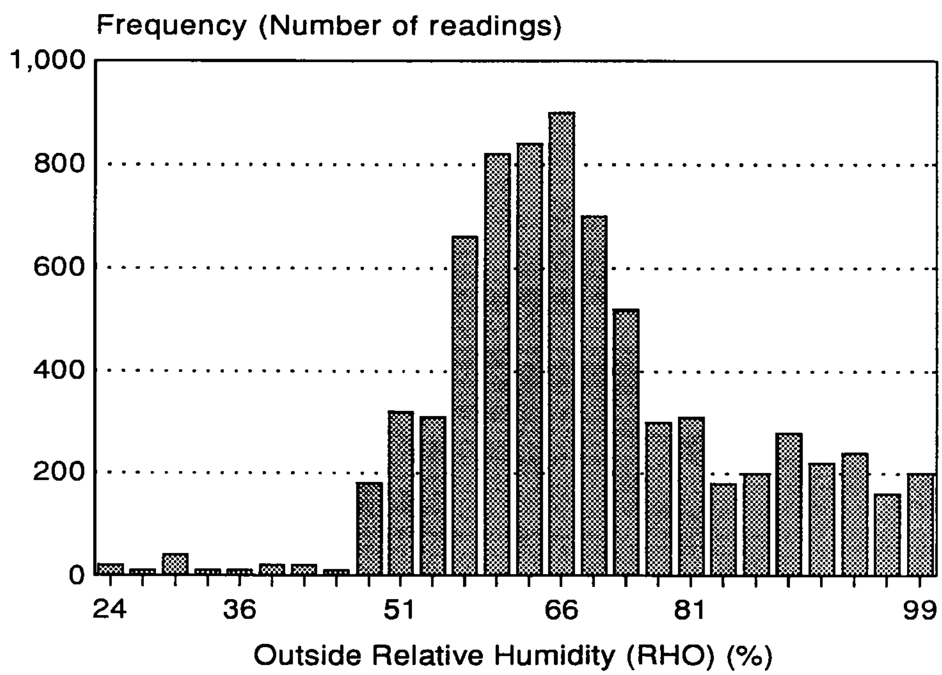

Figure C4. Outside Relative Humidity (Frequency distribution): Experiment #3 - Dry season